Modelling the behavior of the tunnel boring machine and impact on its environment

Mehdi Mahmoudysepehr

N° d'ordre : 411

CENTRALE LILLE

THESE

Présentée en vue

D'obtenir le grade de

DOCTEUR

En

Spécialité : Génie Civil

Par

Mehdi MAHMOUDYSEPEHR

DOCTORAT Délivré par CENTRALE LILLE

Titre de la Thèse :

Modélisation du comportement du tunnelier et impact sur son environnement

Soutenue le 17 décembre 2020 devant le jury d'examen :

Président	Pr. Essaieb HAMDI	Ecole Nationale d'Ingénieurs de Tunis
Rapporteuse	Pr. Tamara AL BITTAR	Université Libanaise
Rapporteur	Pr. Anand PUPPALA	Texas A&M University
Examinatrice	Pr. Anne PANTET	Université du Havre
Examinatrice	Pr. Kaori NAGAI	Université Nihon
Invitée	Mr. Nicolas BRAUD	Bouygues TP (Tunnel Lab)
Invitée	Mr. Julien LARSENEUR	Bouygues TP (Tunnel Lab)
Directeur de Thèse	Pr. Zoubeir LAFHAJ	Centrale Lille
Co-Directeur de Thèse	Pr. Amine Ammar	Arts et Métiers ParisTech, ENSAM Angers

Thèse préparée au Laboratoire de Mécanique Multiphysique et Multiéchelle - LaMCube – CNRS - UMR 9013

Ecole Doctorale SPI 072

Modelling the behaviour of the Tunnel Boring Machine and impact on its environment

---

Turn a great sorrow into a greater work. *(Touran Mirhadi, educator/author)*

Table of Contents

Acknowledgements

Foremost, I would like to express my deep gratitude to Professor Zoubeir LAFHAJ my research advisor and supervisor, for his incredible support, kind and patient guidance and useful critiques of this research work. I am very grateful for all of the things he has taught me. I would like to thank deeply Professor Amine AMMAR my co-advisor, who provided knowledge, guidance, and support, especially when I faced tough and challenging scientific and technical issues. I appreciate his continuous encouraging comments and discussions.

My very sincere gratitude to my director in Tunnel Lab (Bouygues Travaux Public), Nicolas BRAUD. His incredible support to me is unforgettable! His guidance, knowledge, and enthusiastic encouragement is a source of inspiration and self-confidence for me. Further I would like to acknowledge the members of jury Pr.Tamara AL BITTAR, Pr.Anand PUPPALA, Pr.Anne PANTET, Pr.Kaori NAGAI and Pr.Essaieb HAMDI to honor me to participate and provide very useful hints for improving this thesis manuscript, which I have delightedly embraced.

My special thanks go to my colleagues in Bouygues Travaux Public (Tunnel Lab), especially Dr. Nicolas ZIV, Julien LARSENEUR, Estelle LORANT and Guillaume GERARD and all the member of DataTeam of Tunnel Lab who provided a technical, scientific guidance, and support. Our discussion in the office helped me to improve my scientific and technical capabilities and find better solutions for the challenges during my research project. I would like also to acknowledge the helps and advises from my colleagues and friends in Tunnel lab, all experts and engineers from the tunnel department and the methods and prices department of Bouygues Travaux Public, who supported me in different ways and provided a friendly environment.

I would like to acknowledge the helps, supports and advices from Dr.Laure DUCOULOMBIER (head of the construction 4.0 chair) , Ludovic REVERDY and all my colleagues and friends in the construction 4.0 chair and Ecole Centrale Lille within the last few years. Also, I would like to thank Dr. Naeem ADIBI, and Nikzad MOTAMEDI who partly involved in the proof-reading and provided feedback and support on the drafting phase of this work.

And last not the least I wish to express my immense gratitude, appreciation and acknowledge to my family, my father, my mother, my sister and my brother, for their not-ending support and unparalleled love. I am grateful to my beloved fiancée for her support, patience and always being there for me as a best friend. Their endless encouragements, support, patience is unforgettable.

Ecole Centrale Lille - 17/12/2020

Résumé

Les zones urbaines sont de plus en plus peuplées, ce qui oblige les décideurs en matière d'urbanisme à construire des infrastructures sûres, durables, innovantes et de qualité. Le développement des infrastructures souterraines est l'un des choix les plus fiables pour l'aménagement des mégapoles, principalement pour améliorer les systèmes de transport public. Le creusement de tunnels en zone urbaine présente des complexités en matière de durabilité, tels que la sécurité des structures du centre-ville ou la forte densité de population, et des défis techniques comme l'excavation contextes géologique et géomécanique sensibles et complexes ou dans des conditions hydrogéologiques critiques.

Le creusement mécanisé de tunnels est l'une des méthodes les plus courantes pour développer les infrastructures souterraines urbaines, bien qu'il ait été utilisé pour les tunnels de service, le stockage de l'énergie et d'autres ouvrages souterrains. Comme dans d'autres secteurs, l'automatisation et l'optimisation de différentes sous-procédures est une demande et une tendance rapide. La mise en œuvre de nouvelles technologies et d'innovations offre de grandes possibilités de faire évoluer notre compréhension, d'affiner nos connaissances et d'améliorer la conception technique et la prise de décision.

Le tunnelier, l'une des méthodes les plus fiables de creusement de tunnels mécanisés, a des acteurs scientifiques et professionnels de premier plan dans le monde entier, du Japon à l'Europe et à l'Amérique du Nord. Le développement du tunnelier a bénéficié de différentes approches analytiques, numériques et expérimentales. Compte tenu des progrès des nouvelles technologies, les méthodes fondées sur les données peuvent être utilisées comme des outils efficaces pour réaliser et résoudre des problèmes d'optimisation et de fonctionnement. Les approches fondées sur les données nous aident à optimiser la prise de décision sur la base de leur analyse et de leur interprétation. Pour les besoins de cette étude,

nous avons utilisé les données d'excavation opérationnelles du TBM qui proviennent des projets de routes et de tunnels de transport.

Les méthodes analytiques et numériques nous aident à acquérir des connaissances théoriques et techniques essentielles sur les principaux problèmes qui se posent lors de l'excavation et de l'interaction entre le tunnelier et son environnement. Malgré tous les progrès réalisés, les ingénieurs se heurtent à diverses complexités techniques lors du creusement de tunnels sous bouclier. Il existe également un intérêt et une demande énormes pour l'optimisation économique et technique du procédé TBM. Dans ce projet de recherche, nous tentons d'approfondir notre compréhension de l'interaction entre le tunnelier et son environnement et d'utiliser ce développement pour résoudre des problèmes techniques et appliqués, principalement l'optimisation du pilotage du tunnelier.

La première étape consiste à évaluer l'équilibre des forces sur le tunnelier afin de clarifier les interactions inconnues pendant le creusement du tunnel du TMB en se basant sur les complexités géologiques, les incertitudes naturelles suivant les caractéristiques géomécaniques du sol et de la roche et les défis techniques opérationnels. Comme exemples des principales questions scientifiques et pratiques, on peut souligner l'approche visant à évaluer les forces autour du corps cylindrique du tunnelier (tête de coupe, corps principal et la jupe), l'interaction du tunnelier avec son train suiveur, l'interprétation du mouvement de ver (worm-like motion) du tunnelier et certaines interactions internes et externes du tunnelier avec son environnement (comme l'interaction du jupe-revêtement, la poussée et l'interaction des vérins hydrauliques auxiliaires pendant l'excavation et l'inclinaison de la tête de coupe pendant l'excavation).

Au cours de ce projet de recherche, nous avons déterminé l'importance de l'exploration et de l'analyse des données opérationnelles des TBM. Les compétences en science des données, en particulier l'analyse exploratoire des données (EDA), nous permettent d'étudier

les paramètres opérationnels de l'excavation, de découvrir des relations significatives entre les paramètres et de trouver des paramètres efficaces pour décrire plus précisément l'interaction du tunnelier avec son environnement. Ensuite, des algorithmes mathématiques et statistiques (algorithmes d'apprentissage automatique) seront utilisés pour étendre nos capacités de modélisation et d'optimisation du pilotage de la TMB en utilisant des paramètres sélectionnés de l'AED.

Cette étude de recherche nous a permis d'évaluer et d'identifier une méthode applicable pour trouver une corrélation significative entre les paramètres opérationnels du TBM et pour évaluer son comportement avec l'environnement. Cette évaluation basée sur les données nous donne des capacités d'interprétation améliorées pour trouver des paramètres efficaces afin de réduire l'incertitude dans nos opérations techniques. Nous avons également proposé une stratégie instrumentale pour mesurer la déformation du corps cylindrique de la structure (la jupe) et calculer la charge exercée sur la périphérie de la jupe. Les paramètres proposés sont utilisés dans des approches fondées sur les données pour optimiser le pilotage des TBM. Les approches fondées sur les données permettent également aux experts de terrain (ingénieurs de tunnel) d'observer les données opérationnelles mesurées afin d'améliorer la résolution des problèmes. Il leur donne également la possibilité d'étudier les relations statistiques (corrélations) entre les paramètres opérationnels et les paramètres de guidage et d'examiner les algorithmes d'apprentissage de la machine pour optimiser le pilotage du TBM.

L'utilisation d'approches fondées sur les données offre une vision holistique permettant de clarifier et de modéliser les interactions internes et externes des TBM. Cette étude nous a permis de trouver une nouvelle corrélation entre les paramètres opérationnels du TBM, difficiles à distinguer et à expliquer à l'aide d'autres méthodes. L'application d'algorithmes d'apprentissage machine nous a permis de créer des modèles explicatifs et prédictifs plus précis, pratiques pour les experts en tunnels, des ingénieurs aux pilotes de tunneliers.

List of Tables

List of Figures

List of Acronyms

TBM	**Tunnel Boring Machine**
EDA	Exploratory Data Analysis
EPB	Earth Pressure Balance
SPB	Slurry Pressure Balance
VD	Variable Density
FEM	Finite Element Method
JSCE	Japan Society of Civil Engineers
ITA	International Tunnelling Association
PLC	Programmable Logic Controller
PM	TBM Chainage
DTA	Design Axis of Tunnel
ANN	Artificial Neural Network
RQD	Rock Quality Designation
ANFIS	Adaptive Neuro-Fuzzy Inference System
KNN	K-Nearest Neighbours
SVM	Support Vector Machines
LDA	Linear Discriminant Analysis
AI	Artificial Intelligence
CI	Computational Intelligence
SC	Soft Computing
CV	Cross-Validation
MSE	Mean Squared Error
RMSE	Root Mean squared Error
MAE	Mean Absolute Error
R^2	Coefficient of Determination
PCA	Principle Component Analysis
GD	Gradient Descent
SGD	Stochastic Gradient Descent

1. General introduction

Urban areas are becoming more populated, forcing urban planning decision-makers to construct safe, sustainable, innovative, and high-quality infrastructures. Tunnelling in the urban area has different sustainability complexities and technical challenges. These challenges include inner-city structure safety, high population density, technical challenges like excavation in sensitive and complex geological and geomechanical formation and critical hydrogeological conditions. The mechanized tunnelling is one of the most mainstream methods to develop urban underground infrastructures. Similar to other sectors, automation and optimization of different sub-procedures is a rapid request and trend. The implementation of new technologies and innovations provide ample opportunities to evolve our understanding, to fine-tune our knowledge, and to improve engineering design and decision-making. During last decades TBMs are used as one of the most reliable and secured methods for excavation of different types of tunnel specially in urban areas.

Modelling and optimization of the TBM process is an essential demand in the tunnelling industry and an important challenge for researchers and engineers in TBM tunnelling. Understanding the internal and external interactions of a TBM is crucial for finding solutions to TBM operational challenges and problems. There are different approaches which are used to achieve these purposes from analytical (theoretical methods) to numerical methods. Recent progress in computational capabilities and advancement of new technologies to capture more reliable data related to different operations of a TBM give us opportunities to use data-driven approaches. In parallel, development and advancement of data-driven approaches (statistical learning techniques) give us the extra tools to optimize and model complex problems in TBM operations. During this research project, some essential questions are investigated by analytical and data-deiven methods. In this study, an evaluation of the internal and external interactions of a TBM will be studied to find and investigate the important factors and parameters which influence the advancement of a TBM. Improvement of the understanding help find more accurate answers for different technical questions like steering optimization issues, the tail skin blockage, a calculation improvement of required total thrust force and cutter head torque and advancement

speed improvement. The external interactions of TBM (ground-TBM interactions) have an essential role. By using TBM operational data and data represented ground characteristics, the potential associations between these data are studied. Following is presented the brief introduction about the organization of this research project.

The second chapter will cover the state of the art of the analytical methods used to reach a fundamental technical understanding to model TBM interactions. The calculation is proposed and presented by researchers and engineers to better recognize TBM interactions and to find optimal parameters for excavation of a TBM such as required thrust force and cutter head torque. This chapter investigates the interaction of a different part of a TBM. To simplify the observation, TBM body is divided to three main parts: TBM front body, middle body and tail skin. Some analytical approaches are reviewed for estimation of required thrust force and cutter head torque as two important parameters of a TBM advancement. This chapter will demonstrate the review summary of the analytical studies for TBM calculation and design.

The third chapter will provide a brief introduction to data acquisition set up in a TBM. Exploratory Data Analysis will be presented for different TBM operational data, such as excavation chamber pressure, thrust cylinders pressure, injection of mortar and grease pressure and TBM trajectory characterization data (the parameters are investigated based on evaluation of the previous studies, researches and discussions with TBM engineers and experts). Besides, the calculation of the centre of thrust force, centre of moment arm and inclination of cutter head are presented as parameters which will be used in data-driven modelling for optimization and modelling of TBM operation. The visualization techniques are used to find the general association between TBM parameters. Visualization techniques will give us better interpretation capabilities. It will be an essential step to evaluate the TBM parameter and find a meaningful association and probable physical explanation for the phenomena which occurred during a TBM operation. Visualization techniques will be essential and efficient for both pre-processing and post-processing evaluations.

In chapter four, an instrumentation procedure of the TBM's tail skin is proposed to capture data which represent the deformation of tail skin structure. The captured data will be used to calculate the load on the periphery of a TBM. The Finite Element Method (FEM) computation by MATLAB

is implemented to compute the loads. The estimation of load on the periphery of TBM may be beneficial for different evaluation and optimization procedures. The load exerted on TBM body is very important for estimation of friction force created due to interaction of TBM and its periphery. Similarly, it can be used for finding a more precise evaluation of the balance of force on TBM. Also, it can be used for the computation optimization of the required driving force and moment of force of a TBM. Better evaluation of load applied on a TBM body will help engineers find a better interpretation and a solution for the challenges such as tail skin blockage during a TBM excavation.

Chapter five will cover a data-driven approach (finding a statistical learning model) between TBM data (operational parameters, geological parameters and trajectory characteristics) as inputs and steering parameters (Pitch and Yaw) of TBM as the output of the model (Pitch and Yaw considered as horizontal and vertical tendencies of TBM during advancement). As a first step, typical regression algorithms are observed. A spot-check of regression algorithms for this purpose is presented in this chapter. Then Multilayer Perceptron (MLP neural networks model) architecture on our data structure is implemented to find the optimal model for TBM operational data. A hyperparameter evaluation of algorithm is implemented to find the optimal configuration for the proposed model. Finally, the accuracy of the model is investigated by testing the model for different segmentations of the TBM trajectory characteristic.

In conclusion, the results of this research project are discussed. Also, the perspectives are proposed as the next steps for the upcoming improvement and further studies.

1.1 Construction chair 4.0

This PhD thesis is carried out within the framework of the "Construction chair 4.0", an industrial research chair between the École Centrale de Lille, and the industrial partner "Bouygues Construction", as well as public partners such as Europe (via the ERDF), the Hauts-de-France Region and the European Metropolis of Lille (MEL).

In order to move the construction sector on to the fourth industrial revolution, Ecole Centrale Lille and the Bouygues Construction company have signed a 5-year partnership by creating this Industrial Chair, which aims to be a place of reference for research on the modernization of

construction. During these five years, more than thirty researchers, doctoral students, post-doctoral students, interns and student-engineers from Centrale Lille have been working on the theme of construction modernization. They work jointly with collaborators from the company on ambitious and innovative research projects.

1.2 Tunnel Lab

Throughout this thesis, I directly collaborated with Tunnel Lab, I had the chance to exchange a lot with experts and engineers from the Tunnel Lab, the tunnel department and the methods and prices department of Bouygues Travaux Public concerning the technical issues related to the subject. I had many opportunities to work and discuss with different experts from TBM pilots to tunnel engineer and materials engineers of Tunnel Lab to better understand the main challenges regarding excavation of TBM. Also, for installation of sensors, I had chance to experience the applied issues regarding the collaboration with different actors of the big project like line 15(T2A) of Grand Paris Express. I also collaborated directly with the data team of Tunnel Lab for evaluation and development of proposed data-driven approaches. I continued in this approach, because it is important to stay connected to the "technical issues and applied challenges" reality. A thesis is not to advance research for research's sake. It is about bringing, through research, concrete answers to the needs of the field.

The Tunnel Lab is in charge of transforming the ideas and concepts of the Bouygues Travaux Publics teams into prototypes. These prototypes are then deployed on the tunnel boring machines in production. After this crucial first step, the team's second challenge is to work on the industrialization of these innovations, to enable Bouygues TP to offer the best services to its customers. The Tunnel Lab missions lead the team to select partners - small or large companies - to develop these innovations. The team also works in collaboration with scientists, to detect and propose new technologies that meet the needs of business teams. This multidisciplinary team is led by Nicolas Braud. It is composed of experienced project managers and experts in hardware, energy, tunnels, geology, embedded computing, and data analysis.

2. State of the art to mechanized tunnelling by Tunnel Boring Machine

Chapter summary:

This chapter will cover the state of the art of the analytical methods used to reach a fundamental and technical understanding to model TBM interactions. The calculation is proposed and presented by researchers and engineers to better recognize TBM interactions and to find optimal parameters for excavation of a TBM such as required thrust force and cutter head torque. This chapter investigates the interaction of a different part of a TBM. To simplify the observation, TBM body is divided to three main parts: TBM's front body, middle body and tail skin. This chapter will demonstrate the review summary of the analytical studies for TBM calculation and design.

2.1 Introduction

Increasing demand for underground urban area development leads to more tunnelling in soft and complex geological and geomechanical conditions. Based on previous research done by Peck (1969), the main problems related to tunnelling are: keeping the boring front stable, limiting the impact on the surrounding soil and foundations, and keeping the tunnel safe and operational [1]. Fundamental challenges in urban tunnelling arise in the stability of the tunnel environment, especially face and roof collapse and surface settlement. Tunnelling in complex geology/mixed ground is another challenge in tunnelling, especially, for TBM tunnelling. The mixed ground is a simultaneous occurrence of two or more geological formation with different geomechanical characteristics [2]. Cutter head wears, deformation, blocking, tail skin blocking, and steering difficulties are some of the challenges encountered in TBM (shield) tunnelling. In 1997 Baker et al. evaluated aspects related to the feasibility of boring [3]:

- front stability,
- excavation efficiency concerning the soil encountered,
- maintenance and wear of cutter tools,
- unexpected objects.

The large variety of soil formation influences excavation efficiency. With the presence of diverse materials, engineers are encountered diverse geomechanical properties and water-bearing conditions. When there are several diversities in soil formations, it is advised to reduce the speed of excavation to secure the formation on the front of the cutter head. Maintenance and wear of cutter bits are not too much affected by soft soil, but the cohesive behaviour of soil (such as clay) would create more problems[4].

2.1.1 Scope

During the last decades, TBMs are developed to reduce uncertainty and increase safety issues for excavation in complex geological conditions. There are different general TBM classifications [5]. Usually, TBMs classification proposed is based on face supports and muck extraction methods. There are two mains open/closed-face mode and five types of tunnel face support, open-no support, mechanical support, compressed air support, Earth Pressure Balance (EPB) support,

and Slurry Pressure Balance (SPB) support [6]. During this study, the TBMs in soft grounds were mainly studied, TMBs mostly used in soft grounds are EPBs, SPBs or mixed shields and Variable Density (VD).

Table 2-1 Closed type TBM classification, mainly applied for exaction in soft ground (main operations comparison)

TBM Type	Face Support	Muck Extraction	Mode
EPB TBMs	Pressured muck + one or more of water, foam, bentonite, polymer	Dry muck extraction (conveyor belt)	Closed, open
SPB TBMs	Pressured water or water + bentonite /Polymers	Hydraulic muck extraction	Closed, open
Mixed Shields	Combination of SPB and EPB	Combined muck extraction (dry and/or hydraulic)	Closed, open

EPBs are used for many types of soil characteristics from gravelly alluvial sand, to sand, silt and clay, diluvial deposits, and ground with alternating soft and hard sections. Based on face support mechanisms, SBPs are appropriate and operative for high groundwater pressure and wide range of geological and geomechanical characteristics including alluvial gravel mixed with sand; sand, silt , or clay; alternating layers of loosely cemented and soft ground; soil with a high water content that may not form a self-standing of cutting face; diluvial gravel mixed with sand, silt and clay or alternating layer with high water content, sensitive to ground collapse and water inflow in an excavation chamber [7].

2.2 Evaluation and benchmarking on the design and modelling of TBM

In this section, the previous works on TBM design and modelling were investigated to understand TBM behaviour and interactions with its surrounding. There are different classifications for TBMs based on ground characterization and geological complexities; each type has its characteristics to be considered. We focus in this section more on research and

recommendations proposed for soft ground TBMs. Recommendation and research are developed based on experiences and works of each group and region such as European (German, French and British manuals), Japanese, North American and Asian researchers and engineers.

In 1996 B. Maidl et al. described TBM parts into three main sections, front shield, middle shield and tail skin (Figure 2-1). The front shield consists of the cutter head, pressurized chamber, bulkhead and main drive. Loading of the TBM body is divided into external and operational loads, and they considered four general groups of loads in the design and modelling of TBM. These loads consist of [5]:

- Self-weight,
- Radial external load (water pressure, earth pressure and the reaction of forces from steering motion),
- Axial external loading (confining pressure on the excavation chamber, the pressure of tools on the face, thrust cylinder forces and forces from back up train)
- Other loads (skin friction, reaction forces at the shield blade, reaction forces of erector during ring installation, thrust forces from the auxiliary hydraulic cylinders, the reaction force from brush seal and grease chamber pressure and grouting pressure.)

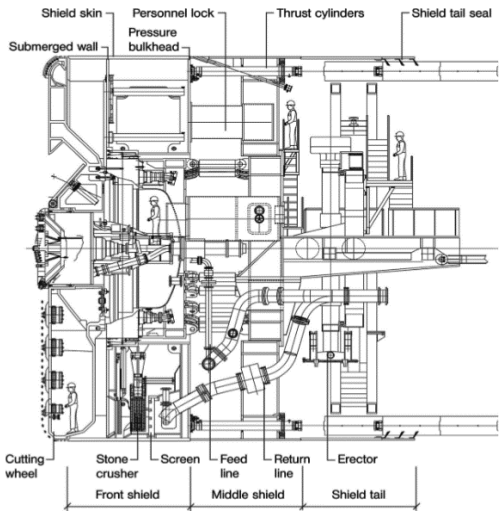

Figure 2-1 Constructional elements of mixed shield _ longitudinal section [5] (Herrenknecht)

Maidl et al. determined that a TBM structure with all its stiffening parts signify a highly structurally indeterminant and asymmetric shell structure. At the same time, they evaluate the moments and forces acting on different parts of the TBM by numerical methods (FEM

computation) [5]. To better clarify loading on different parts of a TBM they used analytical and calculation models for each part, such as calculation of loading on TBM skin, loading on pressure bulkhead and assessment of the necessary thrust force based on individual resistances such as:

- Resistance to advance through friction on the TBM body skin,
- Resistance to advance at the face,
- Resistance to advance with slurry support, earth support and compressed air support,
- Resistance to advance from steering the TBM,
- In the presence of an articulation joint between the middle body and the tail skin reduces moments created due to driving curve.

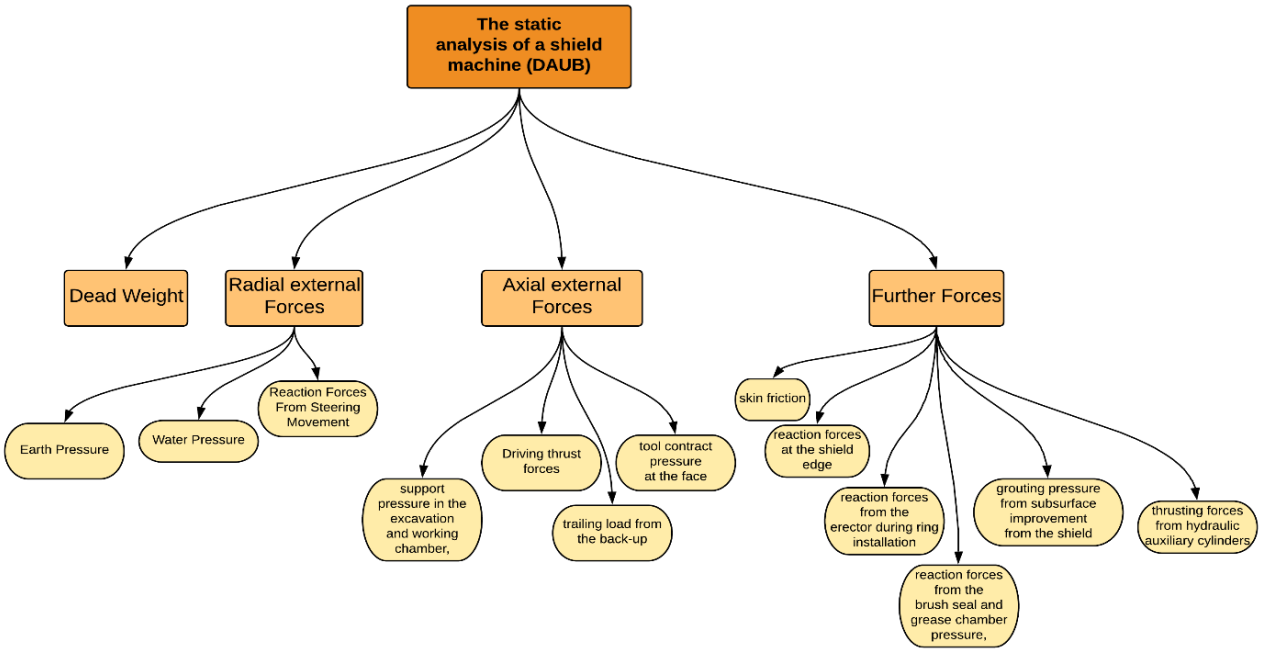

Figure 2-2 A flowchart of the Static analysis of a shield proposed by DAUB (evaluation of main forces excreted on TBM)

They also define a safety margin that includes the forces such as[5]:

- Back up train towing force,
- Tail seal /lining friction,
- Increased cutter tools resistance on obstacles,
- Skin friction increase in grouted zones,
- Skin friction increase due to ground swelling,
- Skin friction increase due to steering and guiding of the TBM.

Another applied recommendation/manual has been developed by the Japan Society of Civil Engineers (JSCE). Japanese guideline for shield tunnelling published in 1969 has been revised four times until today, in 1986, 1996, 2006 and 2016. The Japanese manual refers to the closed-face mode shield tunnelling method. JSCE also proposed two EPB and SPB as main TBM types for excavation in soft grounds Figure 2-3. In this recommendation, they consider two main parts for shield machine, design and analytical modelling of TBMs. They proposed seven main groups of loads to be taken into account[7]:

- Vertical and horizontal earth pressure,
- Water pressure,
- Self-weight,
- Effects of surcharge load,
- Loads imposed by the direction change,
- Cutting face pressure,
- Others.

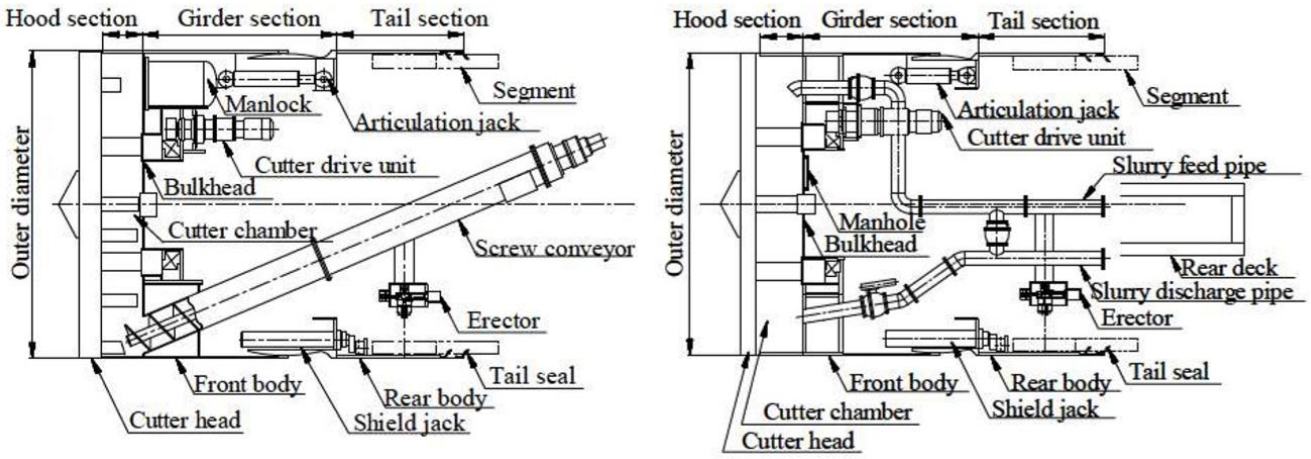

Figure 2-3 Constructional elements of EPB and SPB TBM_Longitudinal section proposed by (JSCE 2006) [7]

For further evaluation of TBM behaviour, the interaction of a TBM based on TBM body parts will be observed in next section. The evaluation will be done for previous analytical modelling and calculation of the critical process in front of TBM and around TBM body separately.

2.2.1 **Process in the front body of a TBM**

In tunnels in urban areas, even if there is no risk of instability, it is known that deformations at the working face during excavation contribute significantly to surface settlement [6]. Confinement or reinforcement of the front is, therefore, a means of controlling the deformations induced on the environment. The front body of TBM consists of two main parts, a cutter head and an excavation chamber. The front body primary responsibilities are digging the ground and providing the stability of the cutting face. The TBM cutter head should be designed and selected based on various considerations from ground characteristics to the tunnel alignment and construction conditions [7]. The contact force of the cutter head to loosen the ground depends on the geomechanical characteristics of the soil and rock. For soft ground, this contact force could be estimated as following [5]:

$$R_{et} = A \times K \times p_v [kN] \qquad \text{Equation 2.1}$$

the resistance of cutter head (excavation tools): R_{et} $[kN]$,

the contact area of cutter head: A $[m^2]$,

lateral earth pressure coefficient: K,

vertical load: $\mathrm{p_v}$ $[\mathrm{kN/m^2}]$.

For the cutter head with displacement cylinders (horizontally and vertically adjustable), the force in the cylinders corresponds to the contact force between cutter tools and the ground.

The front body should be designed based on the type of support. In EPB, it should have enough capacity for mixing excavated ground, and in SPB, it should have a structure not to obstruct slurry flow. In TBM tunnelling, the tunnel face is stabilized by pressured materials (slurry or muck). This pressure should be calculated for the ground pressure. If the calculated pressure is lower than ground pressure, it leads to face collapse or entrance of water in the excavation chamber and finally to the settlement of the surface. If confining pressure is too high, blow-out will occur. The calculation of support pressure in front of earth pressure could be done using different methods such as: analytical, empirical, experimental, and numerical.

Resistance to the advance of a TBM from the earth, water pressure and the support pressure resultant would be part of thrust force exerted by thrust cylinders:

$$W_{ST} > W_E > W_W \qquad \text{Equation 2.2}$$

earth pressure resistance: W_E from investigation of failure body,

water pressure resistance: $W_W = A_0 \times (p_{Wcrown} + p_{Winvert}) \times 0.5$,

resistance for face support: $W_{ST} = A_0 \times (p_{STcrown} + p_{STcrown}) \times 0.5$,

water pressure at the crown: p_{Wcrown},

water pressure at the invert: $p_{Winvert}$,

support pressure at the crown: $p_{STcrown}$,

support pressure at the invert: $p_{STcrown}$,

tunnel face area: $A_0 = \frac{\pi \cdot d_S^2}{4}\ [m^2]$,

Table 2-2 General 3D schematic of EPB and SPB TBM main parts

Earth Pressure Balance (EPB) support	Slurry Pressure Balance (SPB) support
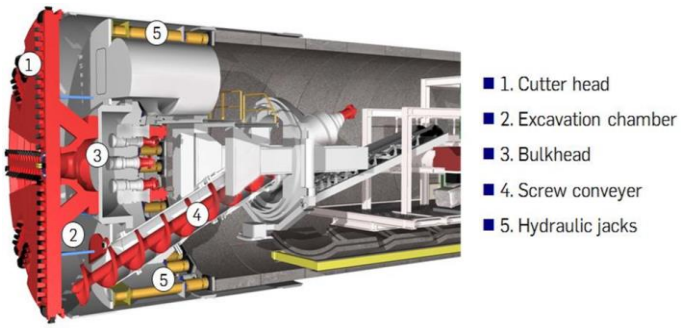	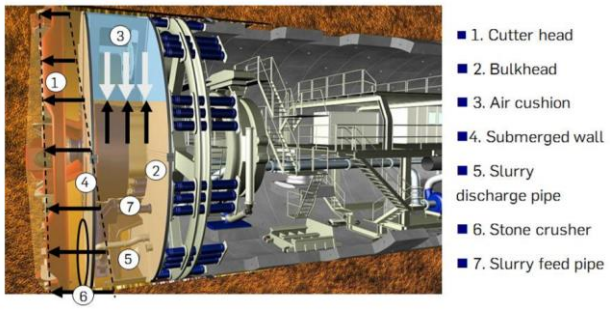

There is a theoretical method suggested by the International Tunnelling Association (ITA) for the estimation of vertical and horizontal earth pressure. In this method, the ITA proposes that the arching height (h_0) should be calculated for estimation of vertical and horizontal earth pressure if the depth of overburden to the crown is greater than two times of diameters of a TBM [8]:

$$h_0 = \frac{\{b_s \cdot (\gamma_b - \frac{C_U}{b_s}) \cdot [\frac{1 - \mathrm{e}^{-K_0 \cdot \tan(\delta) \cdot (h/bs)}}{K_0 \cdot \tan(\delta)}] + \sigma_{\mathrm{Sur}} \cdot \mathrm{e}^{-K_0 \cdot \tan(\delta) - (h/bs)}\}}{\gamma_b}$$ Equation 2.3

$$b_s = \frac{D_{\mathrm{TBM}}}{2} \cdot \cot\left(\frac{\pi}{8} - \frac{\phi}{4}\right)$$ Equation 2.4

$$\sigma_v = \max(\gamma_b \cdot h_0 \ , \gamma_b \cdot 2 \cdot D_{\mathrm{TBM}})$$ Equation 2.5

$$\sigma_h = K_0 \cdot [\sigma_v + \gamma_b \cdot (D_{\mathrm{TBM}}/2)]$$ Equation 2.6

the half-width of arching soil prism: b_s $[m]$,

bulk unit weight of soil: γ_b $[\frac{kN}{m^3}]$,

undrained cohesion of soil: C_U $[kPa]$,

lateral earth pressure at rest (suggested 1.0 by ITA 2000): K_0,

surface surcharge pressure : σ_{Sur} $[kPa]$,

depth of cover to crown: h $[m]$,

excavation diameters of TBM: D_{TBM} $[m]$,

undrained internal friction angle of ground: ϕ [°],

the angle of wall friction of arching prism: δ [°],

vertical earth pressure and horizontal earth pressure: σ_v & σ_h,

Concerning the face pressure in the working chamber of the TBM, the safety margin should be applied to the horizontal earth pressure. When the tunnel is entirely under the groundwater level, hydrostatic pressure should be added to earth pressure, and the buoyant weight of soil should be applied instead of bulk unit weight of soil [9].

In 2016, DAUB (German Tunnelling Committee) also developed and published a complete manual that investigated in detail different methods for face support pressure calculation[9]. A TBM derived in a non-straight trajectory (curved trajectory) by using main thrust cylinders (differential extension of cylinders), and displacement cylinders connected to the main drive (tilting mechanism for cutter head) were studied by DAUB. It means that based on the configuration of TBMs, different cylinders collaborate in the steering of a TBM. To reduce bending created during a curved trajectory, different solutions are proposed and used in design or during operation such as the tapered shape of TBM, creating overcut and lubrication with bentonite through injection nozzles[5].

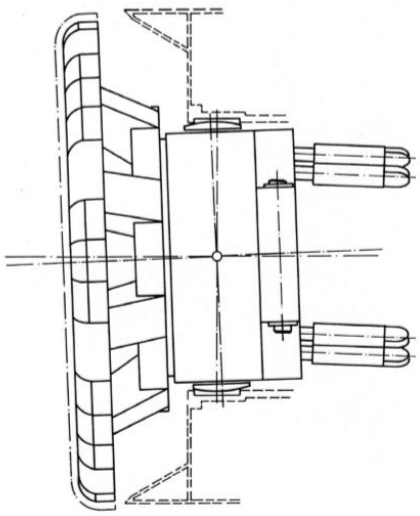

Figure 2-4 Schematic of cutter head-displacement cylinders (schematic to observe how cutter head is inclined) [5]

2.2.2 The process around the middle body and tail-skin of a TBM

The process around the TBM body (middle body and tail skin) are decisive and essential to be studied. Different interactions could occur due to TBM advancement (in straight or curved trajectory). Calculation of earth pressure acting on the TBM body is complex and challenging to evaluate. The first general approach is to understand the earth pressure on the TBM body. JSCE (2006) proposed a general approach (two methods) for earth pressure evaluation. First, the effective stress method (in this method ground pressure is separated from groundwater pressure) is proposed. This method has been mostly used for sandy soils. The second method is the total stress approach, where water pressure is included in-ground pressure (this method is more adaptable for cohesive soil). There are still exceptions which use separated groundwater and soil pressures for cohesive soils (in these cases a cutting face would be highly stable like stiff clay and

consolidated silt). Regarding geomechanical characteristics of soil, the wet unit weight of soil has been used above the groundwater level (effective stress method), and submerged unit weight is used below the groundwater level (total stress method). JSCE proposed that when determining the vertical earth pressure acting on the TBM body, it is better not to consider the arch action of soil when overburden height is less than tunnel diameter (difficult to adapt lessening earth pressure for the design earth pressure). If overburden is one or two times more significant than the outer diameter of the shield, loosening earth pressure is compatible for the design of vertical earth pressure where the arcing act of soil could be expected. Terzaghi equation is usually used for the calculation of loosening earth pressure[7].

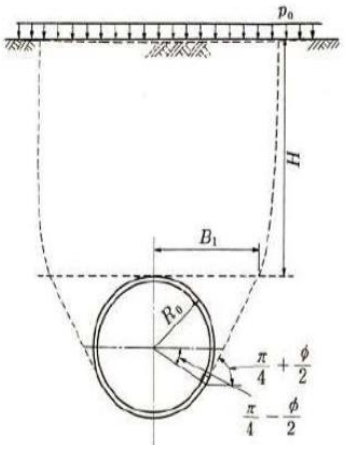

$$\sigma_v = \frac{B_1(\gamma - c/B_1)}{K_o \tan\,\phi} \cdot (1 - e^{-K_0 \tan\,\phi \cdot H/B_1}) + po \cdot e^{-K_0 \tan\,\phi \cdot H/B_1}$$

$$B_1 = R_o \cdot \cot\left(\frac{\frac{\pi}{4}+\frac{\phi}{2}}{2}\right)$$

σ_v : therzaghi's loosening earth pressur
K_o: the ratio of horizontal to vertical earth pressur
ϕ : internal friction angle of soil
po : surcharge load
γ: unit weight of soil
c : cohesion of soil

Figure 2-5 Left: Schematic diagram of Terzaghi arching model, right: formulation of Terzaghi loosening earth pressure

The Terzaghi theory assumed that shearing band rise from the outside of the tunnel cross-section and extends to the ground surface. The lateral earth pressure was less than the static earth pressure on the left and right sides of the collapsed body in the range of 1.5 times the tunnel radius on the crown of the tunnel. Then they consider the range of 1.5 times of tunnel radius as active earth pressure area.

After Terzaghi's calculation, different silo width summarized are shown in Figure 2-6. The yielding points of the shearing bands and their direction would be the differences in these silo widths. Some researchers considered the extension of shearing bands towards the ground surface; others assumed that the shearing bands extended along inclined lines [10].

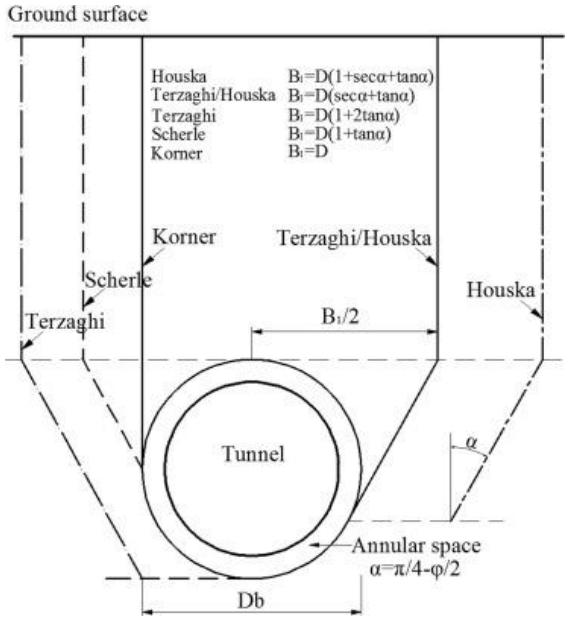

Figure 2-6 Different approach to calculate silos width [10]

Another simplified approached to model (design) the dimensioning of the TBM body skin is the shell model with elastic bedding. Self-weight, earth pressure, and water pressure are applied as external loads[10]. The weight of overburden, traffic and buildings can be used as vertical loading excreted on the body of TBM. The horizontal loading is calculated by the coefficient of lateral earth pressure K and a potential additional horizontal stress. The evaluation of these influences is difficult, and is usually estimated experimentally. K should be selected in such a way that the horizontal load corresponds either to the earth pressure at rest or to the active earth pressure. In this approach, the loaded TBM body skin can be analysed with and without elastic bedding. In the bedding approach shown in Figure 2-7, the roof area with an aperture angle α is not bedded. In the remaining area, the reaction of the ground was modelled by springs. The spring constants, which are referred to as modulus of subgrade reaction, is estimated based on experience. In this model, the interaction between structure and ground is approximated by pre-set load assumptions and assumptions regarding the magnitude, direction, and distribution of the subgrade reaction modulus. By using this model, it is not possible to determine subsidence at the ground surface or the foundations of existing buildings and stress-strain states in the surrounding ground[11].

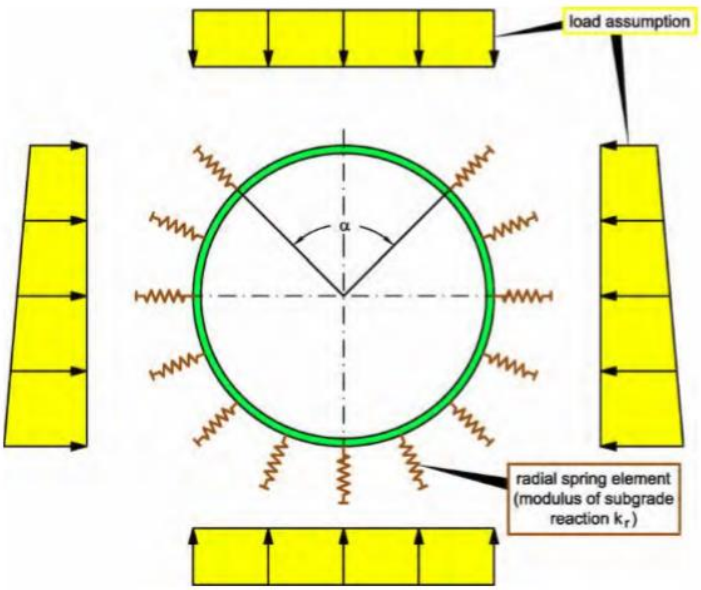

Figure 2-7 Model earth pressure and elastic bedding application to the shield skin (Wittke et al 2007) [11]

The arching in the ground (soil and rock) must be accounted for in the case of tunnels with high overburden. The model with elastic bedding, in such cases, may be applied for approximate calculations [11].

One of the most critical parameters to calculate or estimate would be friction created because of TBM-ground interactions. The loading from earth pressure (radian, horizontal and vertical load), surface loads and load exerted due to the self-weight of the TBM body create friction forces during TBM advancement. There are strategies to reduce this friction, such as conic geometry of TBMs and using overcut and lubrication by bentonite injection around the body. The characteristics of the ground (the type of soil determined the friction coefficient).

Calculation proposed by B. Maidl et al. for the approximation of friction force in shield body – ground interaction[5]:

$$F_b = \mu \times [2\pi \times r \times 1(p_v + p_h) \times 0.5 + W_S] \qquad \text{Equation 2.7}$$

friction force on the shield body: F_b[kN],

friction coefficient (as a function of the wall friction angle): $\mu = \tan\delta$,

perimeter of the shield body: $2\pi.\,\mathrm{r}$ [m],

soil surcharge: $\mathrm{p_{vs}}$ [kN/m^2],

length of shield body: l [m],

vertical load: $\mathrm{p_v} = \mathrm{p_{vs}} + \mathrm{p_{building}} + \mathrm{p_{impossed}} \left[\frac{\mathrm{kN}}{\mathrm{m^2}}\right]$,

horizontal load: $\mathrm{p_h} = \mathrm{K_0}.\,\mathrm{p_v} \left[\frac{\mathrm{kN}}{\mathrm{m^2}}\right]$,

coefficient of earth pressure: $\mathrm{K_0}$,

self-weight of the shield: $\mathrm{W_S}$ [kN].

Other calculation also proposed by JSCE (2007) assumes two cases, the first one with no adhesion (only frictional force) and the second formula for cohesive soil[7]:

$$F_b = \mu_1 \cdot [\pi \cdot D_{TBM} \cdot L_S \cdot P_M + W_S] \quad \textit{for sandy soils} \qquad \text{Equation 2.8}$$

$$F_b = C_A \cdot \pi \cdot D_{TBM} \cdot L_S \quad \textit{for clayey soils} \qquad \text{Equation 2.9}$$

coefficient of friction between steel (shield body) and soil: μ_1,

diameters of TBM: D_{TBM} $[m]$,

shield length: L_S $[m]$,

average earth pressures acting on the shield: P_M $[kPa]$,

adhesion pressure (between the shield body and cohesive soil: C_A $[kPa]$.

Shield body and tail skin friction would be challenging to estimate, but by using an articulated shield, body estimation is simplified.

Tail skin segment interaction and injection of back-fill grout is another important issue to understand in the TBM tunnelling process. To understand these interactions, the annular-gap, steering gap, and tail-skin sealing showed in Figure 2-8 sould be investigated. The tail skin sealing (tail seal brushes) are designed to prevent the inflow of the mortar tail void into the TBM.

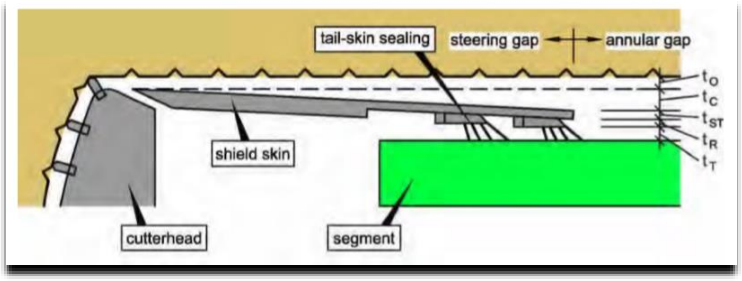

Figure 2-8 Illustration of the theoretical position of steering gap and annular gap (Wittke et al 2007) [11]

overcut: $t_o[mm]$, shield conicity: $t_c[mm]$, clearance of tail skin: $t_T[mm]$, the thickness of brush ring: $t_R[mm]$, steel thickness of tail-skin: $t_{ST}[mm]$.

A steering gap is created by overcutting the cutter head and conicity of the TBM body. A steering gap is needed for passing curves and correcting TBM deviation during the trajectory. In stable ground, the steering gap remains open. During the heading in slurry mode, the steering gap may be filled with slurry. In unstable ground, the shield skin may be bedded with the ground, and so the steering gap may be closed. Also, between the shield skin and the segmental lining, a tail-skin sealing is mounted to avoid leakage of grout into the TBM interior part. This sealing has to resist the injection pressure of the mortar (resulting from rock mass pressure and water pressure). The chambers between the brushes are filled with grease. The grease within the chambers is pressurized to avoid penetration of water or excavated ground into the sealing and to apply a counter-pressure against the grouting pressure[11].

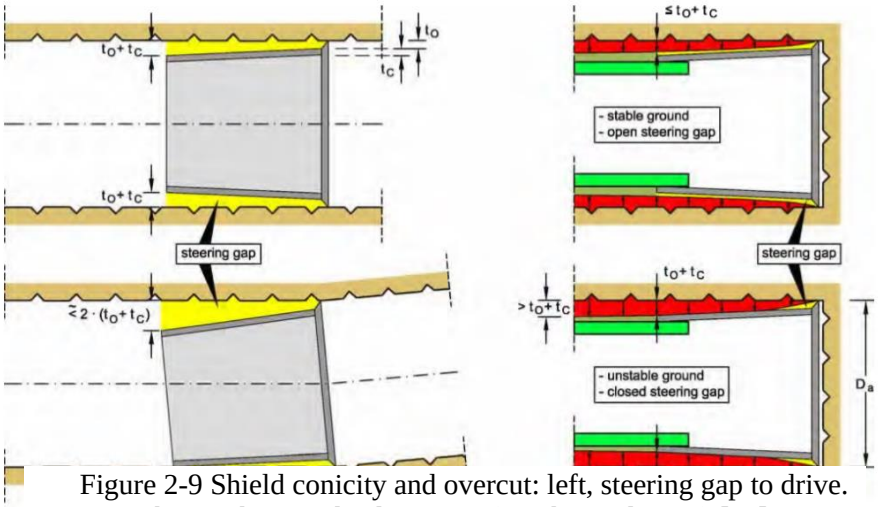

Figure 2-9 Shield conicity and overcut: left, steering gap to drive. right, Rock mass displacement (Wittke et al 2007) [11]

Bentonite and grout flow around the TBM and grout consolidation around the tunnel lining could be considered as important processes that occurred around the TBM body. Bezuijen (2007) [12] and Bezuijen and Talmon (2009) [13] evaluated the distribution of pressure and flow in the steering gap of slurry TBMs using a theoretical calculation model.

They assumed that tail void grout and bentonite slurry are both Bingham fluids and flow is managed by the fluids yield stresses and ground surrounding behave linear-elastic. If there is no flow into the steering gap, then the ground would relax onto the TBM body. If liquids flow into the gap with known pressures, the change in soil radius and, steering gap width could be calculated by the difference of soil and flow pressure.

$$\Delta\sigma = 2\frac{\Delta R}{R}G \qquad \text{Equation 2.10}$$

pressure change: $\Delta\sigma$ [kPa], radius change: ΔR [m], excavated Tunnel radius: $R[m]$,

shear modulus of the surrounding ground: G $[MPa]$.

When bentonite slurry or tail void grout flow into steering gap, their pressure decrease depends on their yield stress and gap width.

$$\Delta p = \alpha_F \frac{\Delta x}{s}\tau_\gamma \qquad \text{Equation 2.11}$$

flow pressure change: $\Delta p[kPa]$, length increment along TBM: Δx $[m]$, gap width: $s[m]$,

yield stress of the flow (bentonite or grout): $\tau_\gamma[kPa]$.

coefficient of friction between soil and bentonite or grout (could be considered 1): α_F

Utilizing these two equations, they calculated gap deformation and pressure along the length of the shield incrementally. Bezuijen (2007) [14] presents three possible flow scenarios in the steering gap, depending on the grouting and face pressures.

- Grout flows from the tail towards the face, and bentonite flows from the face towards the tail. This situation can occur when there is some volume loss in the steering gap.

- Bentonite flows from the face towards the tail, pushing the grout towards the tail. The pressure at the tail is lower than the pressure at the face. This situation cannot be continuous but can occur temporally.
- Grout flows from the tail towards the face pushing the bentonite towards the face. The pressure at the face is lower than the pressure at the tail (grout injection point).

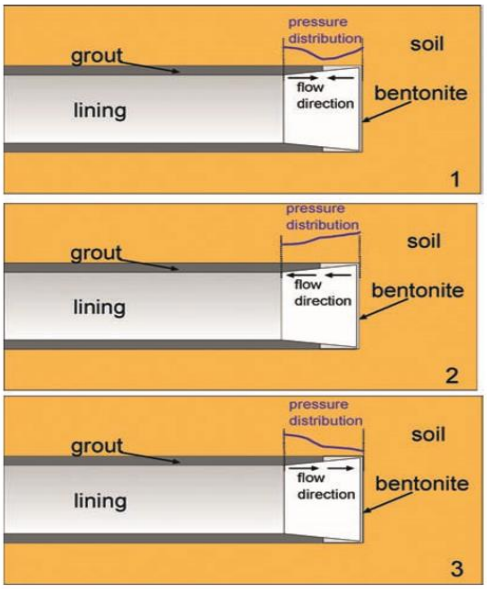

Figure 2-10 Schematic of possible flow scenarios of pressure distribution along TBM body in the steering gap [14]

The results of a 1-dimensional analytical model developed to evaluate the influence of bentonite and grout injection around a TBM and the earth pressure distribution around the TBM. This model showed the influence of flow along the TBM body. Bezuijen concluded in their study that the TBM body is partly in contact with the surrounding soil, although mainly in contact with the liquid grout. Depending on the over cutting, it may also be in contact with bentonite injected at the tunnel face. At high soil pressures and therefore, high grout pressures, this may increase the risk of deformation of the tail skin of the TBM body [14].

One of the challenges in TBM advancement is blockage of tail skin or collision of tail-skin and segments. Deformation of tail-skin leads to the tail-skin blockage or tail skin segment collision. Having a better evaluation of the process occurring around a TBM will help us avoid this problem.

2.3 TBM thrust force, cutter head torque and power evaluation

2.3.1 Thrust force estimation

In TBM tunnelling, the soft ground evaluation and estimation of thrust force have theoretical and operational importance. JSCE proposed five components for an assessment of thrust force.

$$F_{Th} = F_1 + F_2 + F_3 + F_4 + F_5 \qquad \text{Equation 2.12}$$

Total thrust force (normal) in the soft ground TBMs: F_{Th}[kN],

Thrust force to overcome friction (adhesion) between shield and ground: F_1[kN],

Thrust force to overcome the chamber pressure acting on bulkhead: F_2[kN],

Thrust force required to overcome the force caused by steering in curve alignments: F_3[kN],

Thrust force to overcome the friction interaction between segments and tail seal: F_4[kN],

Thrust for to overcome backup train traction force (hauling force of trailing): F_5[kN],

In 2012 Copur added the thrust force to overcome the normal penetration force of cutting tools (F_6).

$$F_{Th} = F_1 + F_2 + F_3 + F_4 + F_5 + F_6 \qquad \text{Equation 2.13}$$

F_1 could be calculated based on equations (8) and (9). P_M is considered to be averages of vertical earth pressure acting on the crown and horizontal earth pressure acting on tunnel spring line (suggested for micro-tunnelling application)[15].

$$P_M = \frac{\sigma_v + \sigma_h}{2} \qquad \text{Equation 2.14}$$

Vertical earth pressure acting at rest on the crown: σ_v $[kPa]$,

Horizontal earth pressure at rest acting on tunnel spring line: σ_h $[kPa]$.

JSCE proposed theoretical estimation for F_2 , F_3 ,F_4 , F_5 [7] :

$$F_2 = \sigma_T \cdot \frac{\pi \cdot D_{\mathrm{TBM}}^2}{4} \qquad \text{Equation 2.15}$$

Face pressure acting on excavation chamber: $\sigma_T[kPa]$,

$$F_3 = \mu_1 \cdot D_{\mathrm{TBM}} \cdot \frac{L_S}{2} \cdot \frac{q}{2} \qquad \text{Equation 2.16}$$

Coefficient of friction between steel and soil: μ_1,

The pressure imposed by direction change of a TBM (assumed to be equal to $\sigma_h \; as \; a$ max): q,

TBM length: L_S $[m]$.

$$F_4 = \mu_2 \cdot \pi \cdot D_0 \cdot L_{SC} \cdot P_M \qquad \text{Equation 2.17}$$

Coefficient of friction between seals and segment: $\mu_{2,}$

Length of contact between segment and tail seal: L_{SC} $[m]$,

$$F_5 = \mu_3 \cdot G \qquad \text{Equation 2.18}$$

Weight of back-up train: G,

Coefficient of friction between wheel and back-up train: μ_3,

2.3.2 TBM cutter head torque and power estimation

Cutter head torque estimation in the soft ground requires many details from TBM specifications. Most of the time, these properties would be unknown during machine selection. JSCE 2016 suggested six torque components for estimation of the total cutter head torque[7].

$$Tq = Tq_1 + Tq_2 + Tq_3 + Tq_4 + Tq_5 + Tq_6$$ Equation 2.19

Total cutter head torque for the soft ground TBMs: Tq [kN.m],

Torque to overcome the cutting resistance of the soil: Tq_1,

Torque to overcome the frictional resistance of the soil: Tq_2,

Torque to overcome the resistance of the soil mixing and stirring: Tq_3,

Torque to overcome the resistance of the main bearing: Tq_4,

Torque to overcome the frictional resistance of the cutter drive unite seal: Tq_5,

Torque to overcome mechanical loses in the reduction gears: Tq_6.

In 1999 Bilgin et al. proposed a theoretical calculation for cutter head torque as follow[16]:

$$T = \frac{N_C \cdot F_R \cdot D_{TBM} \cdot f_L}{4}$$ Equation 2.20

Cutter head torque: T $[kN.m]$,

The coefficient for frictional losses: f_L,

Mean rolling force for one cutter: F_R $[kN]$,

The diameter of the cutter head: D_{TBM} $[m]$,

The number of cutters in a TBM: N_C.

An empirical model also proposed by JSCE, 2016 for estimation of cutter head torque:

$$Tq = \alpha \cdot D_{\mathrm{TBM}}^3$$ Equation 2.21

Torque factor (suggested between 10 to 25 for EPB and 20 for SPB): α,

For rocks and gravel this range could exceed.

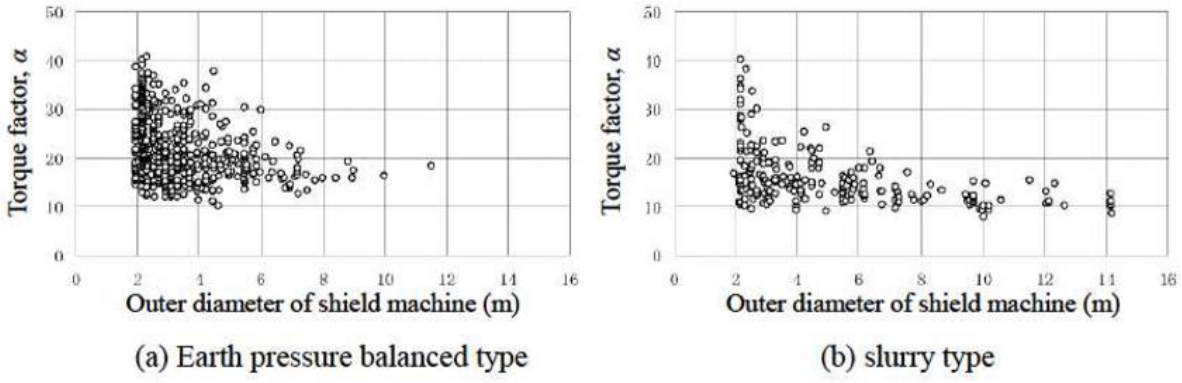

Figure 2-11 torque factor evaluation proposed base on diameters for closed TBM (JSCE-2006) [7]

Cutterhead power requirement of TBM for soft ground could be estimated by[17]:

$$P_{\text{cutterhead}} = 2\pi/60 \cdot Tq \cdot \text{RPM} \qquad \text{Equation 2.22}$$

Cutter head power of TBM: $P_{\text{cutterhead}}$ $[kW]$,

Total cutter head torque: Tq $[kN.m]$,

Cutterhead rotation speed (revolution per second): RPM/60.

There is another approach for the calculation of required torque. Wittke et al. [11] discussed in detail the required torque for a closed mode TBM. In this type of TBM, there is the resisting torque resulting from the excavation tools and the resisting torque resulting from the slurry or earth mud. Required torque for driving a cutter head has to be more significant than resisting torque from excavation tools and the earth mud.

The shear resistance of excavation material in front of the cutter head and the chamber of excavation depends on geomechanical characteristics of the soil, rock and soil/water ratio and the conditioning agent. Witkke et al. investigated two approaches to evaluate the shear strength of excavated materials. Bingham fluid approach described by flow limit τ_0 and the dynamic viscosity η. The second approach is the Mohr-Coulomb approach, shear strength described by friction angle φ and cohesion c [11].

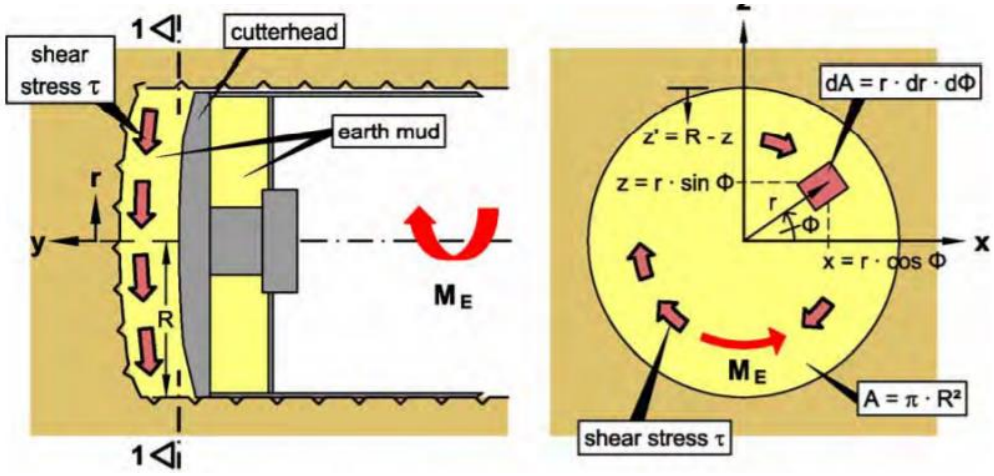

Figure 2-12 Resisting torque evaluation created by excavated material interaction with cutter head (Wittke et al. 2007) [11]

Based on the first approach required, torque is calculated as follow:

$$M_E = \int_A r \cdot \tau \cdot dA \quad \& \quad \tau = \tau_0 + \eta \cdot \left|\frac{\partial v}{\partial y}\right| = \tau_0 + \eta . \frac{\omega}{d_E} . r \qquad \text{Equation 2.23}$$

The absolute value of the gradient of the shear velocity in the direction of TBM advance: $\left|\frac{\partial v}{\partial y}\right|$

Angular velocity of cutter head: ω,

The thickness of the area in front of the cutter head: d_E,

Resisting torque resulting from slurry and earth: M_E.

$$M_E = \iint_{\phi=0, r=0}^{2\pi\, R} r \cdot \left(\tau_0 + \eta \cdot \frac{\omega}{d_E} \cdot r\right) \cdot r \cdot dr \cdot d\phi \qquad \text{Equation 2.24}$$

$$M_E = \frac{2}{3} \cdot A \cdot R \cdot (\tau_0 + \frac{3}{4} \cdot \eta \cdot \frac{\omega}{d_E} \cdot R) \qquad \text{Equation 2.25}$$

By using the Mohr-Coulomb approach, shear resistance is calculated as follow:

$$\tau = p_s \cdot \tan\varphi + c \quad \& \quad \mathrm{p_s}(\mathrm{z}') = \mathrm{p_{so}} + \mathrm{Y_E} \cdot \mathrm{z}' \qquad \text{Equation 2.26}$$

Supporting pressure on the face: p_s,

The angle of friction of excavated earth: φ,

The cohesion of excavated earth: c,

Supporting pressure at the crown level: $\mathrm{p_{so}}$,

Unite weight of excavated earth: $\mathrm{Y_E}$.

$$M_E = \iint_{\phi=0, r=0}^{2\pi\, R} r^2 \cdot [c + (p_{so} + \gamma_E \cdot (R - r \cdot \sin\ \varphi)) \cdot \tan\ \varphi] \cdot dr \cdot d\phi \qquad \text{Equation 2.27}$$

After the calculation of integrals, the required torque to overcome shear resistance of excavated materials is calculated as follow:

$$M_E = \frac{2}{3} \cdot A \cdot R \cdot ((p_{so} + Y_E \cdot R) \cdot \tan\ \varphi + c) \qquad \text{Equation 2.28}$$

2.4 General comparison of two models for TBM behaviour evaluation

In 2002 Sugimoto et al. [18] developed a theoretical dynamic model of the load acting on the TBM body during excavation. In this model, five main forces are considered: force due to the self-weight of the machine (f_1), the force on the shield tail (f_2), the force due to the jack thrust (f_3), the force acting at the face (f_4), and force acting on the shield periphery (f_5). Their model is a function of the TBM behaviour, TBM operations and ground properties. TBM operations signify operational control of TBM such as confining pressure and thrust force of cylinders and moment of thrust cylinders. The TBM behaviour shows deviation and rotation of the TBM thorough excavation. The ground properties in this model represent frictional parameters, coefficients of earth pressures and coefficient of ground reaction.

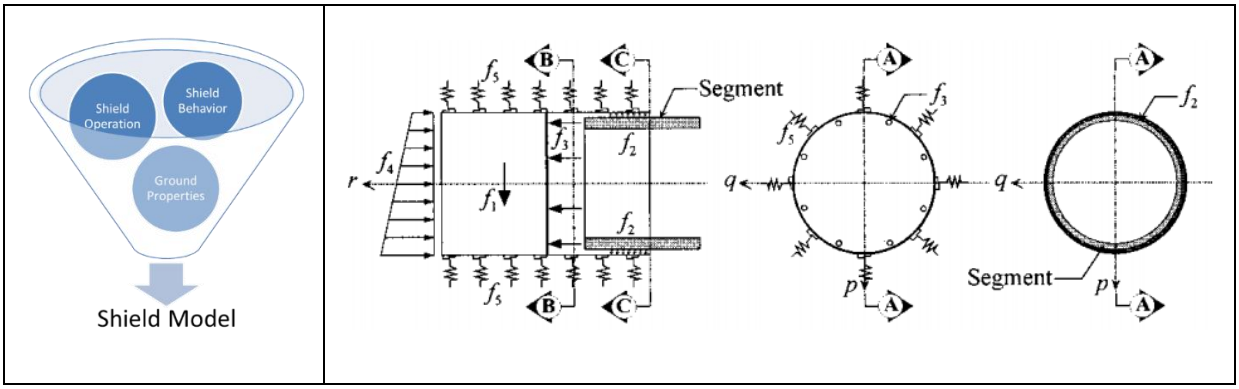

Figure 2-13 left: configuration of load model, right: schematic of model proposed for evaluation of acting load on a shield (Sugimoto et al. .2002)[18]

Their study concluded the following results:

- Ground displacement (ground reaction) was the most crucial factor in TBM behaviour.
- The tail clearance (especially tail skin contact with the segment in the brush section) influences TBM behaviour in curve alignment. The decrease of the tail clearance and the increase of the spring constant of the brush limit the TBM rotation.
- The cutter face rotation direction influences the TBM behaviour when there is unsymmetrical face pressure.

- The thrust cylinders influence TBM behaviour. Face pressure is highly sensitive to the TBM advance speed. The cylinder moment is effective for rotating the TBM in soft ground where the ground reaction in the passive state is small.
- The acting point of force on the cutter head influences the TBM behaviour.

The Bouygues TP Price and Design Bureau proposed a calculation method for estimating the total thrust force required for TBM advancement based on their experiences and expertise. Figure 2-14 represents the comparison of components for two different total thrust force estimations proposed by Bouygues TP and Sugimoto et al. [18].

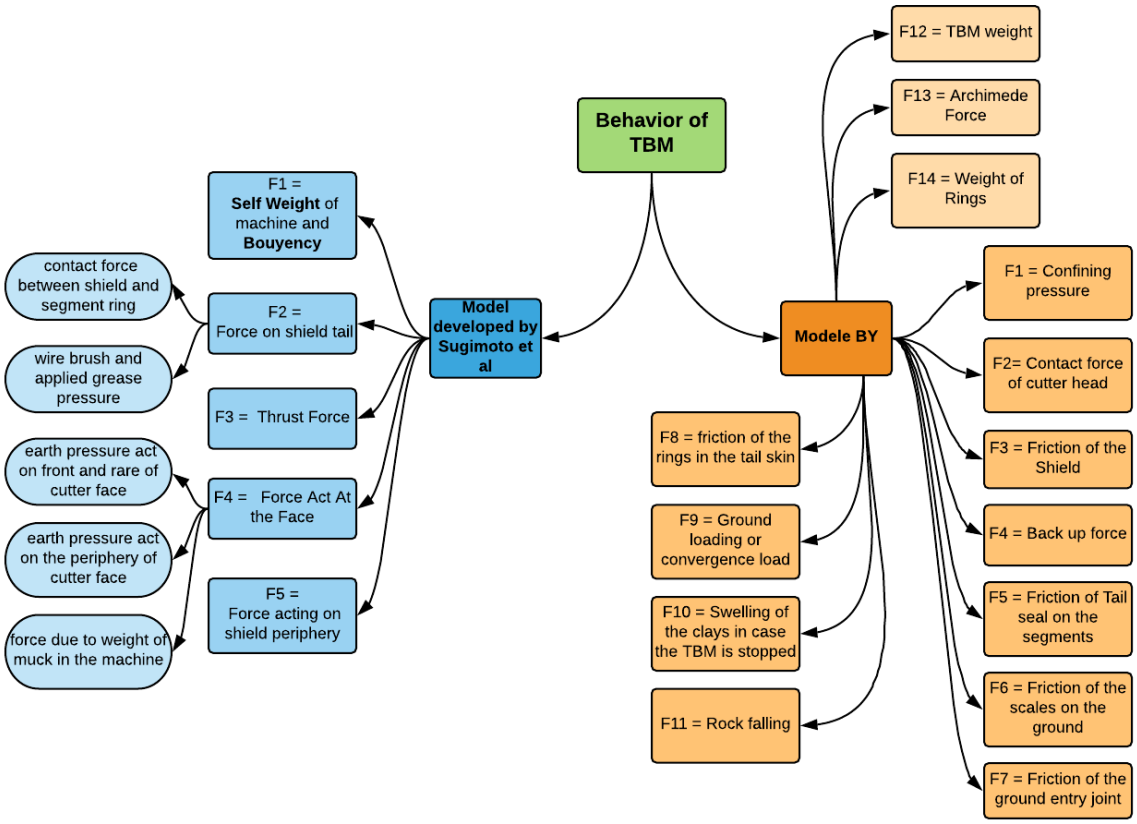

Figure 2-14 Comparison of components of JSCE model and Bouygues TP thrust force estimation components

2.5 Conclusion

TBM tunnelling in soft ground has different challenges from geological complexities and uncertainties to safety sensibilities in underground development in an urban area. TBM design and modelling is essential to purify our understanding of the structural design of TBMs, and the interactions during TBM tunnelling. There are various methods such as analytical (theoretical), empirical and numerical methods to optimize TBM design and operation.

Analytical and theoretical (mathematical) models have many effects on TBM behaviour evaluation, assessment and modelling. As a TBM is a huge machine, there are different analytical and theoretical studies to explain the interaction of different parts of TBM. In this study, the summery of some the previous studies is presented to observe in detail some of the main issues and challenges encountered in two main parts of TBMs, the front body and main body.

Assessment of force exerted on TBM during excavation and estimation of required total thrust force and required torque is significant for every stage of TBM operation. In this chapter, different analytical and theoretical calculations proposed by researchers and tunnelling experts were observed for the evaluation of force exerted on TBM and evaluation of required thrust force and cutter head torque.

In the next chapter, these analytical and theoretical calculations will be used for the evaluation of operational data captured during excavation. A TBM has different internal and external interactions. TBM interactions and their complexity due to geological uncertainties create problems that cannot be considered in a unique model. The data captured during excavation will be used to evaluate better and estimate more accurately TBM operations. The captured data will be served to solve the operational problems and to optimize TBM operations such as steering.

3. Data-Driven Methods in TBM Tunnelling Process Evaluation

Chapter summary:

This chapter will provide a brief introduction to data acquisition set up in a TBM. Exploratory Data Analysis will be presented for different TBM operational data, such as excavation chamber pressure, thrust cylinders pressure, injection of mortar and grease pressure and TBM trajectory characterization data (the parameters are investigated based on evaluation of the previous studies, researches and discussions with TBM engineers and experts). Besides, the calculation of the centre of thrust force, centre of moment arm and inclination of cutter head are presented as parameters which will be used in data-driven modelling for optimization and modelling of TBM operation. The visualization techniques are used to find the general association between TBM parameters. Visualization techniques will give us better interpretation capabilities. It will be an essential step to evaluate the TBM parameter and find a meaningful association and probable physical explanation for the phenomena which occurred during a TBM operation. Visualization techniques will be essential and efficient for both pre-processing and post-processing evaluations.

3.1 Introduction

Development of new technologies and tools such as data acquisition systems, vast new-designed sensors, computational techniques and tools facilitate the process of investigation and provide more data for different operations. This ability to collect data help experts and engineers to deepen their insight into the different aspects of problems and improve their evaluations and design. In 2013 Sukumar et al. stated that within the last few years we had seen a paradigm shift in the knowledge discovery workflow[19]. They displayed this shift as moving from the data-to-decision-process triangle to a constantly-at-work gear system as illustrated in Figure 3-1.

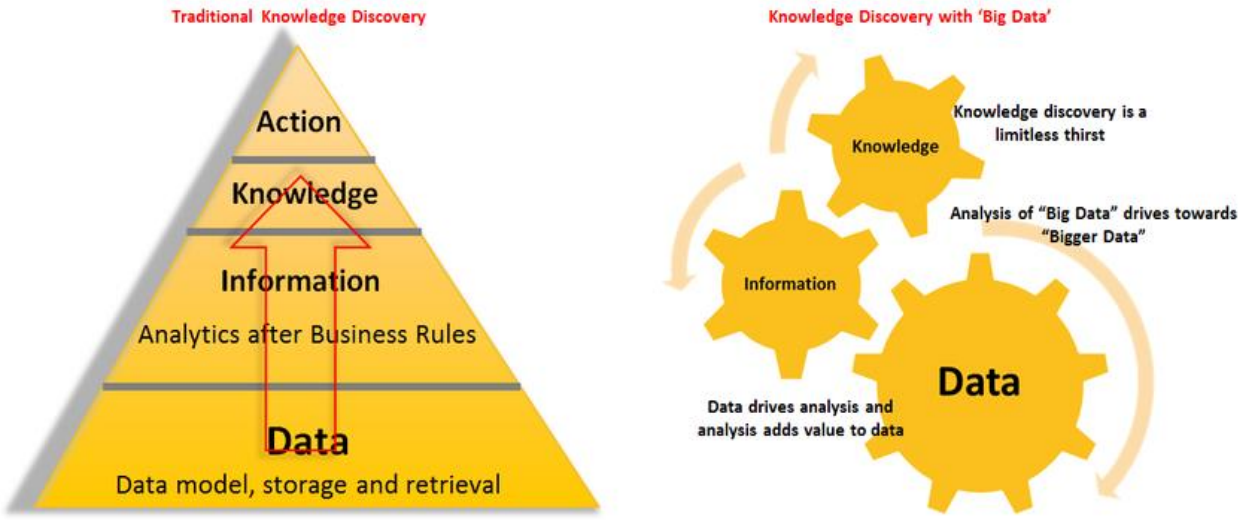

Figure 3-1 Evolution of knowledge discovery in the era of data [19]

Access to a vast amount of data will lead to the forced paradigm of science which is data-driven discovery. Data-driven approaches would improve our analytical capabilities. For 5000 years, the human-being built tunnels for different purposes. In the 19th-century, shield tunnelling was invented for excavation in the loose ground and underwater condition. During the last two centuries, various methods from experimental and empirical approaches to theoretical and numerical methods have been used to increase and deepen our knowledge in tunnelling. Figure 3-2 shows the general concept of the paradigm of science for tunnelling. This concept is adopted from recent approaches of material science[20].

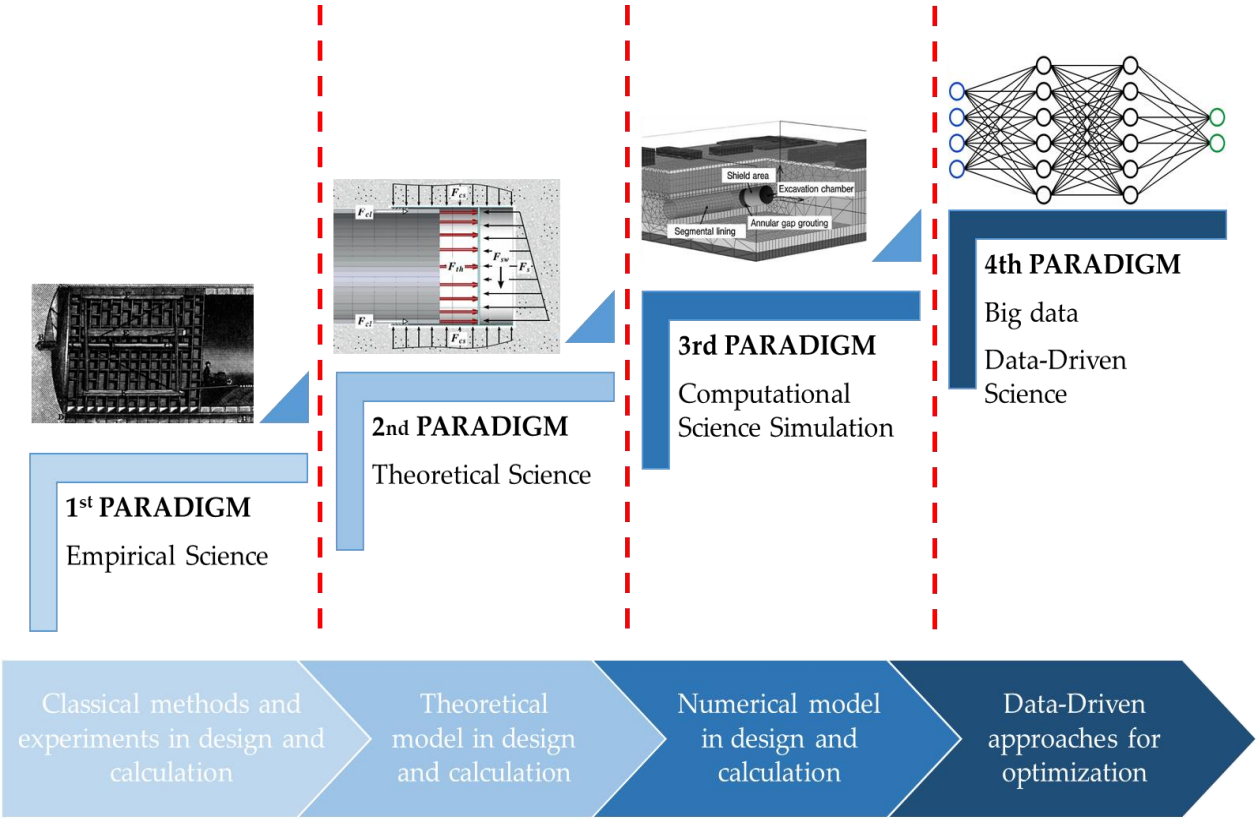

Figure 3-2 Potential paradigm of science for tunneling process optimization

TBM tunnelling generates a large amount of data. This data is helpful for different purposes such as, identifying subprocess control and evaluations, finding underlying causes of breakdowns, to implementing corrective decisions and predictive modelling. TBM data acquisition system compiles information about TBM excavation, lining installation, muck extraction, ground control investigation and logistic, while providing continuous display and visual representation of measured data. There are three main operating phases for TBMs, advance, ring built and standstill. Some of the most common graphs for data representation during TBM operation are advance speed of TBM, thrust force, cutter head torque, confining pressure in excavation chamber, cylinders pressure and extensions and fluid injection pressure and volumes. Despite many facilities and development of these systems, still, TBMs face some operational issues during excavation.

Nowadays, data usage is widespread and efficient to solve complex issues and problems in different sectors from health to financial and industrial sectors. Due to development and advances in computational capabilities, advances in various mathematical and statistical algorithms (data-driven approaches), researchers and engineers can improve their analysis by using data-driven

strategies. Nowadays Tunnel engineers have access to an enormous amount of data for the different operations of TBM. All operations performed by TBM recorded and documented allow engineers to have real-time analysis and evaluation. The other approach of using these significant volumes of data would be the optimization of TBM operation. In this study, operational parameters of TBM and guiding parameters is mainly investigated.

3.2 Instrumentation and data acquisition system in a TBM

3.2.1 Instrumentation

There are different sensors in a TBM. Sensors to capture confining pressure, hydraulic pressure sensors, the extension sensors to measure cylinders elongation, temperature sensors, an injection pressure sensor to measure fluid injection pressure and sensors to measure volume injection (Figure 3-3).

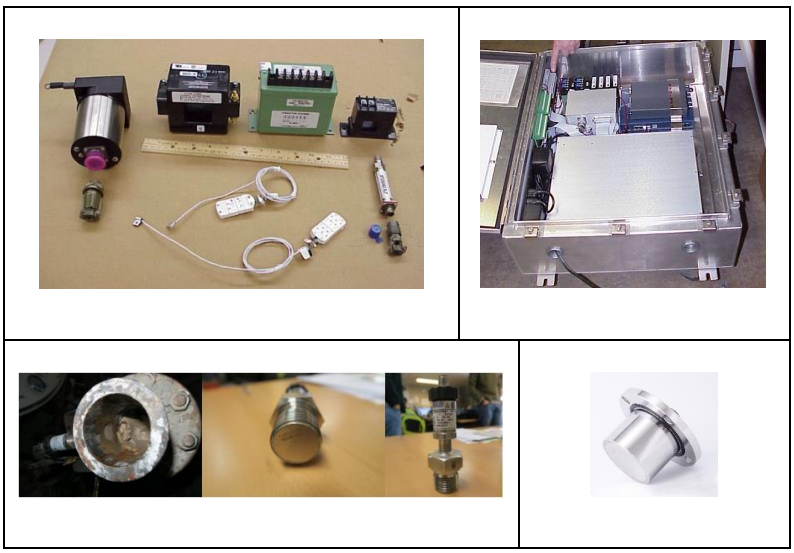

Figure 3-3 Example of sensors in a TBM data capturing system

3.2.2 Data monitoring general setup

Another essential issue in TBM data management is the general setup of a data monitoring system. Figure 3-4 provides data monitoring system (for different data captured during TBM tunnelling) proposed by Tunnelsoft. It shows different types of measurable data with varying aims

for evaluation of ground settlement and TBM operational parameters representation and interpretation.

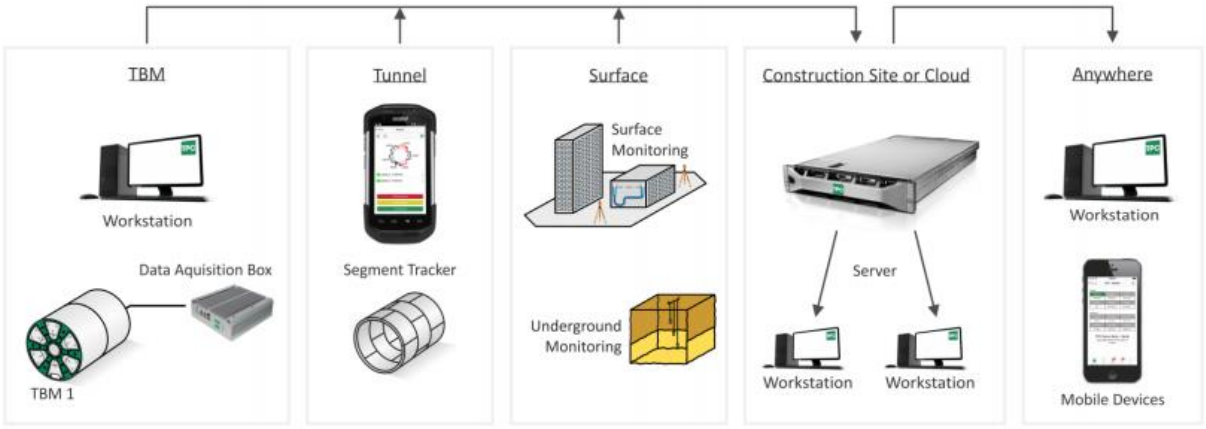

Figure 3-4 Schematic of new data monitoring set up [tunnelsoft.com]

3.2.3 **Case studies general information and data volume**

During this research, the data came from the Tunnel Lab project database. Table 3-1 provides general information about the projects used in our studies. All the data assessment tasks realized came from these two projects. During these two projects, different mixed shields are used for excavation of the 11 km tunnel. The configurations of these machines are different (articulated shield and cutter head). The TBM for the tramway project in Nice has articulation cylinders in the tail skin section and cutter dead displacement cylinders. The TBM for the TMCLK project has only cutter head displacement cylinders.

In this chapter, the results and studies on data from the Tramway Nice project in the South of France were presented and discussed. The same investigation and observation were implemented for the other two machine's (TMCLK project) data.

The Tramway Nice project was carried out between the Var sedimentary basin in the West and the mountainous area of the Alpine formation in the East part. The bedrock is strongly tectonized and presents substantial irregularity. It is covered by alluvial formation showing a considerable heterogeneity. The specificity of the encountered formation is that it has a heterogeneous behaviour with strong anisotropy and is characterized by an irregular succession of rock limestone and alluvial soil layers.

Table 3-1Characteristics of the case studies (the TBM used for the studies during this research project)

			
Project	***Nice (S955)***	***TMCLK (S882)***	***TMCLK (S881)***
Tunnel type	Rail-way	Road-way	Road-way
Tunnel length	2900m	4160	4160
TBM type	SPB (Mixed Shield)	SPB (Mixed Shield)	SPB (Mixed Shield)
Cutter head diameter	9680mm	14000mm	14000mm
TBM body front diameter	9640mm	13950mm	13950mm
Tail skin diameter	9610mm	13910mm	13910mm
Nominal advance speed	60mm/min	60mm/min	60mm/min
TBM weight (TBM + Back-up train)	872t+475t (1347t)	NA	NA
TBM length	10330mm	15125mm	15125mm
Number of thrust force cylinders	30(15*2)	36(18*2)	36(18*2)
Number of active articulation cylinders	NA	NA	NA
Number of articulation cylinders (tail skin)	15	NA	NA
Displacement cylinders	6	15+3	15+3

Table 3- 2 represents the total size and volume of the operational data frame that is used for our studies and analysis. The volume of data is so large which generate challenges for manipulation and analysis.

Table 3-2 Total data volume of the case studies, investigated during this project

Project	Data Size				
	Raw Numbers		Column Numbers		Volume
	Total	DataFrame	Total	DataFrame	Total
Nice Tramway Tunnel	49,469,046	7,455,369	993	102	250 GB
TMCLK Tunnel	60,492,586	12,604,781	1774	161	460 GB

3.3 Exploratory Data Analysis of TBM data

3.3.1 The general concept of exploratory data analysis

Data-Driven approaches would be a practical skill or competence to optimize previous development and help us find better solutions and an explanation for complex problems. A significant challenge of data-driven approaches is to connect raw data into actionable information. A data-driven essential step is Exploratory Data Analysis. EDA is detective work--numerical detective work-- or counting detective work--or graphical detective work [21]. EDA may request a significant amount of time and efforts. Still, mostly it is an investment in a data-driven approach to create a better understanding of the problem and to present a better model. Key drivers of this discipline are the rapid development of new technology, access to a more significant volume of data, and the greater use of quantitative analysis in a variety of fields [22].

Performing EDA, manipulating data and cleaning the data are not only essential steps but also an excellent opportunity to lay the foundation for a robust statistical model (machine learning and deep learning model). EDA reveals insight on data and different essential interaction in TBM process; it helps tunnel engineers and experts explore relations or correlations between TBM operational parameters and its steering parameters. TBM data used for this study is composed of two types of structured data, most of the TBM's data in this study is numeric, and parts of data are categorical.

All the visualizations (charts) are developed by python visualization libraries such as Matplotlib, Seaborn and Plotly. Matplotlib is a 2D graphics package used in Python for application development, interactive scripting, and publication-quality image generation across user interfaces and operating systems[23]. Plotly's Python graphing library makes interactive, publication-quality graphs[24]. For the scientific computation and manipulation of data during this study, python scientific computation libraries such as SciPy, NumPy and Panadas are used. SciPy is an open-source scientific computing library for the Python programming language[25]. NumPy is the fundamental package for scientific computing with Python[26]. Pandas is a library which aims to facilitate working with data sets and to provide a set of fundamental building blocks for implementing statistical models[27].

3.3.2 **TBM parameters flowchart proposed for evaluation of TBM behaviour**

Based on the principle operations of TBM, the essential parameters of a TBM were investigated. Choosing parameters is based on the provided state of the art in chapter one and interviews and discussions with tunnel experts and TBM pilots. The interviews allowed to understand and find the operational parameters with more influence on TBM interactions.

During the excavation of a TBM and installation of the segment, various parameters were investigated in detail to give us a better evaluation of TBM behaviour in straight advancement or curve advancement. In this study, this parameter was divided to five leading groups. 1- Lining position 2- Machine position 3-1 Force acting on TBM 3-2 Operational parameters 4- Ground characteristics 5- Over-cut (over-excavation).

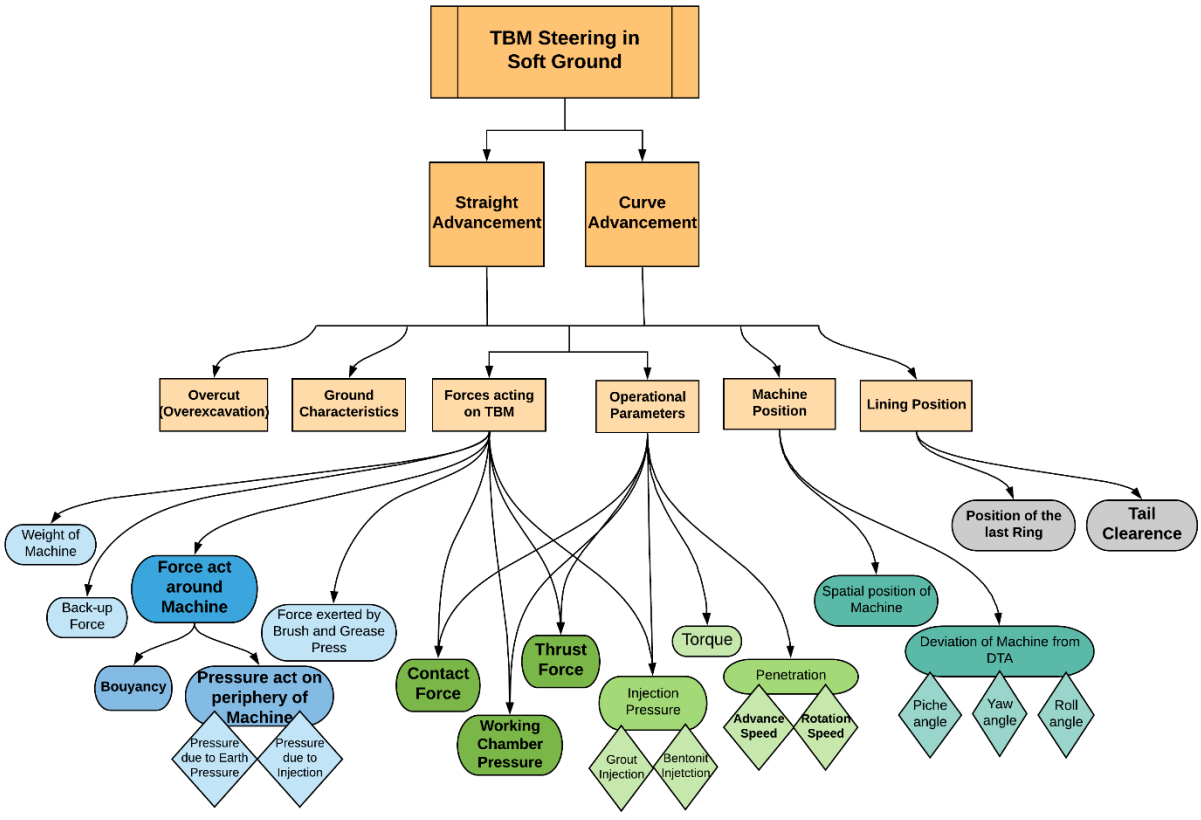

Figure 3-5 Flowchart of parameters required for evaluation of TBM interaction during advancement

Availability of the data for all these parameters has its challenges and special procedures. Some of the parameters proposed are calculated based on theoretical methods. Ground properties

(geological and geomechanical characterization) have various data resources and types. These properties include laboratory test results, in-situ test and borehole results and geological plans (which could be assumed as the resume of geological expertise). The guiding system of TBM could calculate guiding parameters (position and localization of machine and lining). Operational parameters of TBM are captured and evaluated by TBM data acquisition systems.

3.4 EDA of TBM operational data

Based on benchmarking of the theoretical and analytical model provided for design and modelling of TBMs and discussion with Tunnel engineers, experts and pilots of TBM of Bouygues TP the operational and guiding parameters for an EDA were chosen. The TBM schematics and its configuration for each part are shown in Figure 3-6. During this study, the data from TBM S955 (Nice Tramway project) was used.

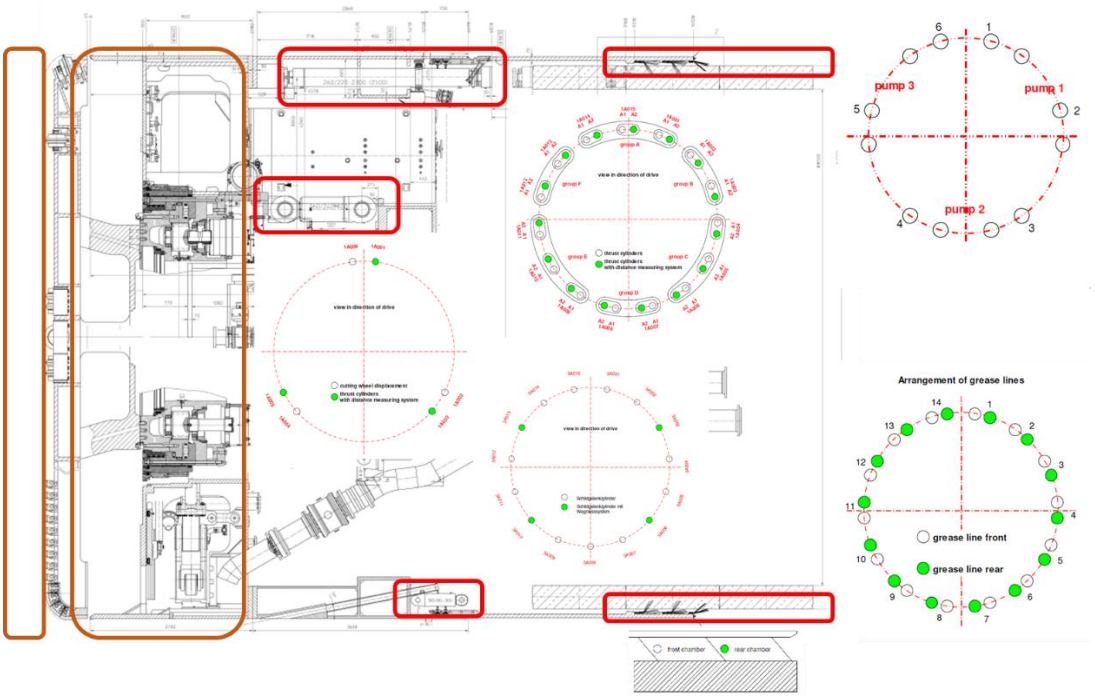

Figure 3-6 Longitudinal section of Nice Tramway TBM configuration details (courtesy of Bouygues TP)

Parameters include pressures the captured in excavation chamber (confining pressure), contact force calculated based on displacement cylinders of the cutter head, mortar injection pressure, grease injection pressure and the thrust cylinders pressures.

Thrust cylinders have an essential role in TBM advancement and behaviour. Thrust cylinders provide total thrust force for the advancement of the TBM and are used to pilot TBMs in different alignment (curve or straight or correction of a TBM trajectory).

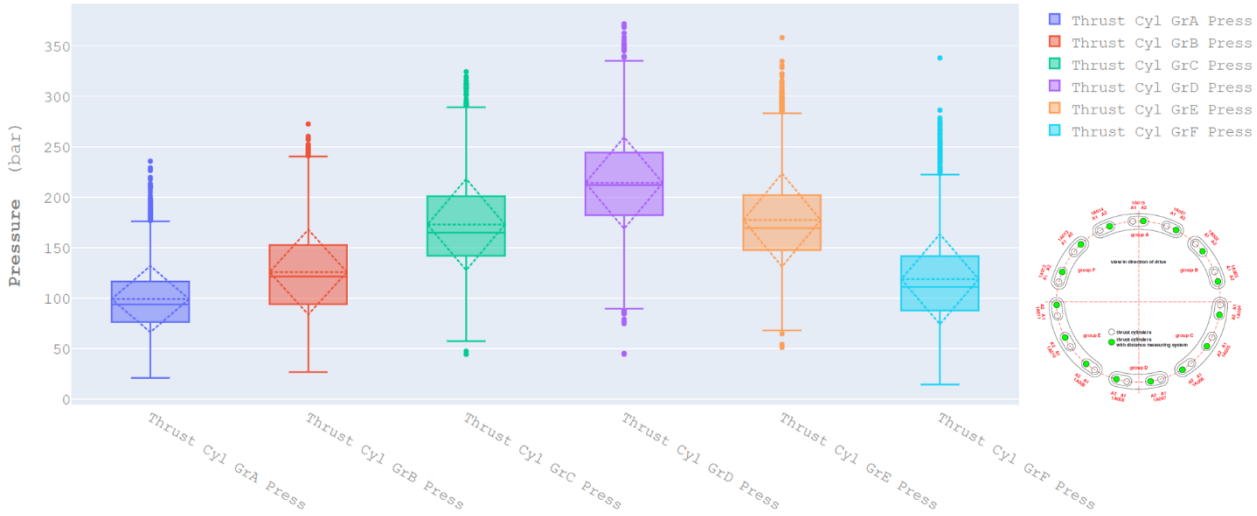

Figure 3-7 Distribution of pressure for each group of thrust cylinders (box plot)

In Figure 3-7, the box plot of thrust cylinders for each group of cylinders is represented. For this example, there are six groups of cylinders. Box plot is usually used to show the distribution of data, an indication of how the values in the data are spread out. Box plots have a significant advantage when user wants to compare distribution between many groups of data.

Box plot would give us the capability to display the standardized distribution of data based on five values (minimum, first quartile, median, third quartile, and maximum). However, the average and standard deviation of data are also accessible in the interactive visualizations (developed by Plotly library).

- Median (50th Percentile): the middle value of the dataset.
- The first quartile (25th Percentile): the middle number between the smallest number (not the minimum) and the median of the dataset.
- The third quartile (Q3/75th Percentile): the middle value between the median and the highest value (not the maximum) of the dataset.
- Interquartile range (IQR): 25th to the 75th percentile.

As shown in Figure 3-8, more significant values for three groups of cylinders are identified. These values are located in the lower part of the machine; this distribution of the cylinders pressures is utterly reasonable with the excavation procedure.

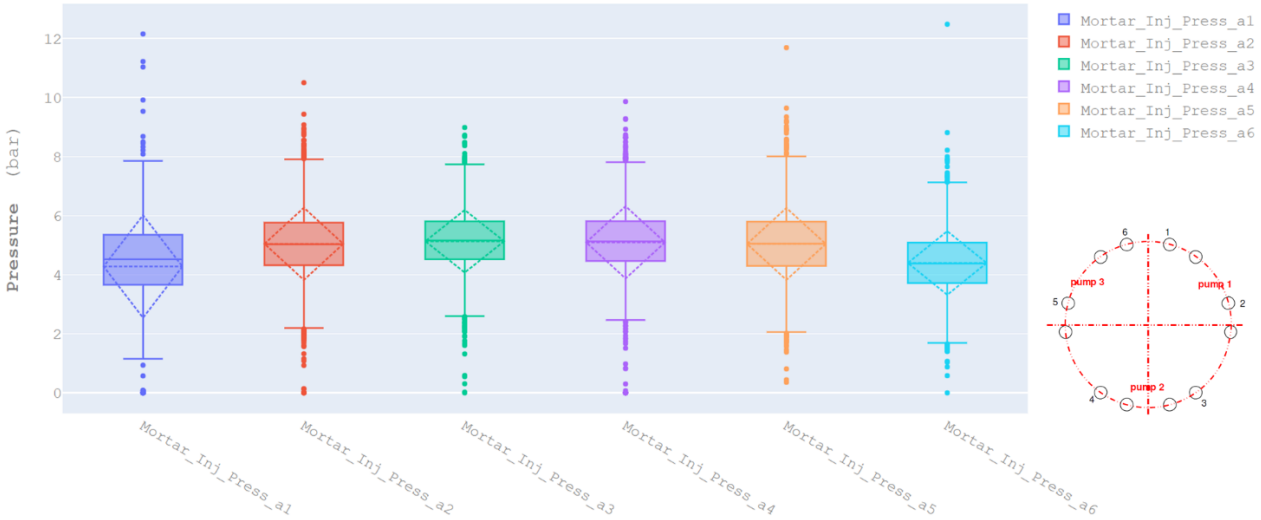

Figure 3-8 Distribution of mortar injection lines pressure (box plot)

Figure 3-8 provides the configuration of mortar injection lines. Six groups of injection line are present. The box plot shows us that the average value of mortar injection for line 2-3-4 and 5 are similar and bigger than line 1 and 6.

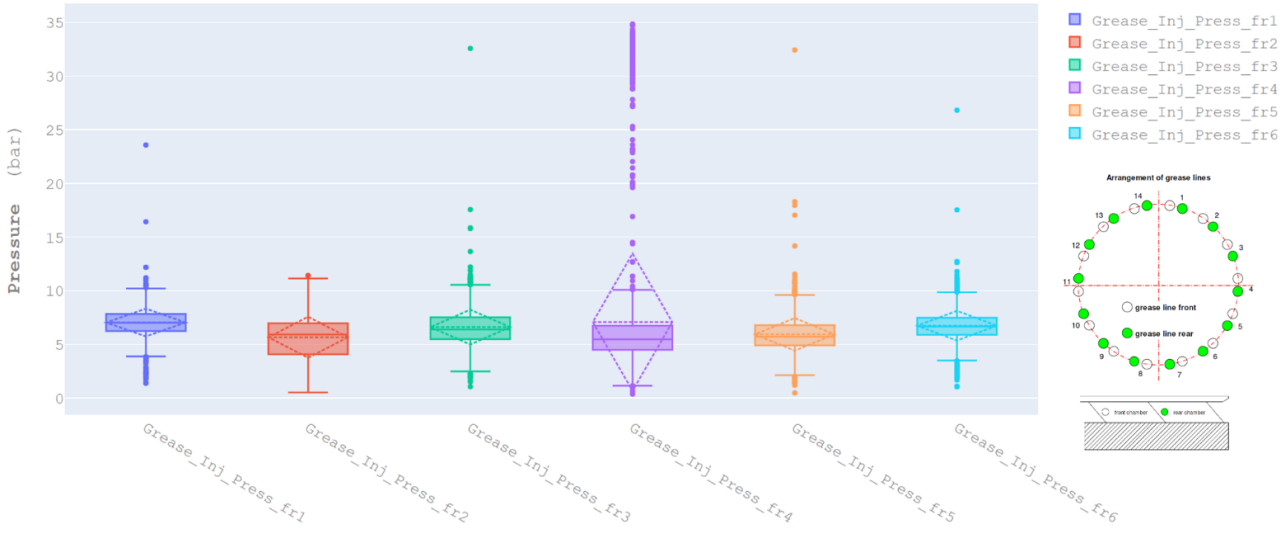

Figure 3-9 Distribution of the grease injection lines pressure (box plot)

Figure 3-9 represents the distribution of grease injection (tail sealing pressure) in the front line. As we can see in this case study, two injection lines (front and rear) with 14 injection tubes are present. These lines were divided into two six groups on injection lines, to improve the investigation.

Group 4 (average of line 7 and 8) was observed with an abnormal distribution, but the average value of different groups had the same range. This abnormal situation was considered in our observation for future study and modelling.

3.4.1 **EDA of excavation chamber pressure and tail sealing pressure**

As observed in the first chapter, during shield tunnelling, one of the main challenges is the evaluation and calculation of safe and optimal confining pressure. EDA was done on the data captured in the excavation chamber during the excavation phase. The exploratory evaluation of the excavation chamber pressure gave us a better capability to observe the abnormal situation during excavation and to improve the use of this data for future modelling. For each machine, three to five pressure sensors were installed in confining pressure. These sensors gave a real-time confining pressure fluctuation. Confining pressure is an important factor in evaluating coherence of TBM operations. Also, it is one of the significant parameters for data-driven modelling and TBM assessment process.

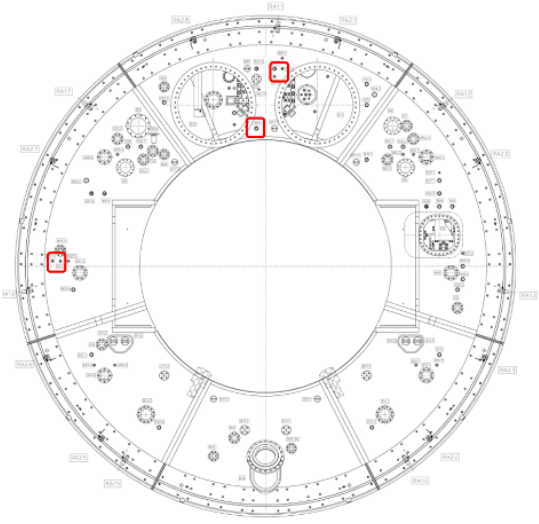

Figure 3-10 transversal section of TBM bulk head configuration,
position of pressure sensors (courtesy of Bouygues TP)

Figure 3-10 shows the location of pressure sensors in the axis and crown of the excavation chamber for the Nice Tramway TBM. Sensors measured bubble pressure and earth pressure in the excavation chamber. Figure 3-11 illustrates the distribution of confining pressure captured by three sensors and an average pressure of tail seal grease injection.

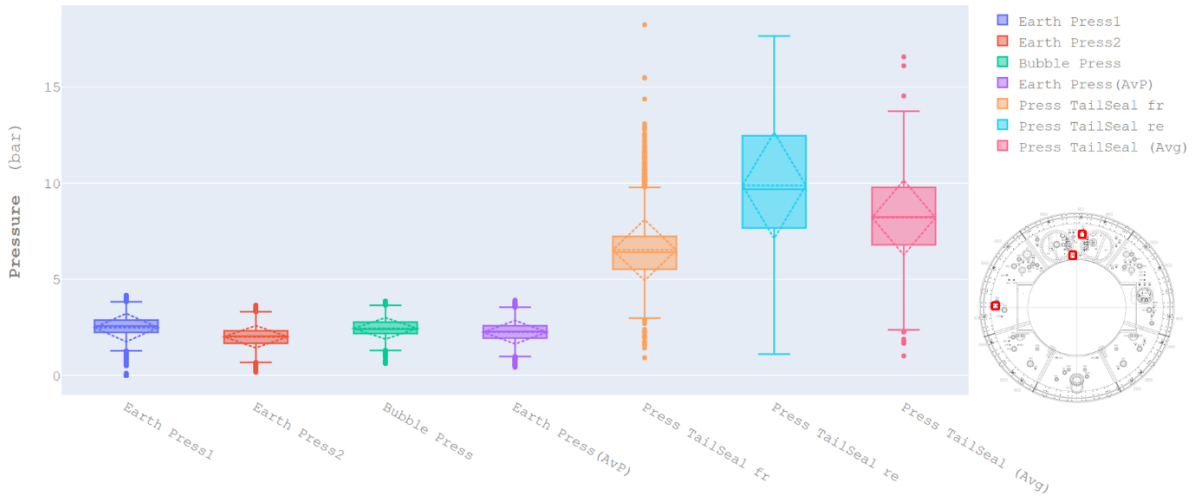

Figure 3-11 Distribution of confining pressure captured by 3 sensors and average of tail seal grease injection pressure (box plot)

Earth pressure is measured in two locations (axis and crown) of the excavation chamber. Bubble pressure is measured at the crown of the excavation chamber. In Figure 3-11, Earth Press1 shows the distribution of pressure at the axis of the tunnel; Earth Press2 is the pressure at the crown and the Bubble Press represents pressure of compressed air in the mixed shield. Earth Press (AvP) is the average value of Earth Press1&2.

The Press TailSeal (front and rear) shows the distribution of grease injection pressure between the tail skin and the segments for tail sealing of TBMs. This pressure is measured at the beginning of the tail skin structure. A Press TailSeal shows the average value for both grease pressure at the front and at the rear line of injection. The distribution of earth pressure and grease injection pressure was observed in the same plot as these two parameters are used for the evaluation of the steel brush, segment interaction and estimation of friction force between the steel brush and the segments.

Figure 3-12 displays the line plot of confining pressure and trajectory characteristics (evolution of altitude and slope) variation for the advancement of tunnel per metre. Confining pressure shows

an obvious correlation with the altitude changes; the Figure 3-12 shows the evolution of confining pressure with altitude. Also, changes were observed in the confining pressure (both earth pressure and bubble pressure) within the slope of trajectory.

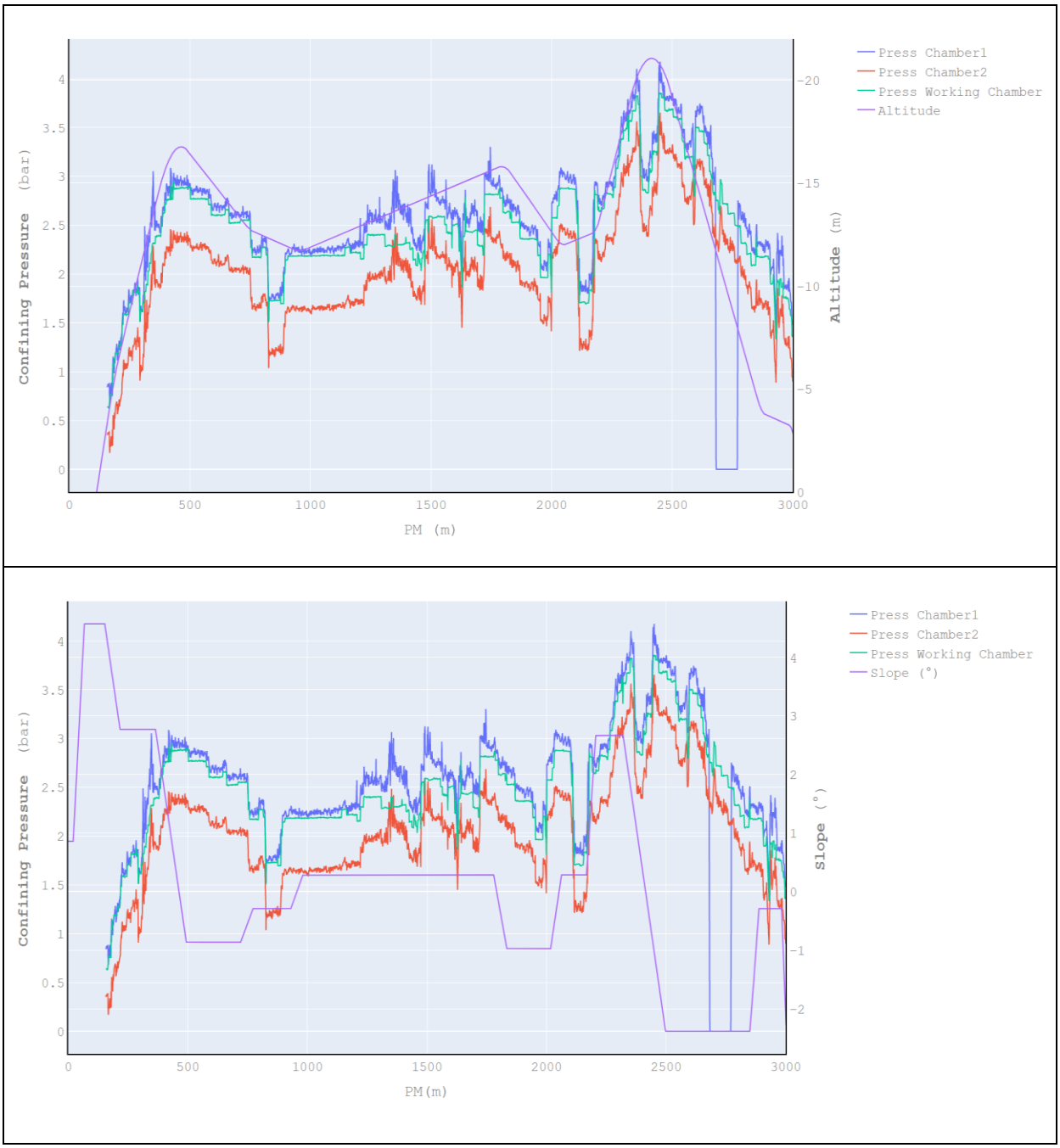

Figure 3-12 Evaluating observation of confining pressure and its potential relation with trajectory's slope and altitude

3.4.2 **EDA of force exerted on TBM based on its external and internal interactions**

Interaction of a TBM with its environment depends on the configuration of the TBM. In this study, three different types of configuration that were encountered for close TBMs in soft ground (Figure 3-13) were evaluated. This configuration mostly helps TBM engineers and crews to facilitate TBM advancements in straight and curve alignment. There are different cylinders which play leading roles in TBM advancement: thrust cylinders, active articulation cylinders, passive articulation cylinders, displacement cylinders and back-up train cylinders.

In the first configuration Figure 3-13(a) thrust cylinders, displacement cylinders, and back-up train cylinders are appearing. Thrust cylinders create main thrust force for the advancement of TBMs. Displacement cylinders are connected to the main drive and give translation displacement to the cutter head. It will also give us the capability to measure the tilt force of cutter head moment and inclination in the horizontal and vertical plane. Furthermore, data captured from these cylinders provide an estimation of the contact force in front of the TBM cutter head.

In the second configuration Figure 3-13(b), thrust cylinders, displacement cylinders, passive articulation cylinders and back-up train cylinders are appearing. Articulation cylinders are developed to help the shield to pass through smaller curvature in curve alignment. This cylinder helps TBM engineer to have a better estimation regarding the friction force of the tail skin.

(a)

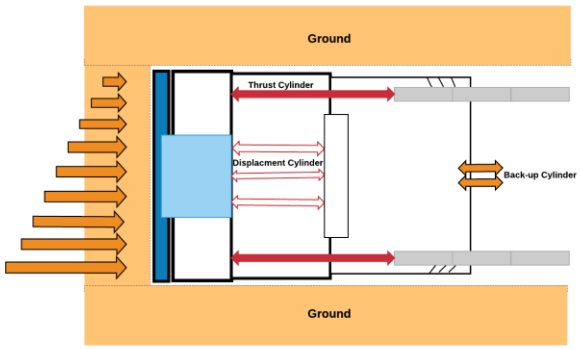

(b)

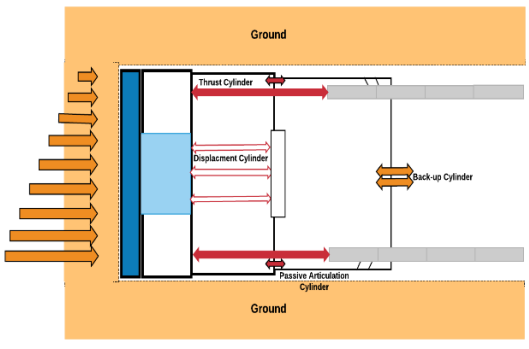

(c)

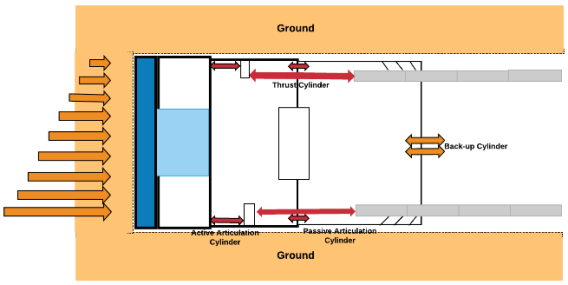

Figure 3-13 Simple schematic for three different configurations of a mixed TBM

In the third configuration Figure 3-13(c), thrust cylinders, active articulation cylinders, passive articulation cylinders and back-up train cylinders are appearing. Active articulation cylinders are mainly used for two purposes: first enabling the advancement of the shield in a smaller curve, and second, the estimation of contact force of the cutter head with its front.

During excavation based on data captured by different sensors, forces created during excavation are estimated. These forces will give us information about:

- real-time total thrust force required for excavation,
- estimation of force due to the interaction of cutter head and ground (contact force),
- force in the chamber of excavation due to confining pressure,
- force calculated based on articulation cylinders,
- the traction force of the back-up train,
- friction force estimated based on the pressure of injection of tail seal grease.

Figure 3-14 illustrates the distribution of these forces. Total thrust force and Contact force are directly from a Programmable Logic Controller (PLC) calculation. The others are calculated as follow:

$$F_{\mathrm{CP}} = A \cdot Pcc \qquad \text{Equation 3.1}$$

Force exerted on bulkhead due to confining pressure in the excavation chamber: $F_{\mathrm{CP}}[KN]$

Confining pressure (bubble pressure or the average of two pressure sensors): Pcc[bar]

$$F_{CFC} = F_{CF} - (A_{MD} . Pcc) \quad \text{Equation 3.2}$$

The surface of Main drive: A_{MD} $[m^2]$,

Contact force: $F_{\mathrm{CF}}[KN]$,

Contact force correct: $F_{\mathrm{CFC}}[KN]$.

$$F_{tailseal} = \mu \cdot \pi \cdot D_0 \cdot L_{SC} \cdot P_{Gr} \quad \text{Equation 3.3}$$

Coefficient of friction between seals and segment: μ,

Length of contact between segment and tail seal: L_{SC} $[m]$,

Grease injection pressure: $P_{Gr}[bar]$.

$$F_{AT} = F_{CFC} + F_{\mathrm{CP}} + F_{AC} + F_{BK} + F_{tailseal} \quad \text{Equation 3.4}$$

Anti-thrust force: $F_{AT}[KN]$,

Force calculated based on articulation cylinders: $F_{AC}[KN]$,

The traction force of back-up train: F_{BK}[KN],

Frictional resistance force due to tail seal interaction: $F_{tailseal}[KN]$.

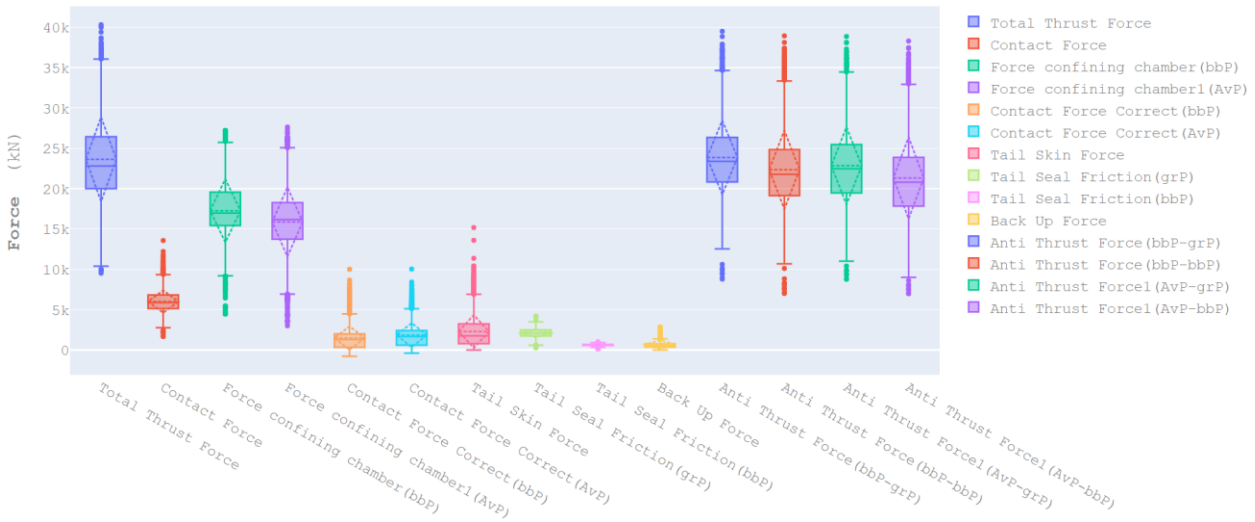

Figure 3-14 Evaluation of the distribution of force and anti-thrust force components

In Figure 2-14, forces are calculated based on two scenarios, considering bubble pressure as confining pressure, and/or considering the average value of the measured pressure in the excavation chamber.

3.4.3 **Calculation of centre of thrust force**

The centre of thrust force gives information about the position of the centre of forces exerted by all thrust cylinders. This parameter is calculated based on several thrust cylinders and the position of each cylinder. Hereunder is presented the essential parameters for calculation of the centre of thrust force in the case study.

Number of cylinders: Nv (15)	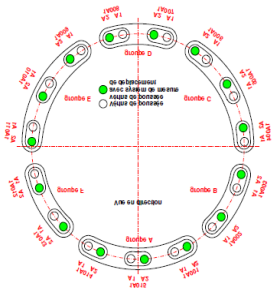
Unite angle: 0.419 rad	
Extrados diameter: 9.3	
Intrados diameter:8.5 m	
R cylinders:4.452 m	

Position of the instantaneous centre of thrust force	Average for each meter of excavation
$\boldsymbol{X = \frac{\sum_{i=1}^{Nv} F_i x_i}{\sum_{i=1}^{Nv} F_i}}$	$\overline{X} = \frac{\sum_{i=1}^{N} X_i}{N}$
$\boldsymbol{Y = \frac{\sum_{i=1}^{Nv} F_i y_i}{\sum_{i=1}^{Nv} F_i}}$	$\overline{Y} = \frac{\sum_{i=1}^{N} Y_i}{N}$

Figure 3-15 and 3-16 represent 2d distribution and 3D visualization of the centre of thrust force calculated for each meter of excavation in the Nice Tramway project.

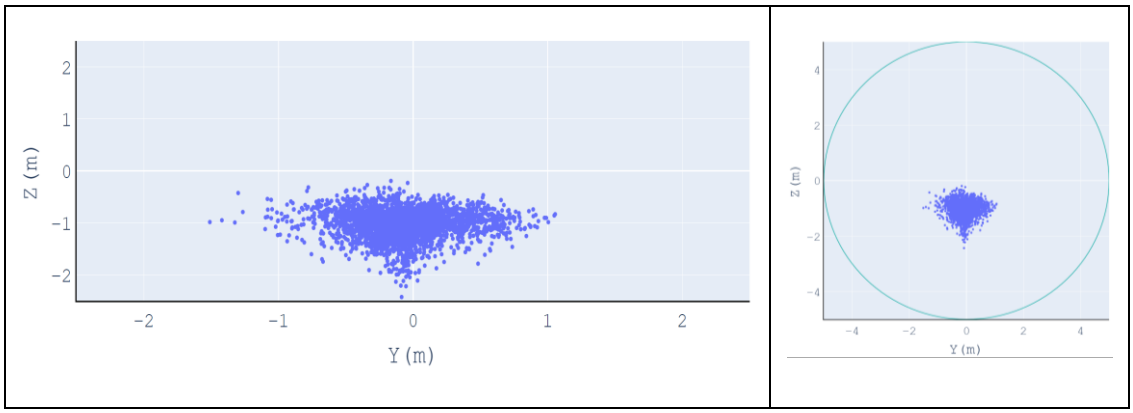

Figure 3-15 Visualization of the calculated centre of thrust force

The distribution of the centre of thrust force was visualized in the 3D plot as follows:

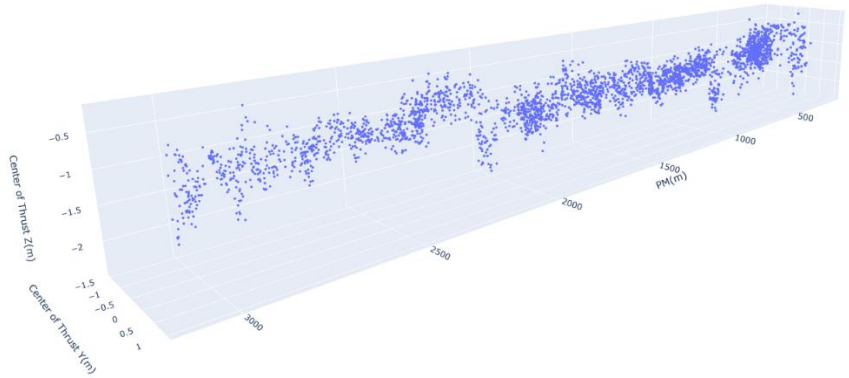

Figure 3-16 3D visualization of center of thrust force for each meter of excavation

3.4.4 **EDA of moment force and inclination of the cutter head**

Investigation of the cutter head moment force give information to better observe the behaviour of TBMs during excavation and the interaction of the cutter head with its front ground. Using displacement cylinders which are directly connected to the main drive of the cutter head give us the ability to instantly capture and analyse moment force exerted on the cutter head in the horizontal and vertical directions (X-Y). Also, the inclination of the cutter head by using the difference of elongation between different groups of cylinders is calculated. These parameters are used in data-driven approaches. Figure 3-17 shows the configuration of displacement cylinders on the main drive for the Nice Tramway TBM.

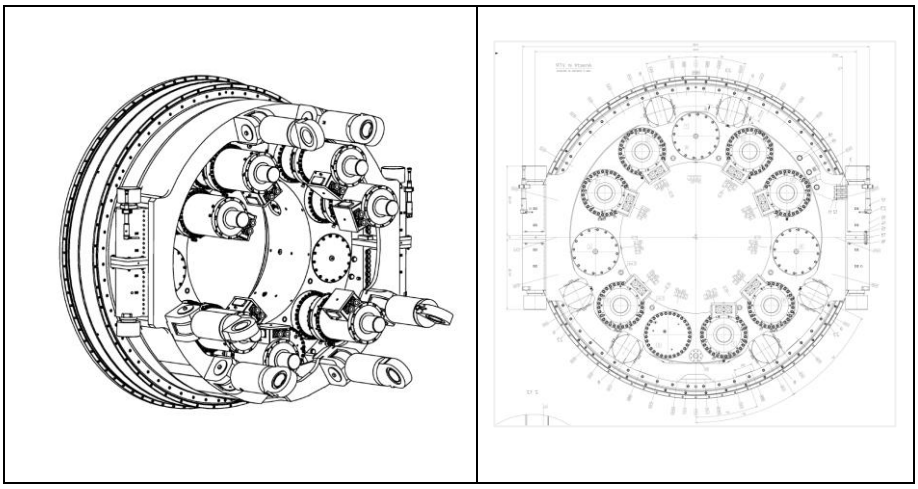

Figure 3-17 Main drive cylinders configuration, left: 3d schematic, right 2d transversal section (courtesy of Bouygues TP)

As displayed in Figure 3-17, three groups of cylinders (4h, 8h, 12h) connected to the main drive are presently supporting us to gain useful information about the inclination of the cutter head, cutter head moment force and cutter head moment arm. In Figure 3-19, the importance of displacement cylinders elongation can be observed. By using the difference of elongation between each group, the angular position of the cutter head in a horizontal and vertical plane is calculated. Figure 3-18 shows the distribution of moment force and projection of moment force on X and Y.

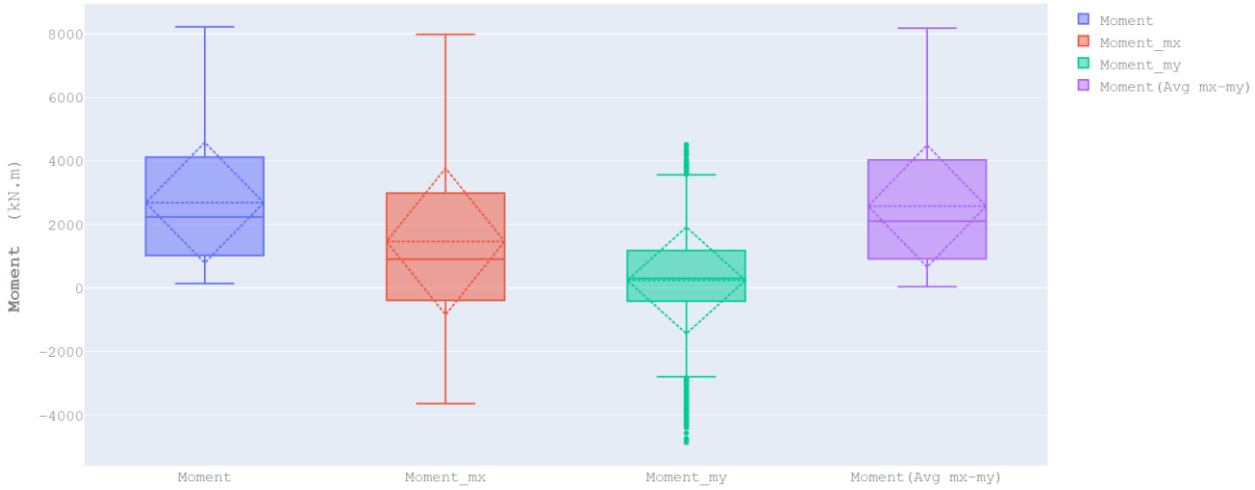

Figure 3-18 Cutter head moment force distribution evaluation (box plot)

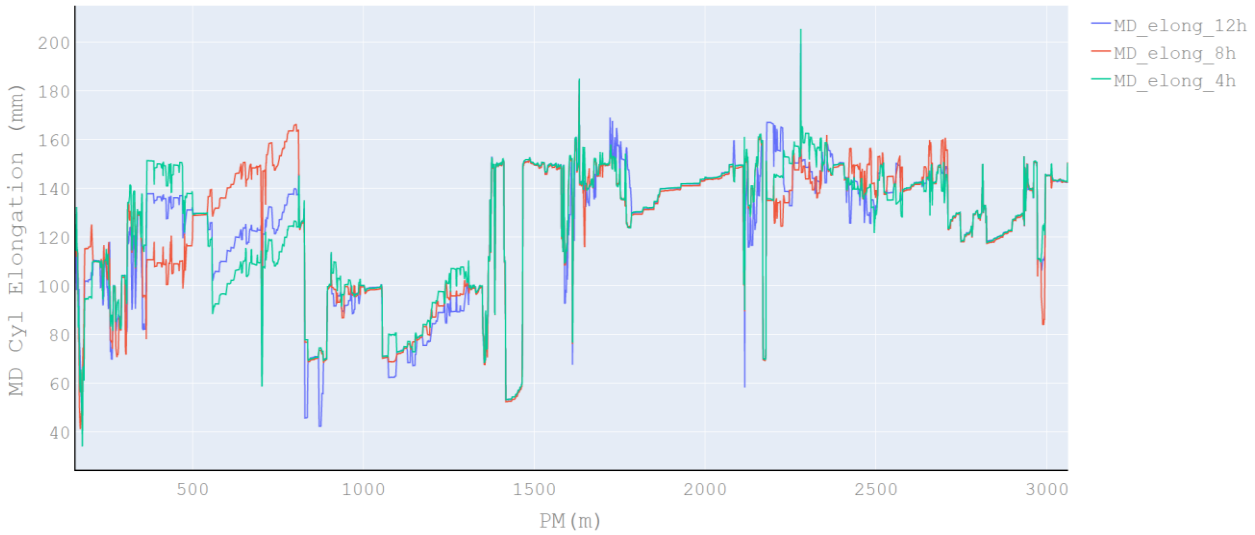

Figure 3-19 Evolution of elongation of displacement cylinders

Also, the moment arm and projection of moment arm for machine Y-Z reference (X-Y of general reference) are measured.

In Figure 3-19, the parts of the trajectory can be seen differentiating the displacement cylinders elongation used for steering (guiding) of TBM, e.g. between TBM chainage (PM) 550-850m. For the estimation of moment arm and moment arm projection on two main axes, the following calculation is used:

$$d_M = {M_T}/{F_{CF}} \quad d_{Mx} = {M_x}/{F_{CF}} \quad d_{My} = {M_y}/{F_{CF}}$$ Equation 3.5

Contact force: $F_{\mathrm{CF}}[KN]$,

Total Moment: $M_T[KN.m]$,

Moment Arm: $d_M[m]$.

In figure 3-20 and 3-21, the position of moment arm is visualized (2D and 3D visualization) during the trajectory of TBM per meter. This parameter will be used as input parameters for the future data-driven model. It gives useful information about cutter head ground interaction.

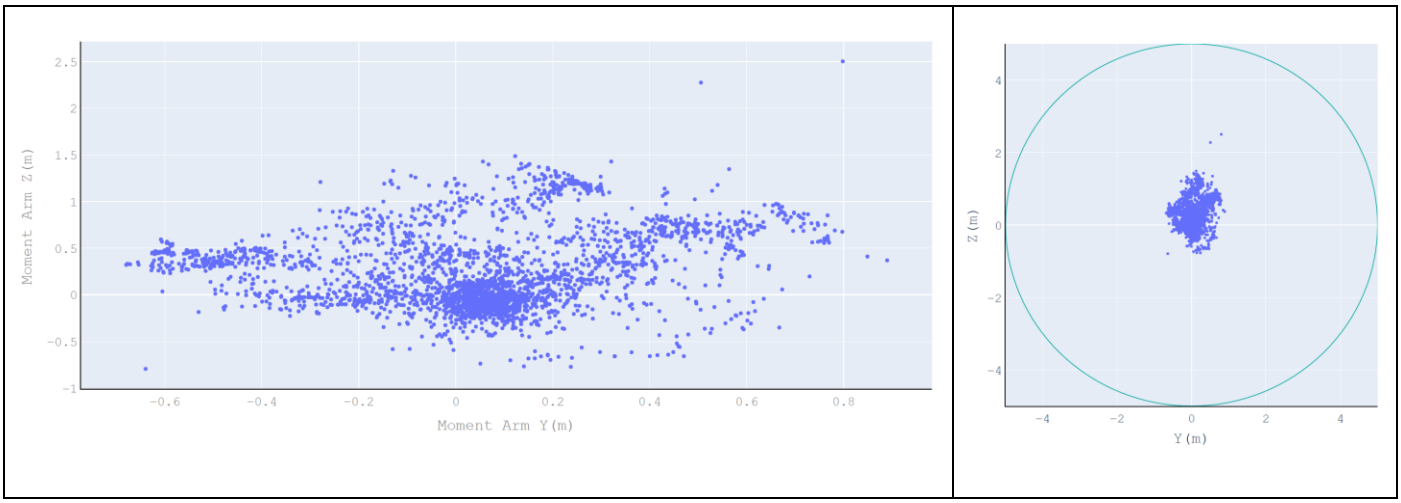

Figure 3-20 2D scatter plot-visualization of the moment arm

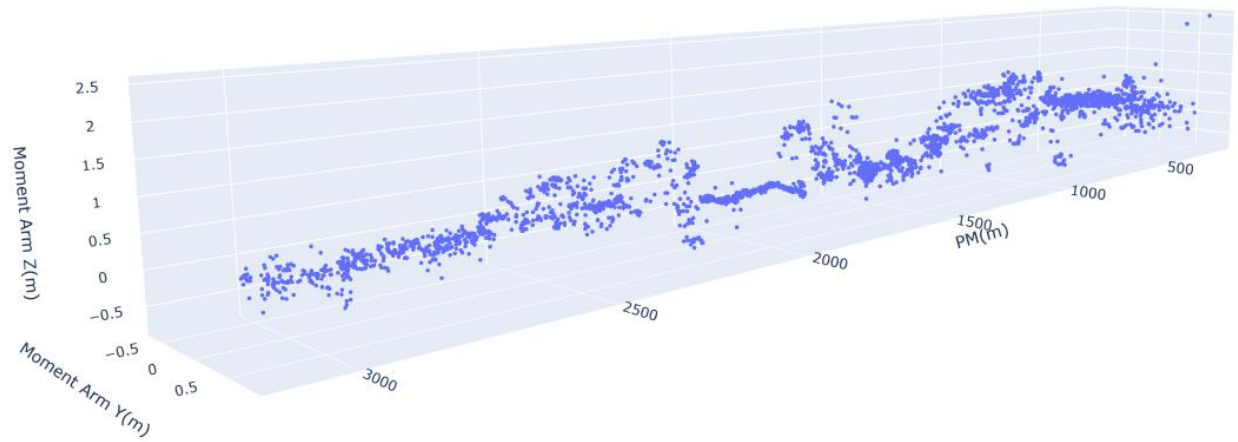

Figure 3-21 3D visualization of the moment arm projection on Y-Z direction of advancement of TBM during chainage of TBM

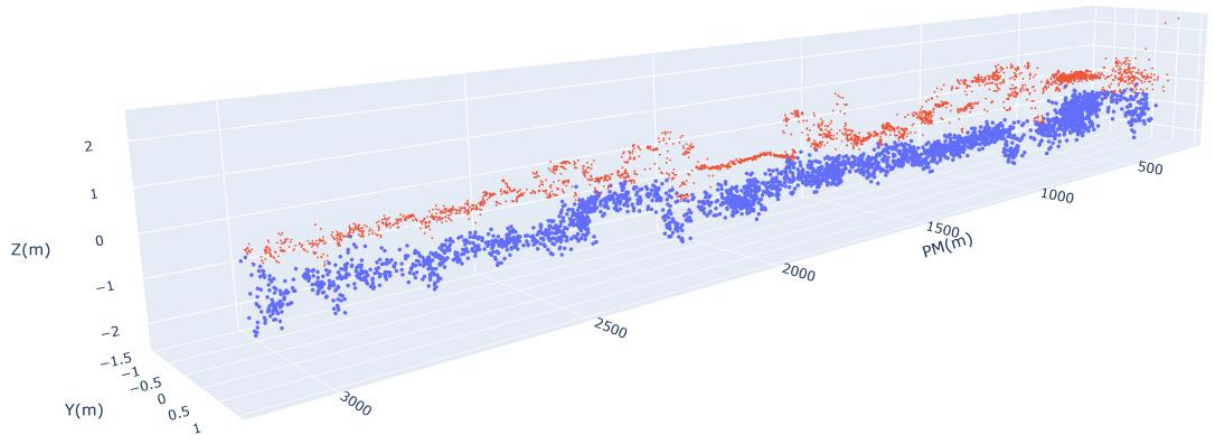

Figure 3-22 3D visualization of the moment arm and center of thrust force evaluation during chainage of TBM

Figure 3-22 displays the position of the centre of thrust force (blue points) and moment arm (red points) in the same 3D visualization. It is observed that the centre of thrust force is located lower than moment arm position in all trajectory of this project.

The inclination of the cutter head

Estimation of the cutter head spatial position can be helpful for the interpretation of TBM internal and external interactions. Similarly, it provides information about the situation pilots use displacement cylinders for steering the TBM. The inclination of the cutter head in the horizontal and vertical plane are two potential parameters for future investigation in data-driven modelling. For the calculation of cutter head inclination in the horizontal and vertical plane, elongation of displacement cylinders and their installation configuration (Figure 3-17) are used.

Following is the calculation of cutter head inclination:

$$\Delta d_h = e_{4h} - e_{8h} \quad \text{Equation 3.6}$$

$$\Delta d_v = e_{12h} - ((e_{4h} + e_{8h})/2) \quad \text{Equation 3.7}$$

$$c = 2R \sin\frac{\beta}{2} \quad \text{Equation 3.8}$$

$$h = R(1 - \cos\frac{\beta}{2}) \qquad \text{Equation 3.9}$$

$$\alpha_h = \tan^{-1}(\Delta d_h / c) \qquad \text{Equation 3.10}$$

$$\alpha_v = \tan^{-1}(\Delta d_v / (D_{MD} - c)) \qquad \text{Equation 3.11}$$

Chord length in the circular segment: c $[m]$,

Segment height: h [m],

Diameters of main drive: $D_{MD}[m]$,

Cutter inclination in the horizontal plane: α_h,

Cutter inclination in the vertical plane: α_v.

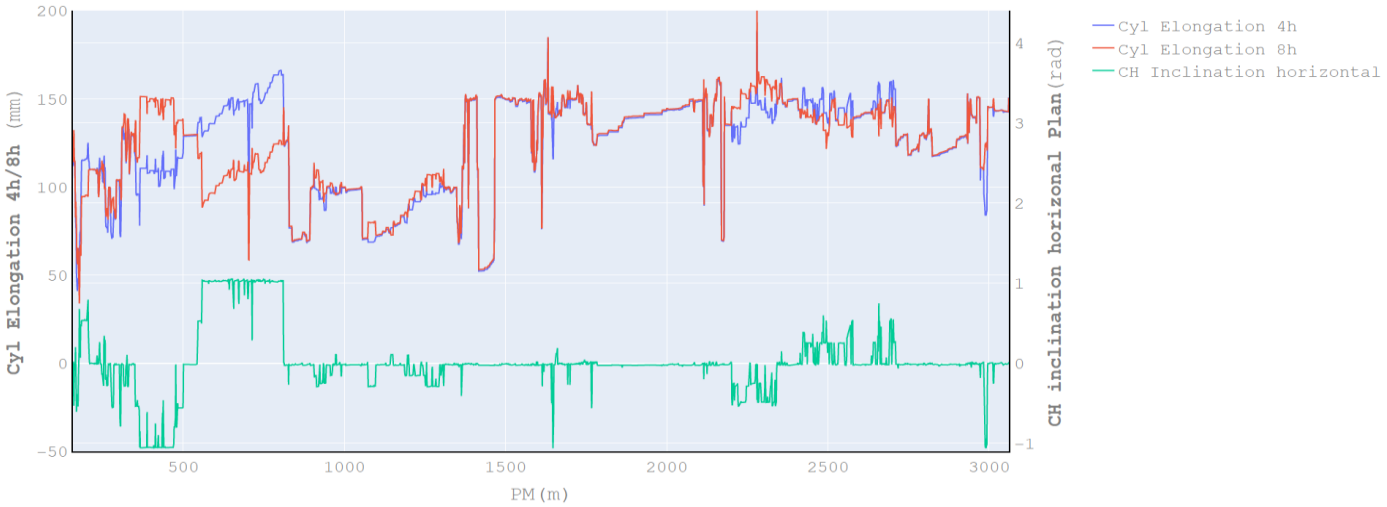

Figure 3-23 The cutter head inclination evolution and elongation of displacement cylinders 4h-8h

Figure 3-23, The right axis represents the cutter head inclination on the horizontal plane through the trajectory of a TBM (green line) and the left axis represents the elongation of cylinders (4h & 8h).

Figure 3-24, the right axis represents the cutter head inclination on the vertical plane through the trajectory of a TBM (green line) and the left axis represents the elongation of the cylinders (12h & 4-8h).

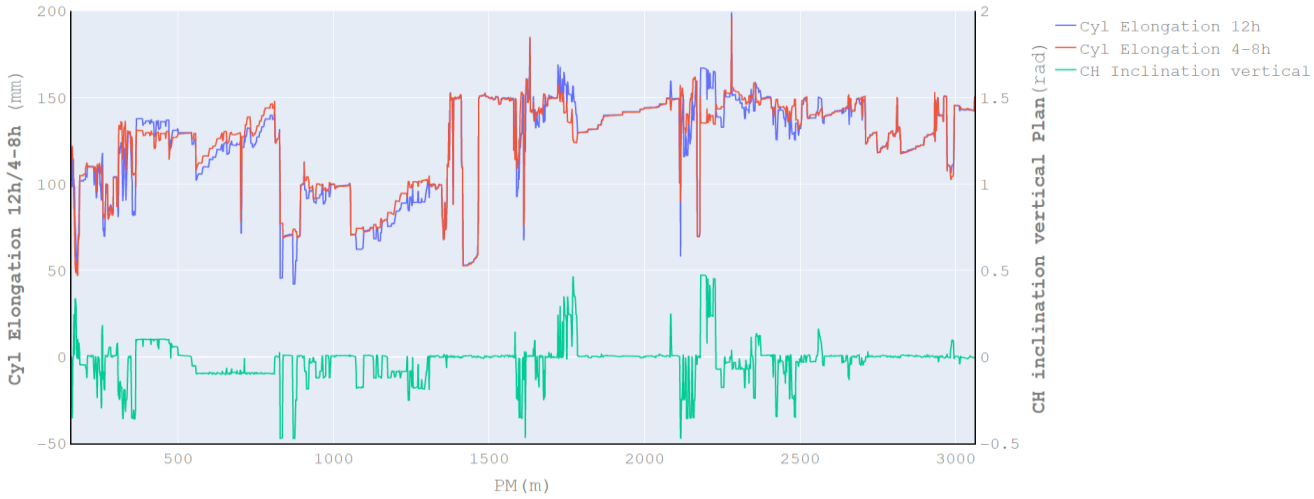

Figure 3-24 The cutter head inclination evolution and elongation of displacement cylinders 12h vs 4h-8h

3.4.5 EDA of guiding parameters

A TBM guiding system is composed of three essential stages. The first stage is called preconstruction, the second stage, construction and the last stage the post-construction. In this study, these stages are not discussed in detail. The general aspect of the guiding system and important parameters are highlighted in this section. Then, some essential parameters of the trajectory of a TBM such as slope and curvature are calculated. Finally, the potential correlation between these parameters with operational parameters of a TBM is observed.

The representation of a 3D displacement is difficult to draw on a screen or on a paper. Therefore, it is usual to split the representation into a horizontal view and a vertical view, as illustrated in Figure 3-25. The current theoretical position at the front of the shield, the red dot, can be described by its coordinates X and Y. However, it is preferred to give the currently covered distance from the project start defined as the chainage (PM), (here 987.234 m from the project start symbolized by the blue cross where the chainage is 0 m). The distance is computed along the horizontal view axis (i.e. on the projected map) and not as the 3D curvilinear distance. The vertical view of the axis represents the theoretical project elevation as a function of the chainage. So, for a known theoretical curve, knowledge of the chainage allows the corresponding theoretical coordinates: X, Y, Z to be defined.

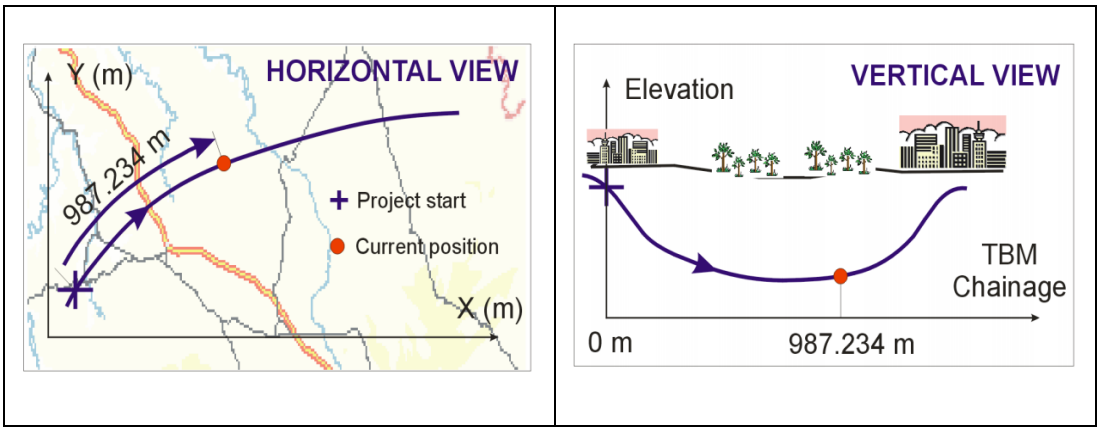

Figure 3-25 Sample horizontal and vertical view of a trajectory [28]

The Design Axis of Tunnel (DTA, Tunnel axis derived from the project axis) is the main parameters for real-position calculation of a TBM. This axis is used as the reference axis for all computations relative to guidance and ring positioning in TBM tunnelling. DTA will be used to calculate slope and curvature (in the horizontal and vertical plane) of trajectory. By using guiding parameters (Pitch and Yaw), also the real-time position of a TBM is recalculated as a general reference.

Shield positioning

Three references are considered for TBM positioning Figure 3-26:

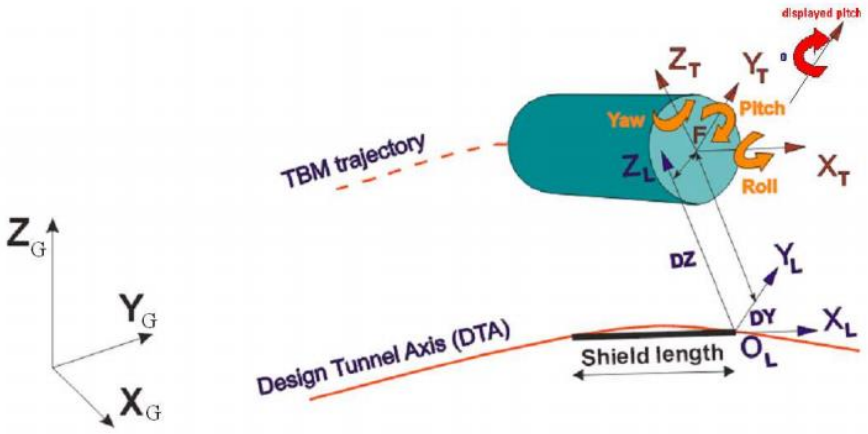

Figure 3-26 Reference system for TBM guiding[28]

The general reference system of the project in which the DTA is described (X_G, Y_G, Z_G): An offset can be applied in the three directions to ease the input in the Pyxis application. The local reference system as a function of the chainage (X_L, Y_L, Z_L): The TBM front point chainage

projected on the DTA defines a local system as shown in Figure3-26. The X_L-axis is not tangent to the theoretical curve. The position where the front and back of the shield lies is considered ideal on a theoretical axis. It defines the X-axis. The two other axes are deduced with a null cross-slope. Shield roll, pitch and yaw angles are relative to these axes. The TBM axes (X_T, Y_T, Z_T): The TBM front point, head retracted, is the origin of the TBM axes as shown on the Figure 3-27.

The front of the shield has been set up on the theoretical axis. Although most of the time, this is not the case as the TBM is wiggling around the theoretical axis. The horizontal view and vertical view can also be used to represent the position of any point P of the space known by its coordinates: X, Y and Z (Figure 3-26).

1. The point P is projected as P' on the 3D theoretical axis.
2. Chainage C at P' is computed.
3. Projected horizontal distance DY of P to P' is computed.
4. Vertical distance DZ is given as Z – Z'.

By convention, the sign of $\Delta Y$is positive when point P is on the left of the curve when looking towards the shield progression. So, ΔY is positive in Figure 3-27. One point, for instance, the front of the shield F, is not sufficient to completely define the position of a rigid bod. It is also necessary to know the attitude of the body relative to its theoretical position. The attitude is defined with three shown angles, as presented in Figure 3-28.

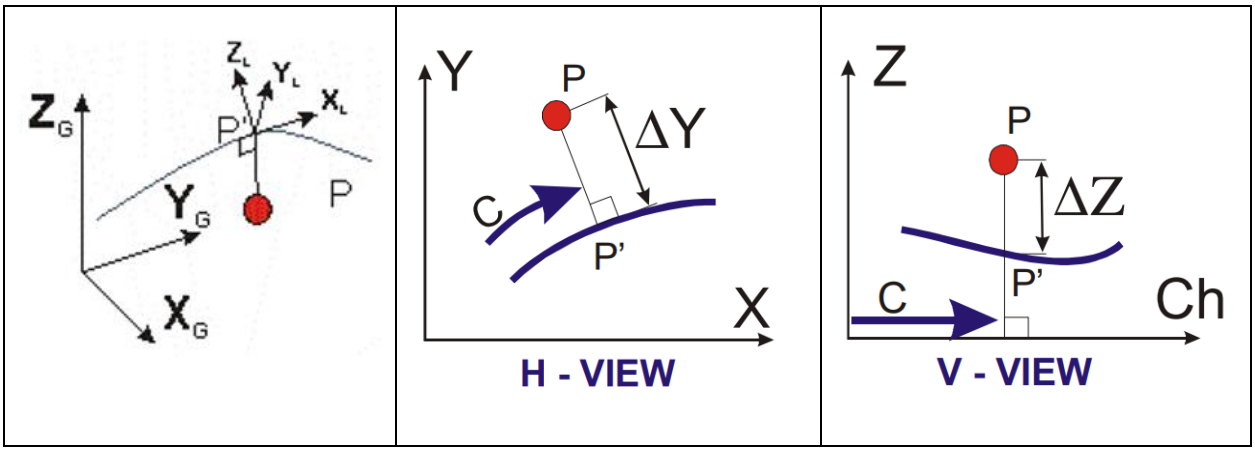

Figure 3-27 Horizontal view and vertical view used to represent the position of any point[28]

By convention, the sign $\Delta Y$is positive when point P is on the left of the curve when looking towards the shield progression. So, ΔY is positive in the above figure. One point, for instance, the

front of the shield F, is not sufficient to define the complete position of a rigid body. It is also necessary to know the attitude of the body relative to its theoretical position. The attitude is defined with the three shown angles:

• The roll is the rotation around the main shield axis, the cylinder axis. The roll is positive when the shield is rotating clockwise when looking from the rear of the shield towards the shield progression.

• The pitch is the vertical attitude of the shield. It shows how the shield is going up or down. The pitch is positive when the shield is moving upwards.

• The yaw axis is the horizontal attitude of the shield. It shows the attitude of the shield to leave a trajectory on the left or right when looking at the horizontal view. The yaw is positive when the shield is heading towards the left of the trajectory.

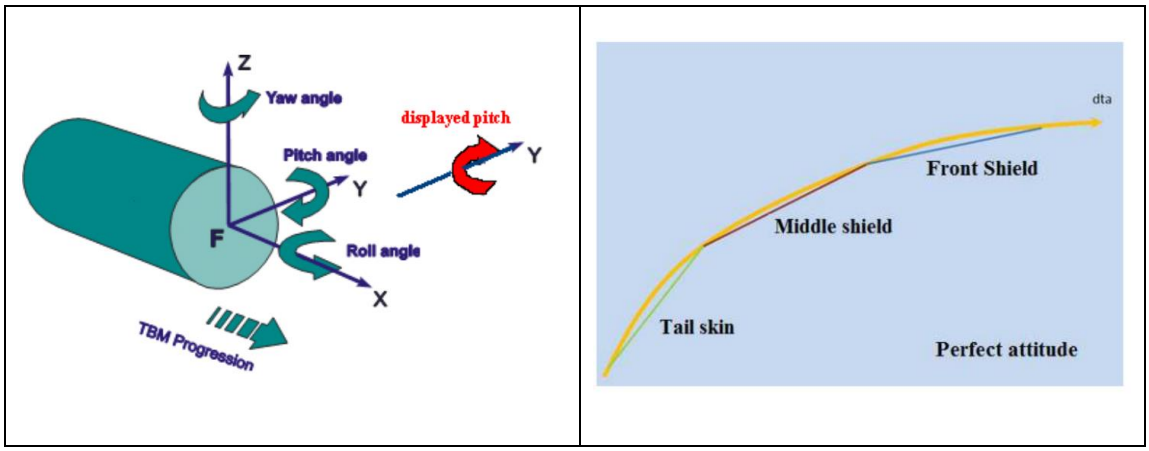

Figure 3-28 Schematic of theoretical position in a TBM advancement [29]

The theoretical attitude mentioned above is defined as the best TBM attitude. It is assumed that this best attitude is reached when the centre of the cutter head, the articulation centres and the rear of the tail skin are on the theoretical curve as shown in Figure 3-28 (and not when the shield is tangent to the trajectory) [29].

Table 3-3 Representation of DTA file

PM	Est (m.)	Nord (m.)	Alt. (m.)
0	1042509.376448	6297440.265758	6.280000
1	1042510.239294	6297440.771226	6.265003
2	1042511.102139	6297441.276694	6.250007
3	1042511.964984	6297441.782161	6.235010
4	1042512.827830	6297442.287629	6.220013
….	….	….	….
3101	1045048.020878	6298244.504083	-0.047836
3102	1045048.573618	6298243.670729	-0.027843

Table 3-3 shows an example of DTA data representation. The DTA data frame was used to calculate slope and curvature in a horizontal and vertical plane. Figure 3-29 represents Horizontal view and vertical view of DTA (design trajectory of TBM)

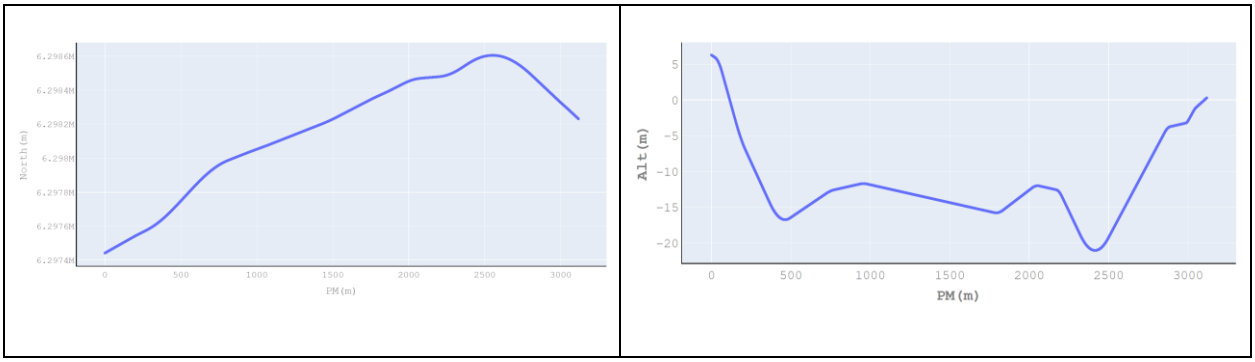

Figure 3-29 Horizontal and vertical view in the Nice Tramway project

The slope in a TBM trajectory

DTA gives us required data for calculation of TBM trajectory characteristics such as slope, and curvature in the horizontal and vertical plane. The chainage (PM) of TBM was used as a label of our data frame then the slope for each meter of the advancement of a TBM was calculated as follow:

$$S_{pm} = \tan^{-1}(\Delta Z) * 180/\pi$$ Equation 3.12

Slope of TBM for each meters of advancement: S_{pm} [radian],

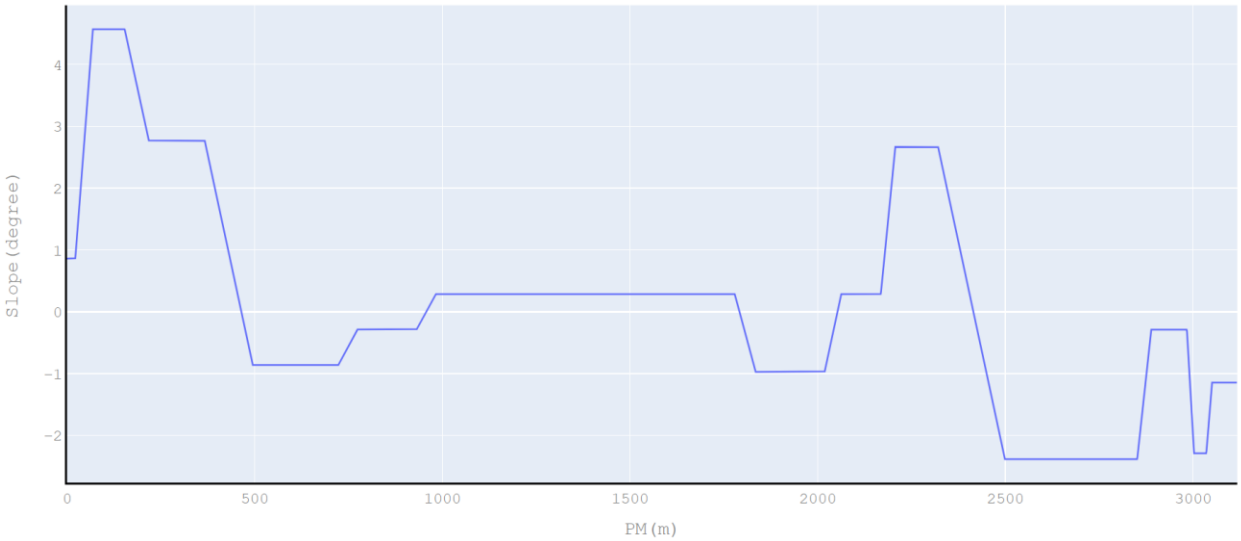

Figure 3-30 Evolution of slope through excavation trajectory in the Nice Tramway project

Curvature in TBM trajectory

In each curve trajectory, a fundamental property of curve is the curvature at a point on the curve. The curvature at a point is defined to be the rate at which the unit tangent vector changes direction. The arc length is independent of its parametrization (how faster or slower the curved trajectory was passed). Therefore, the following curvature, defined by arc length, will be independent of its parametrization.

Let's consider $\vec{r}(s) = (x(s), y(s), z(s))$ to be a vector-valued function parameterized in terms of the arc length of a smooth curve that is traced out by $\vec{r}$. Then the curvature of the curve at the point $\vec{r}(s)$ denoted:

$$\kappa(s) = \| \frac{d\hat{T}(s)}{ds} \| = \| \frac{d\hat{T}(s)/dt}{ds/dt} \|$$ Equation 3.13

$\kappa(s)$ is the length of derivative of $d\hat{T}/ds$.

For plane curve the curvature was calculated by following equations:

$$\text{Speed} = \frac{ds}{dt} = |\mathbf{v}(t)| = \sqrt{(x')^2 + (y')^2} \qquad \text{Equation 3.14}$$

$$\mathbf{v} = \frac{ds}{dt}\mathbf{T} \quad \& \quad \mathbf{T} = \frac{\mathbf{v}}{\frac{ds}{dt}} \qquad \text{Equation 3.15}$$

$$\mathbf{a}(t) = \frac{d^2s}{dt^2}\mathbf{T} + \kappa(\frac{ds}{dt})^2\mathbf{N} = \frac{d^2s}{dt^2}\mathbf{T} + \frac{v^2}{R}\mathbf{N} \qquad \text{Equation 3.16}$$

$$\kappa = \frac{d\mathrm{T}}{ds} = \frac{|\mathbf{a} \times \mathbf{v}|}{|\mathbf{v}|^3} \qquad \text{Equation 3.17}$$

$$\mathbf{r}(t) = x(t)\hat{i} + y(t)\hat{j} \ : \qquad \kappa = \frac{|x''y' - x'y''|}{((x')^2 + (y')^2)^{3/2}} \qquad \text{Equation 3.18}$$

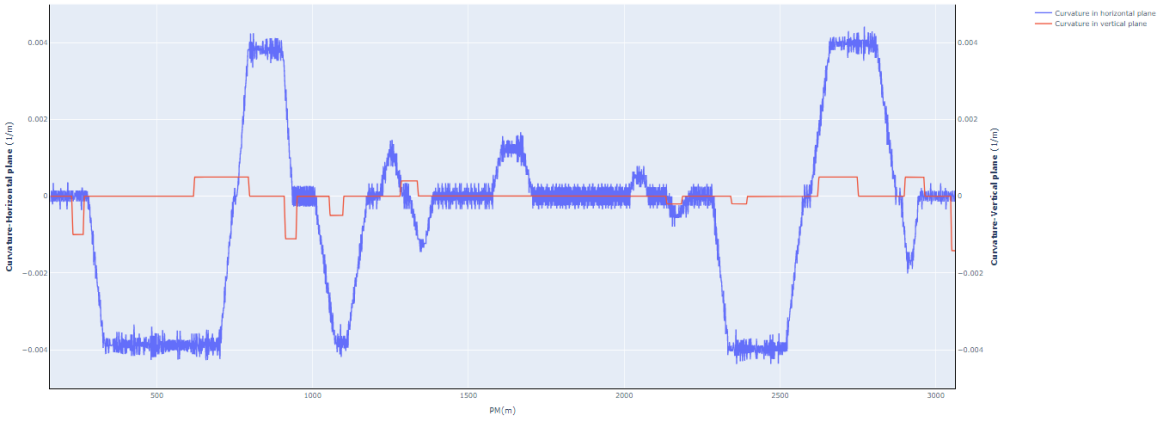

Figure 3-31 Ecolution of the curvature of DTA in horizontal and vertical plane in the Nice Tramway project

Figure 3-32 shows the slope of the trajectory (blue line), curvature in the horizontal plane (red line) and curvature in the vertical plane (green line) during advancement of the project. All the parameters are calculated by DTA parameters and validated by the longitudinal profile of the project.

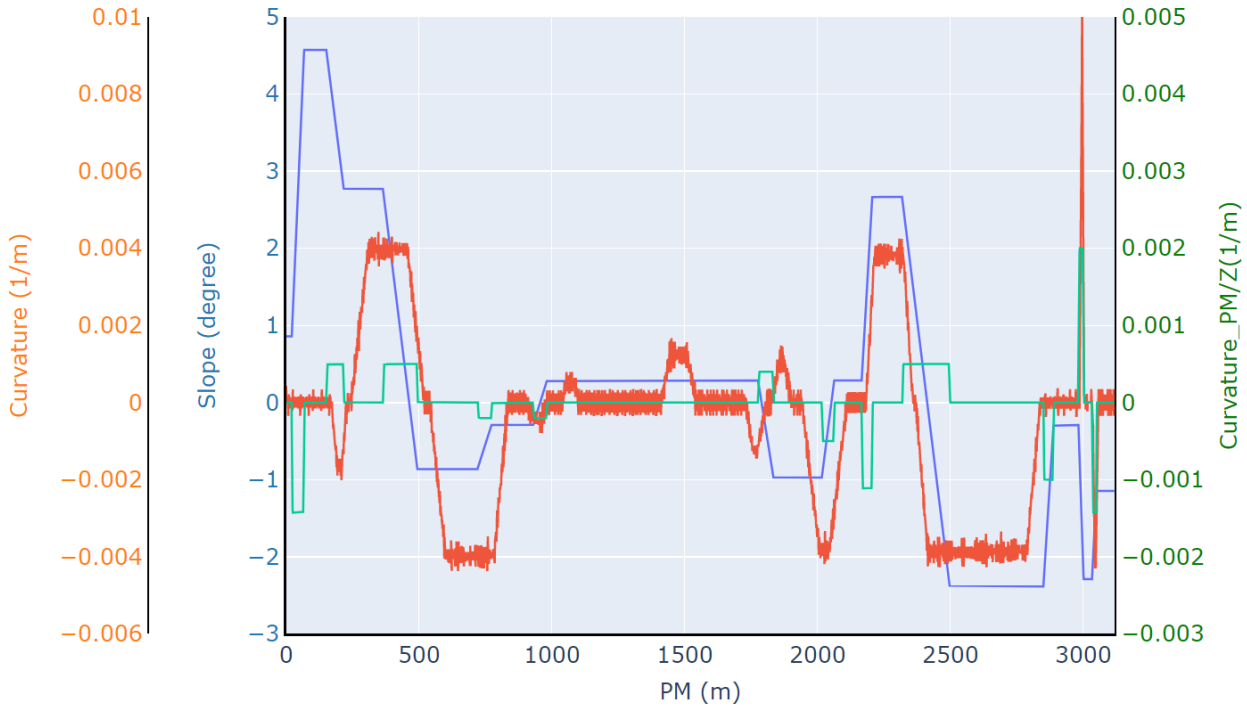

Figure 3-32 Evolution of slope, curvature in the horizontal and vertical plane of DTA in the Nice Tramway project

Calculating the location of a TBM by DTA, pitch and yaw

In this section, the real position of a TBM is calculated by using DTA and deviation of machine (Delta Y and Delta Z). By a given point, slope and a distance along that slop, the second point is calculated (in investigation of the local position of TBM in comparison with DTA).

For two-point $(x_1, y_1) and\ (x_2, y_2)$:

$$m = \frac{y_2 - y_1}{x_2 - x_1} = \frac{\Delta y}{\Delta x} \quad \& \quad n = -1/m \qquad \text{Equation 3.19}$$

$$x_l = x_i \pm \frac{d_x}{\sqrt{1+m^2}} \quad , \quad y_l = y_i \pm \frac{d_y * n}{\sqrt{1+m^2}} \qquad \text{Equation 3.20}$$

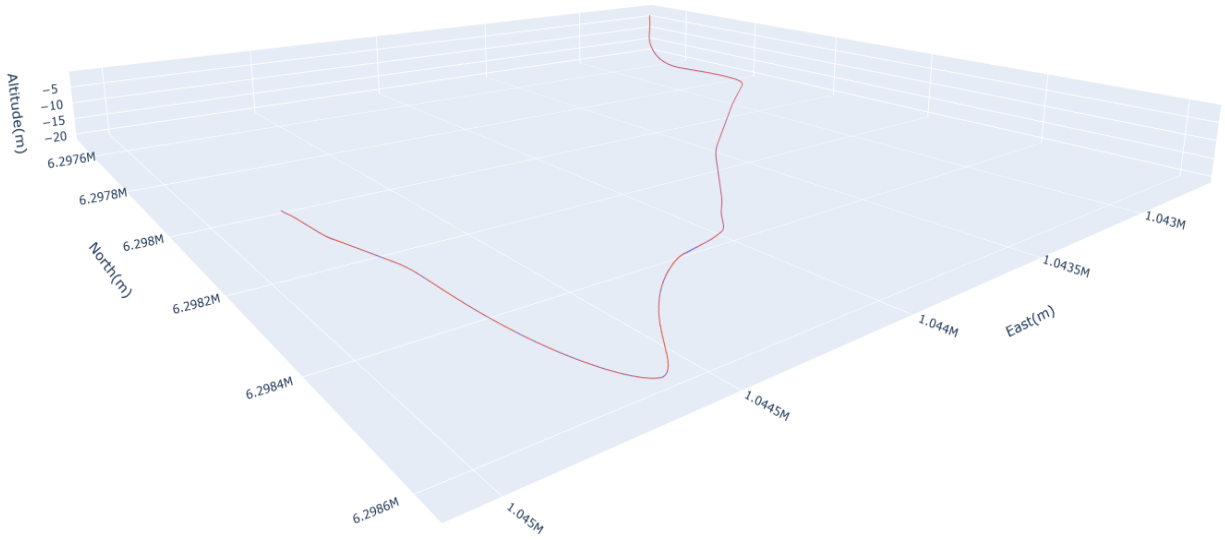

Figure 3-33 3D visualization of DTA and local position of TBM in the Nice Tramway project

Figure 3-33 represents TBM trajectory and DTA in a same interactive plot. As the deviation of a TBM is too small around mm to cm, here the difference between two values of a DTA and TBM local position is not observable. Still, in the interactive visualization, it is clearly observable.

3.4.6 **Evaluating the association between TBM operational and steering parameters**

Two important statistical terms for every statistical and probabilistic investigation are correlation and covariance. Essentially these two terms are used for measuring the association between parameters. They are essential to give general views when there are some complex problems with many involved parameters.

Correlation measures the direction and strength of the linear relationship between two variables. Covariance specifies the linear relationship between variables. Correlation is a function of the covariance. The difference between covariance and correlation is that correlation values are standardized, whereas covariance values are not. The correlation coefficient of two variables is calculated by dividing the covariance of those variables by the standard deviation of the values. In reality, by dividing the covariance values by the standard deviation, we scale the value to a range

of -1 to 1. This range is the range of the correlation value. The covariance of two variables is represented as follow:

$$\mathrm{Var}(X) = \frac{\sum(X_i - \overline{X})(X_i - \overline{X})}{(n-1)} \qquad \text{Equation 3.21}$$

$$\mathrm{Cov}(X) = \frac{\sum(X_i - \overline{X})(Y_i - \overline{Y})}{(n-1)} \qquad \text{Equation 3.22}$$

The correlation coefficient (Pearson's correlation coefficient) has mathematical representation as follow:

$$\mathrm{Corr}\ (X,Y) = \frac{\sum(X_i - \overline{X})(Y_i - \overline{Y})}{(n-1)\sqrt{\mathrm{Var}\ (X)}\sqrt{\mathrm{Var}\ (Y)}} \qquad \text{Equation 3.23}$$

If the value of the correlation coefficient is closer to +1 or -1, the variables are more related. The positive correlation shows that if a value increases, the other would also increase (two variables change in the same direction). The negative correlation indicates that the two variables are changing in the opposite direction. A correlation coefficient of zero or near zero shows no relation in changing variables. As general estimation for the correlation coefficient, if this value is between 0.7 and 1, there is a strong correlation between two variables. If the correlation coefficient is between 0.25 to 0.7, there is a moderate correlation, and the values smaller than 0.25 represent the weak correlation. Correlation is dimensionless. Covariance accepts the units from the product of the units of the two variables.

There are different applications for correlation analysis, such as feature selection and multivariate analysis in data pre-processing and exploration. Correlation gives us the capability to investigate and establish a relationship between variables. Using the correlation matrix for feature selection could be completely helpful for any kind of statistical modelling or data analysis. Generally, the correlation matrix may be used when the scale of variables differs. The covariance matrix may be used when the variables have similar scales.

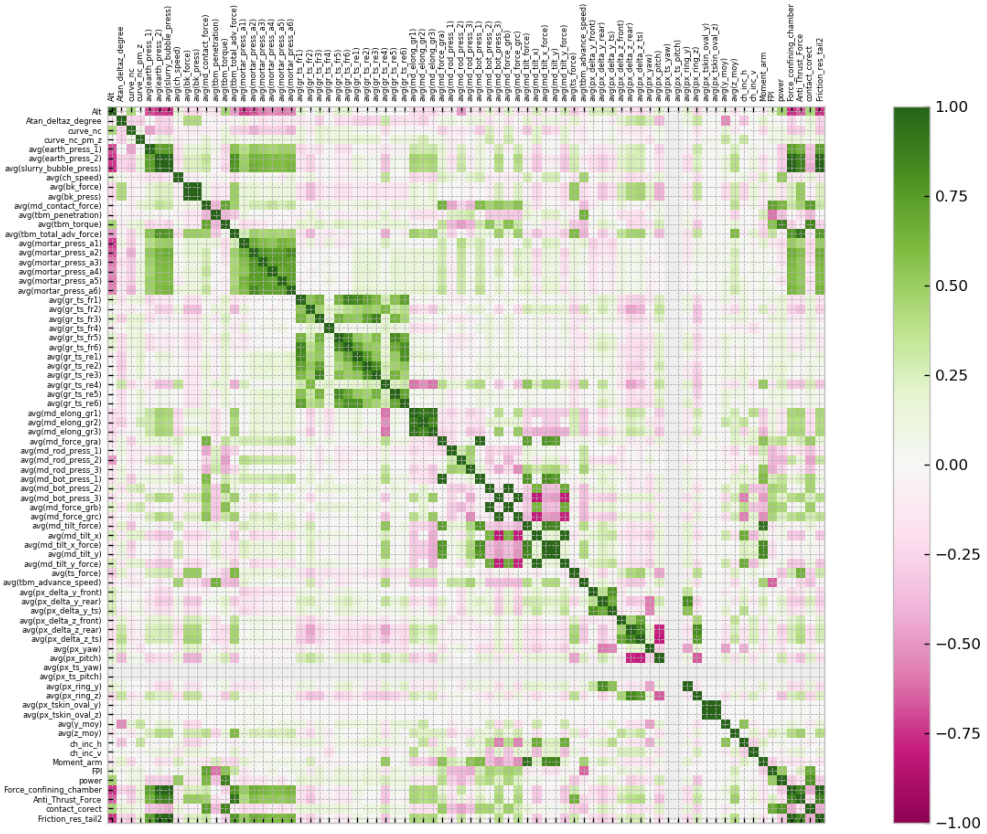

Figure 3-34 Correlation matrix of parameters for the Nice Tramway project

Figure 3-34 represents the correlation matrix for our case study with 76 parameters. In this part, the potential relation (correlation) between operational parameters and parameters related to the steering of TBMs such as altitude, slope, curvature on the horizontal plane and curvature on the vertical plane was observed. The first plot shows the change of total thrust force with the slope, and curvature on the horizontal and vertical plane through the trajectory of a TBM for about 3 km of the Nice-Tramway project (Figure 3-35).

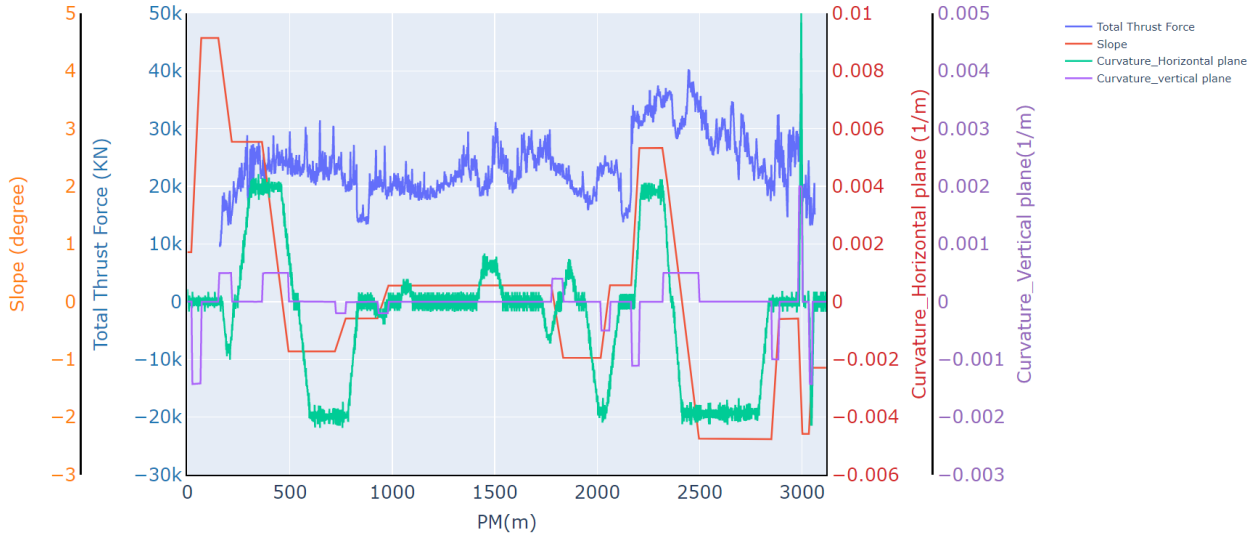

Figure 3-35 Thrust force evolution vs slope, curvature in horizontal and vertical plane

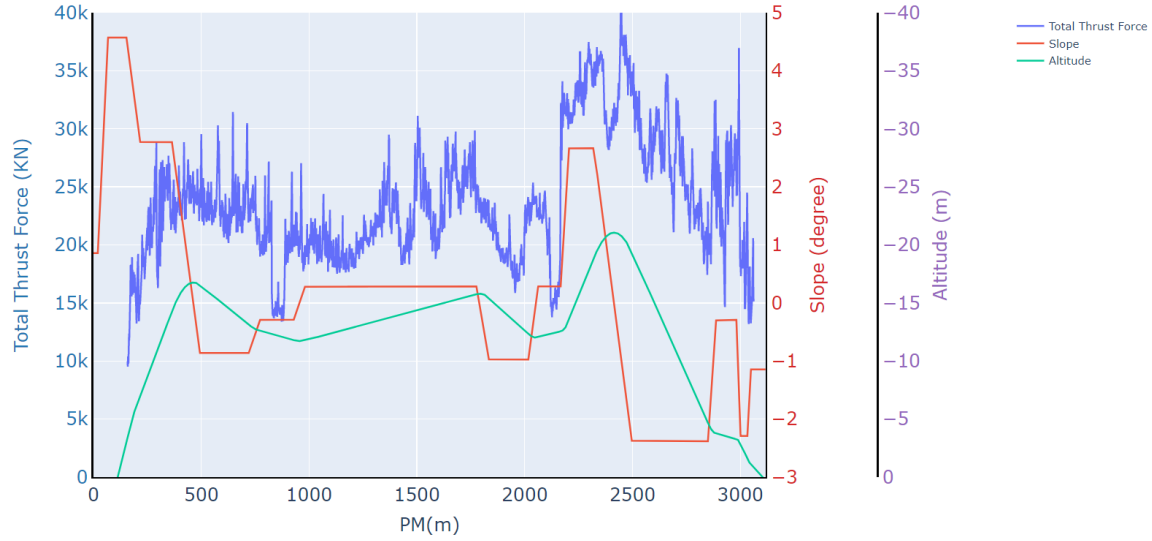

Figure 3-36 Show evolution of the thrust force vs altitude and slope in the Nice Tramway project

Figure 3-36 represents the changes of total thrust force with slope and altitude.

Figure 3-36 illustrates the fluctuation of the total thrust force in comparison with slope and altitude. It is observed that there is a correlation between changes in total thrust force and altitude and slope.

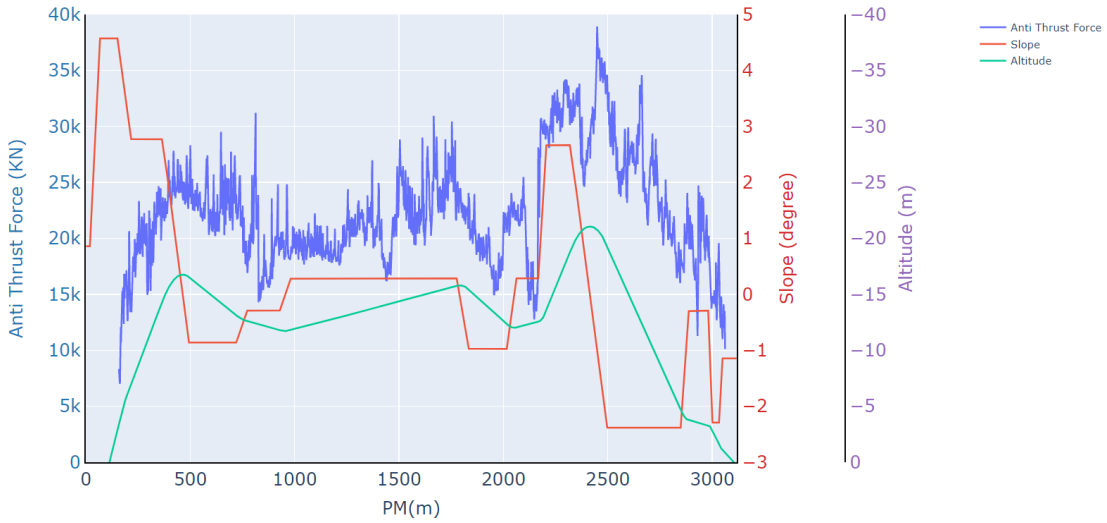

Figure 3-37 Antithrust force evolution vs altitude and slope in the Nice Tramway project

Other parameters which represent forces against the advancement of TBM is anti-thrust force. Figure 3-37 represents the variation of anti-trust force in comparison with slope and altitude. A correlation is observed between changes in anti-thrust force values and altitude and slope of trajectory.

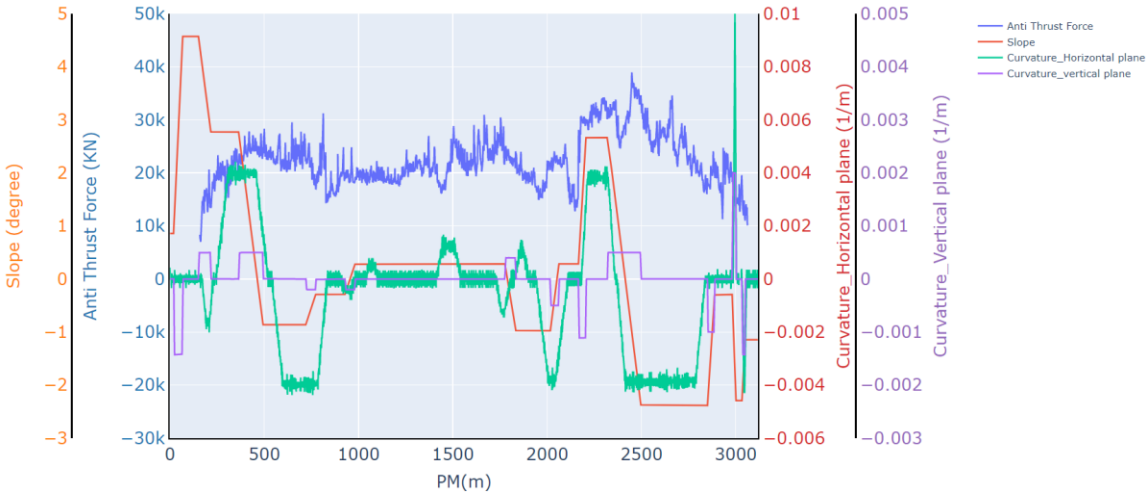

Figure 3-38 Antithrust force evolution vs slope and curvature in horizontal and vertical plane

Figure 3-38 demonstrates the changes of anti-trust force, slope, and curvature in the horizontal and vertical plane during advancement of a TBM.

Back-up train interaction with a TBM is another interaction which is not investigated in detail. Here the observed data frame had 37486 rows of data for back up force, advance speed and thrust cylinders elongation. Here Figure 3-39 is very dense as the resolution of data is very small.

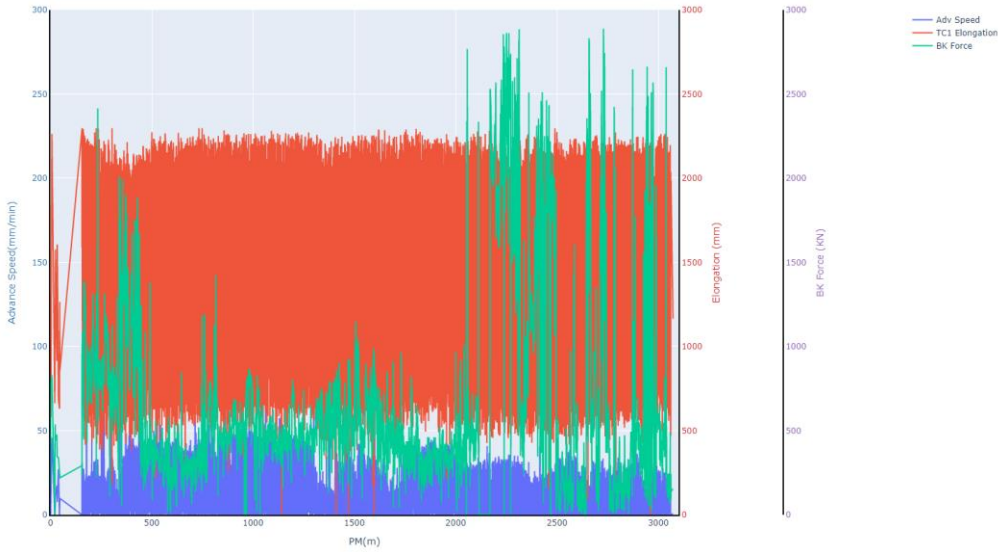

Figure 3-39 Variation of the advance speed vs back up force in a complete trajectory in the Nice Tramway project

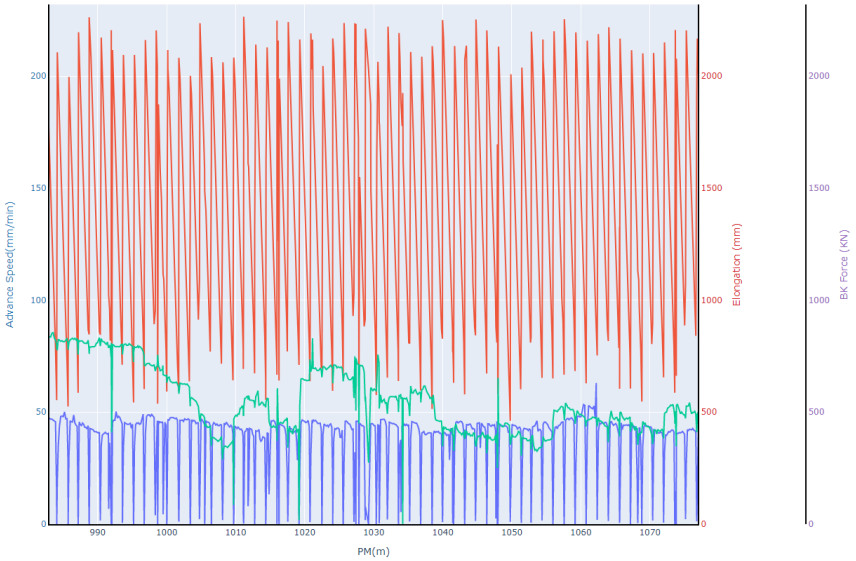

Figure 3-40 Observe correlation between back up force and advance speed in the Nice Tramway project

Figure 3-40 displayed more observable view of back up force, elongation of thrust cylinder and advance speed of a TBM. A correlation between back up force and advance speed of a TBM is observed. Also, the correlation between altitude and slope of trajectory with back up force is investigated in Figure 3-41.

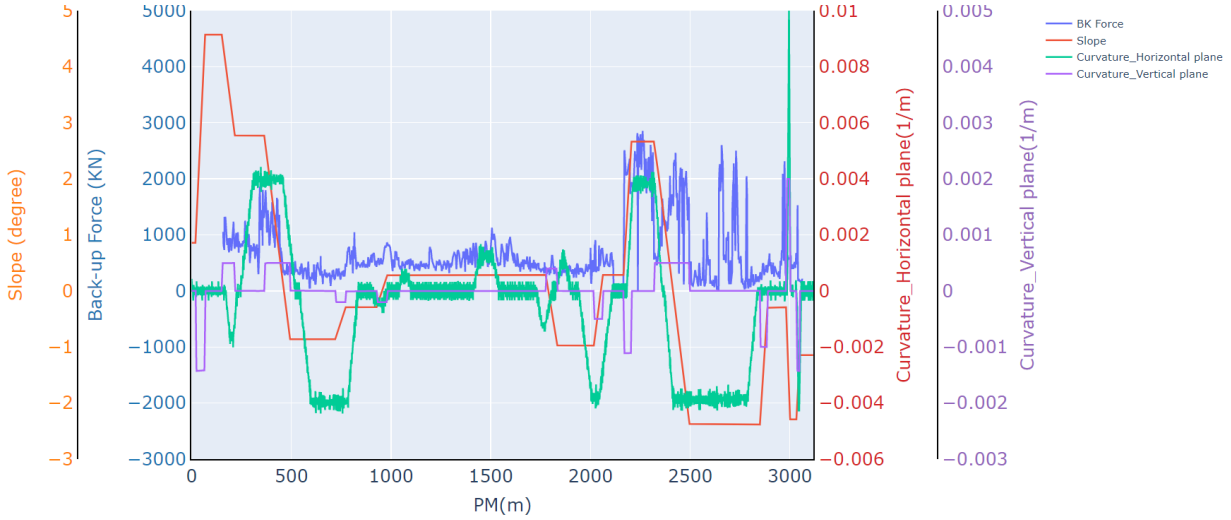

Figure 3-41Evolution of the backup force vs slope and curvature in horizontal and vertical plane

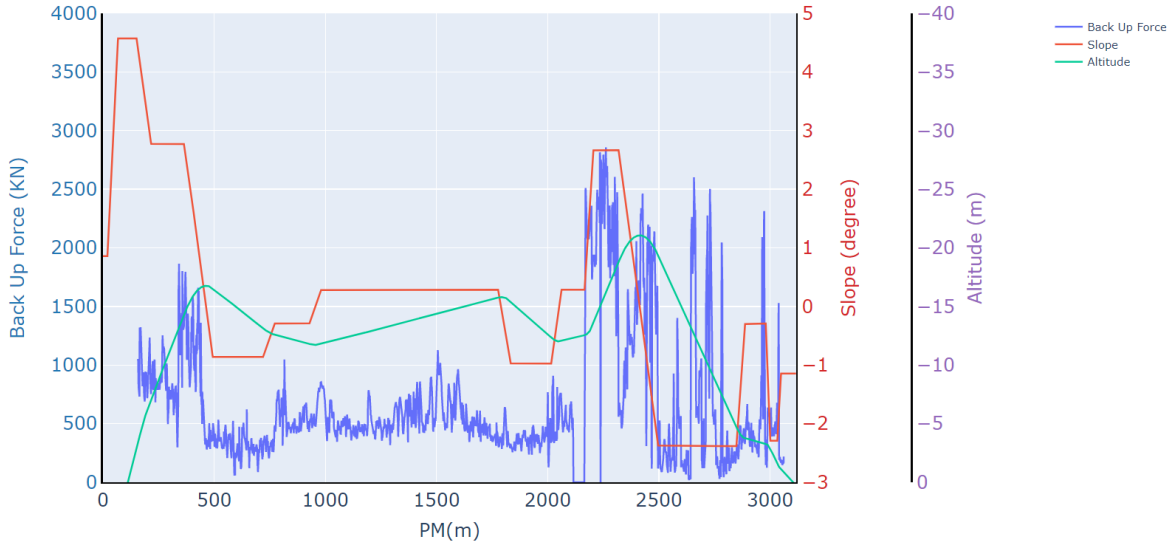

Figure 3-42 Back up force evolution vs altitude and slope of trajectory

In figure 3-42, the changes in the backup force versus curvature in the horizontal and vertical plane and slop of trajectory is observed.

In Figure 3-43, histogram2Dcontour plot for total thrust force vs trajectory characteristics parameters (slope, curvature in the horizontal and vertical plane) is displayed. the different zones of functionality based on the relation between total thrust force and trajectory characteristics were investigated.

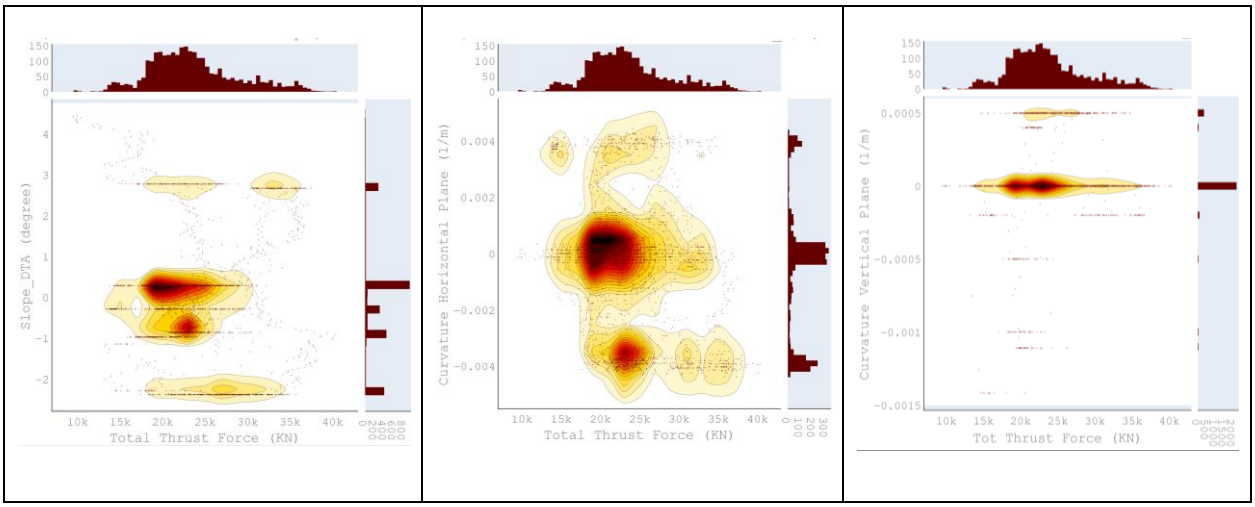

Figure 3-43 Histograme2DConture plot: total thrust force vs trajectory characteristics

Figure 3-44, is shown the histogram2Dcontour plot for anti-trust force vs trajectory characteristics parameters (slope, curvature in the horizontal and vertical plane). Also here the different zone of functionality base on the relation between anti-thrust force and trajectory characteristics were observed.

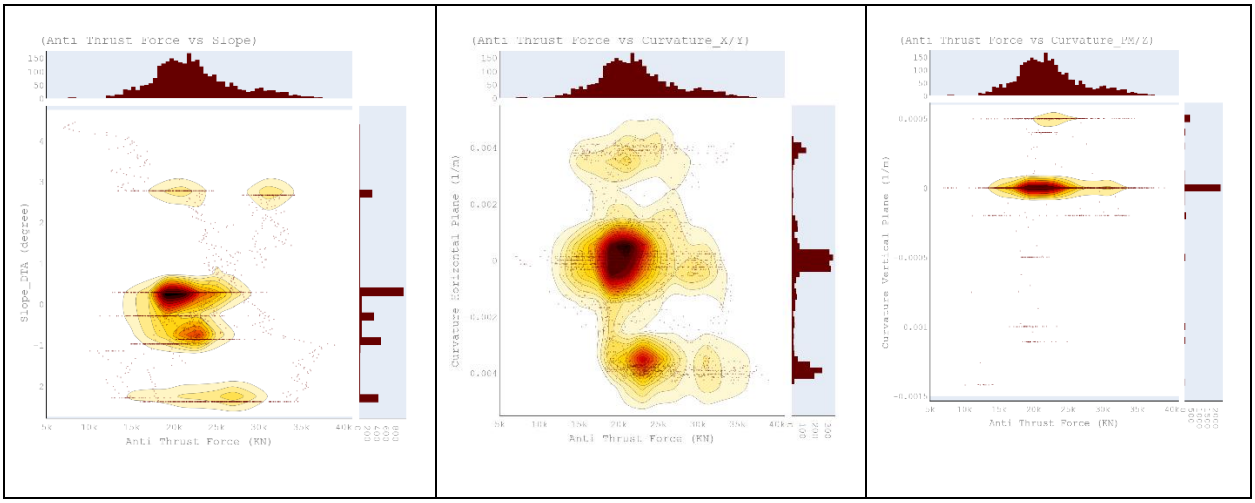

Figure 3-44 Histograme2DConture plot: Anti-thrust force vs trajectory characteristics

3.5 Conclusion

In this chapter, the importance of using data is investigated to discover knowledge for complex problem optimization, especially for the TBM process. The exploratory data analysis was presented for TBM operational and steering parameters. EDA is an essential step for pre-processing data and finding a relation between different parameters. It's also necessary to have a broad understanding for data-driven modelling (machine learning and deep learning model for the optimization of the TBM process). Different tools are available to perform Exploratory Data Analysis. In this chapter, computational and visualization tools (libraries) of python are used to better analyse and visualize the data. The most important advantage of these tools is that they are compelling and efficient for data analysis and free for use.

There are over a thousand parameters that are captured during a TBM operation. This study focused on operational data and steering parameters (trajectory characteristics). The operational data mainly is observed to understand the interaction of a TBM and evaluate forces excreted on TBM. Specially the antithrust force is proposed as an ensemble of the forces against advancement of a TBM. The antitrust force is consisting of different components such as, the force exerted on bulkhead due to confining pressure, the corrected contact force, the articulation cylinders force, the back-up force, and the tail seal friction resistance. The box plots are presented to assess the distribution of forces exerted on different parts of TBM based on data captured during TBM excavation.

Some variables such as the centre of thrust force, the inclination of the cutter head and the cutter head moment arm were calculated by using the TBM data. These variables give more comprehensible understanding of behaviour of TBM. The centre of thrust force is calculated using cylinders' geometry and thrust cylinders force. Cutter head inclination is calculated by using displacement cylinders data. The slop of the trajectory and curvature in the horizontal and vertical plane is calculated using DTA data. Then, the EDA is realized to find the association and potential correlation between operational data of TBM, the trajectory characteristics and the steering parameters. Finally, these variables will be used for data-driven modelling for TBM optimization in chapter five.

4. Evaluation of load on shield body, instrumentation of tail skin

Chapter summary:

In this chapter, an instrumentation procedure of the TBM's tail skin is proposed to capture data which represent the deformation of tail skin structure. The captured data will be used to calculate the load on the periphery of a TBM. The Finite Element Method (FEM) computation by MATLAB is implemented to compute the loads. The estimation of load on the periphery of TBM may be beneficial for different evaluation and optimization procedures. The load exerted on TBM body is very important for estimation of friction force created due to interaction of TBM and its periphery. Similarly, it can be used for finding a more precise evaluation of the balance of force on TBM. Also, it can be used for the computation optimization of the required driving force and moment of force of a TBM. Better evaluation of load applied on a TBM body will help engineers find a better interpretation and a solution for the challenges such as tail skin blockage during a TBM excavation.

4.1 Introduction

Understanding behaviour of a TBM and improving our knowledge of the physics governing the interaction of a TBM and its surrounding environment is an essential issue in TBM tunnelling. This understanding is important and beneficial for both the design stage and optimization of different operations during advancement of a TBM. There are different challenges such as uncertainties in prediction of soil settlement, evaluation of balance of force exerted, and estimation of the required torque and driving force during the TBM tunnelling advancement. As reviewed in the first chapter, there are many studies and applied research (using different methodology) to enhance reliability of computation and to improve uncertainties in TBM tunnelling. Even so, there is simplification or assumption for estimation of required thrust force and moment force as two important parameters for the evaluation of TBM behaviour. Having better evaluation regarding interaction of a TBM main body and its surroundings (evaluation of force exerted on a TBM Periphery) can help us solve previous challenges.

In 2006 Kasper et al developed a three-dimensional finite element model to analyse the influence of TBM operation parameters and design parameters for a shallow tunnel in soft soil. They presented a numerical sensitivity study on the face support pressure, the grouting pressure, the weight and taper geometry of the TBM [30]. In 2009 Nagel et al presented a finite element framework for the modelling of partially saturated soil that has been developed for the evaluation of the TBM and the surrounding ground interactions[31].

In 2011 and 2012 Festa et al developed data approaches to improve understanding of the interaction between a TBM and surrounding soil. They quantified the ‘missing link’ to equilibrate the system of forces and moments in TBM tunnelling in soft soil. Although, they had challenges for modelling the external reaction acting on the TBM (surrounding soil, excavation fluids, and interaction with the already installed tunnel lining) [32][33]. In 2013 Festa et al implemented the experimental approach based on capture of the settlement data of soil around TBM to investigate kinematic behaviour of a TBM. They captured soil displacement monitoring data by extensometers and inclinometers. They concluded that there is a relation between TBM-shield kinematic behaviour with the soil response. They also determined that in certain condition tail void grouting had an essential role on the kinematic effects of shield advance[34][35].

In this chapter a data driven approach is proposed to measure structural deformation of tail skin by installation of system of measurement. Then the calculation of load is implemented in the periphery of tail skin by numerical computation with MATLAB.

4.2 Evaluation of loads on TBM periphery

The load estimation around a TBM body has different advantages. This helps engineers improve the estimation of friction between the TBM body and its surroundings. Load calculation is useful to investigate and evaluate some technical challenges during TBM excavation such as tail skin blockage. Load evaluation on the shield body is also valuable to improve the estimation of required thrust force. Similarly, this parameter will be used in a data-driven modelling process in TBM tunnelling.

For calculation of load an indirect approach is proposed. The inclination of the tail skin structure is captured during operation of a TBM and by using the deformation parameters, the loads on the tail skin structure are computed.

4.2.1 Installation of system of measurement

For capturing data, system of measurement (nodes) is used. The instrumentation system is a nodes arrangement for measuring deformation of structures in real time. Each node is composed of different types of sensors: three analogue accelerometers, one digital 3-axis accelerometer (MEMS), one digital 3-axis magnetometer and 1 digital temperature sensor. Figure 4-1 represents a master node and normal node of a measurement system chosen for this study.

Figure 4-1 System of Measurement (master and normal nodes)

The data collected by the system is transmitted by a master node in ethernet on a local server or in 4G on the cloud depending on the needs. The data collected by this network is then processed and merged, providing a means of monitoring the structures in real time.

Table 4-1 System of measurement (nodes) characteristics

Node Characteristics	
Measures	
Deformation	Resolution 0.1 mm/m
Vibration	Maximum Frequency 1 KHz
System dimensioning	
Acquisition frequencies	40, 100, 200, 500 or 1000
Distance between nodes	1 to 50 m
Maximum deployment distance	500m

Table 4-1 contain information about the measurement characteristics and dimensioning of deployment and installation of sensors.

The placement of installation of nodes is chosen after discussion with Tunnel Lab and worksite experts. Here also it should be considered structural constrains in the interior parts of a TBM, operational limits and the accessibility of the location in the interior parts.

Figure 4-2 Placement of chain nodes (proposed for installation on longitudinal and transversal section)

Considering all technical issues, the sensors were installed on the interior skin of the tail skin. As shown in Figure 4-2, first it was proposed to install thirteen sensors on the radial section of the tail skin and five along the longitudinal section however the longitudinal line of nodes had to be disassembled due to operational issues, also it was not possible to install any nodes on the lower

section of tail skin. Finally, thirteen nodes were installed on the upper section of the tail skin. The final configuration of installed nodes is represented in Figure 4-3.

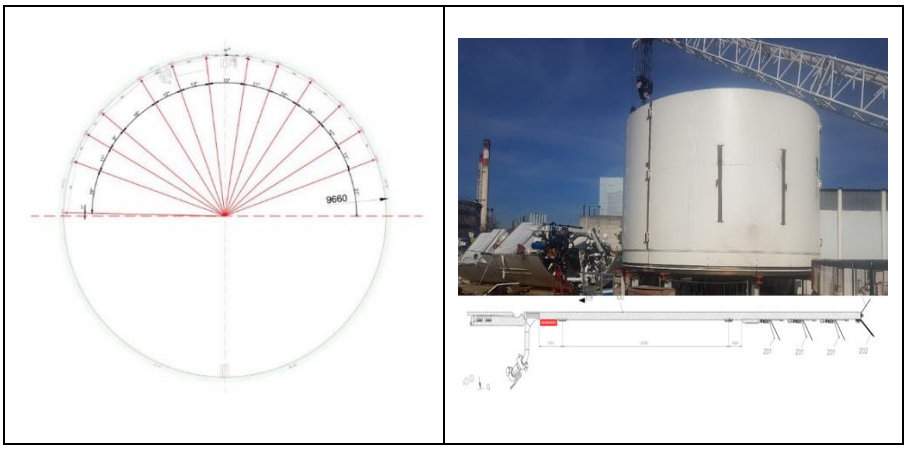

Figure 4-3 Final position of nodes, installed on the tail skin

After installation of the measurement system on the tail skin, the data was captured and the pre-processing visualization was displayed on the platform developed for this measurement system. In this platform the visualization of the captured parameters based on their time are accessible. The brut parameters and calculated values are exported as a CSV file. The difference between the reference of measurement on the TBM and the system of measurement should be considered before computation of load (Figure 4-4).

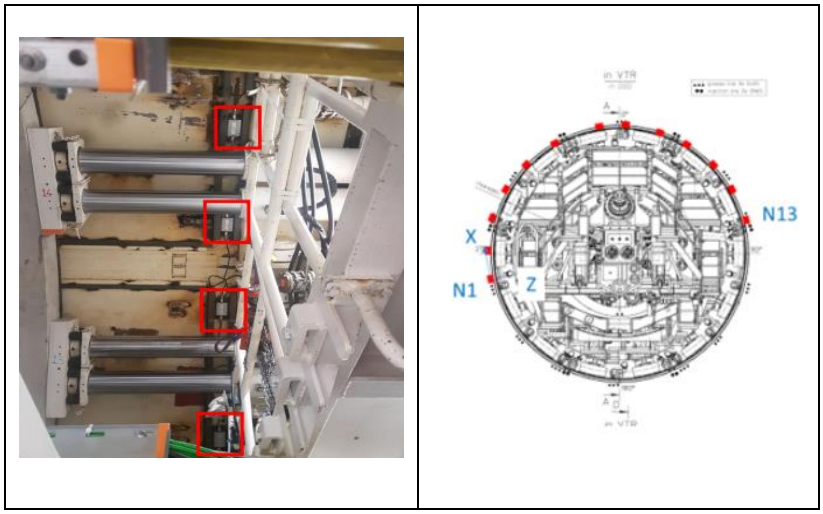

Figure 4-4 Left: position of sensors in the tail skin, right: sensor direction conventions

4.2.2 **Sensors measurement principles and indicators**

This section presents the principle of node measurement, arrangements and the main indicators that are calculated, including so-called static indicators (inclination, roll, static deformation) and so-called dynamic indicators (frequencies, spectra, dynamic deformation).

To introduce the indicators accessible by the sensors, first the measurement model of a 3-axis accelerometer is recalled. Accelerometers used in sensors measurement nodes are sensitive to the proper acceleration and acceleration linked to gravity. Each axis measures the projection of the total acceleration on the gravity axis. For a 3-axis accelerometer, this is formalized by the following measurement equation:

$$m(t,x) = R(t,x)(g - a(t,x)) \qquad \text{Equation 4.1}$$

- $m(t,x)$ is a vector of 3 dimensions which contains the measurements at the moment t of the 3-axis measurements,
- $R(t,x)$ is a 3 x 3 matrix containing the vectors $u\,(t,x)$, $v\,(t,x)$, $w\,(t,x)$ of the 3 measurement axes of the accelerometer,
- g is the vector of earth gravity,
- $a(t,x)$ is proper acceleration.

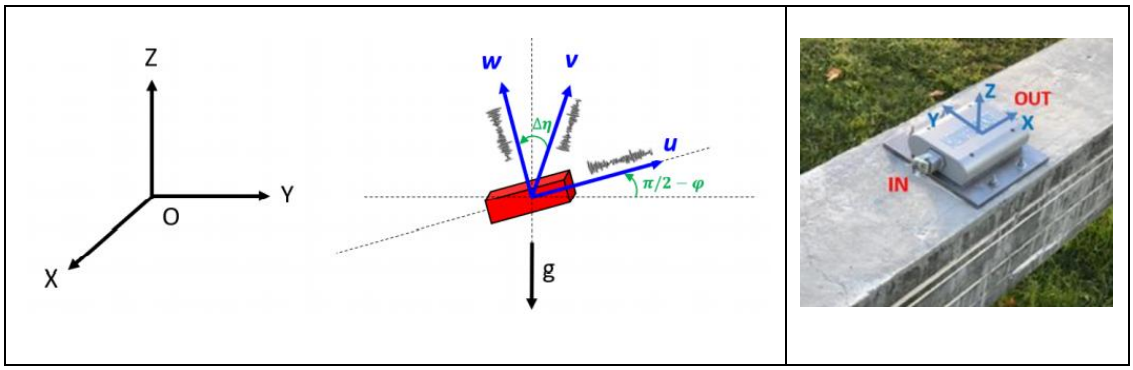

Figure 4-5 Convention and representation of the sensor axis

$m\,(t,\,x)$ is the first indicator captured by sensors systems, it is the acceleration measurement which has not undergone any post-processing (apart from calibration and temperature

compensation). It is the most general indicator. From this indicator, more specific parameters (static, seismic, statistical, among others) can be extracted according to the application context.

To introduce the static and dynamic indicators accessible via the node arrangement, the fundamental equation of accelerometer is broken down into two parts:

$m(t,x) = m_{\text{sta}}(t,x) + m_{\text{dyn}}(t,x)$	$m_{\text{sta}}(t,x) = R(t,x).g$	$m_{\text{dyn}}(t,x) = -R(t,x).a(t,x)$

This decomposition makes it possible to introduce quasi-static and vibratory modes (or hypotheses). The quasi-static hypothesis concerns the time intervals [t_0, t_0+T] where the proper acceleration is low in comparison to gravity. The measurement m (t, x) is then an approximation of the static part of the measurement. The relation becomes exact in the pure static case when the proper acceleration is zero. In the quasi-static context, the accelerometer measurement is directly related to the tilt φ and the roll η of the measurement node by the following relation:

$$m_{\text{sta}}(t,x) = g \times \begin{bmatrix} \cos(\varphi(t,x)) \\ \sin(\varphi(t,x))\cos(\eta(t,x)) \\ \sin(\varphi(t,x))\sin(\eta(t,x)) \end{bmatrix} \qquad \text{Equation 4.2}$$

Quasi-static and vibratory modes can be linked to real structure tracking configurations. The mode actually depends on the loading sources of the instrumented structure. The so-called static or quasi-static sources are related to slow phenomena which are interpreted/processed by the static structure equations i.e. where the frequency considered is zero or quasi-zero. The weight of a truck at rest on a bridge, the load of a rock on a tunnel, the difference in water height upstream/downstream on a lock gate, the dead weight of a bridge deck, the thermal fluctuation of a steel girder are examples of static sources. In the quasi-static mode, the static deformation is accessible using the inclinations measured by the measurement nodes. These inclinations are related to the angles of the tangent to the measurement points. The static deformation is deduced from these inclinations by an interpolation/integration algorithm.

4.3 Computation of load by inverse approach

After installation of measurement system, the captured data and visualization of measured data were accessible as follows. Figure 4-6 displays the inclination fluctuation of the TBM structure for each node.

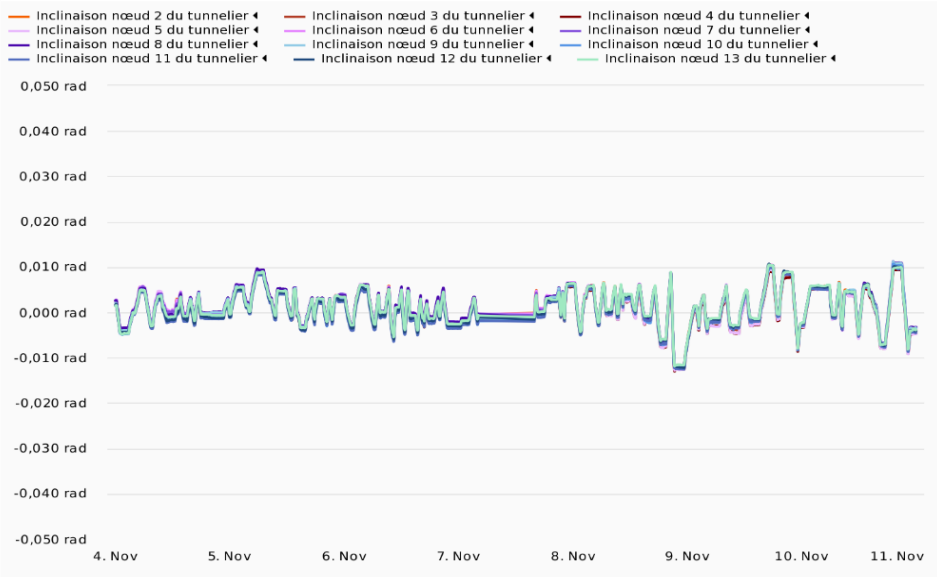

Figure 4-6 Visualisation of the measured inclination of the structure of tail skin by sensors

For computation of load the angular displacement of the TBM structure is used as input parameter, in the finite element method.

A problem of elasticity is solved if we know the displacement vector in any point of the solid. Our problem is therefore defined by an infinite number of parameters. Such a system is said to be continuous. The finite element method replaces the continuous system by a discrete model characterized by a finite number of parameters. The main steps of the finite element method are:

- Geometry is decomposed into domains of a simple geometric form (elements) linked together at points called nodes. The element used is the rectangular element with four nodes in this study, Figure 4-7.

- The displacement field in each element is defined according to the element displacement of the nodes. The state of deformation and the state of stress at any point of the element as well as the deformation energy of the element and its stiffness matrix are derived from this.
- The overall stiffness matrix is constructed from the elementary stiffness matrices.
- After setting up the boundary conditions, the unknown displacements are calculated and then, in each element, the stress and strains are calculated.

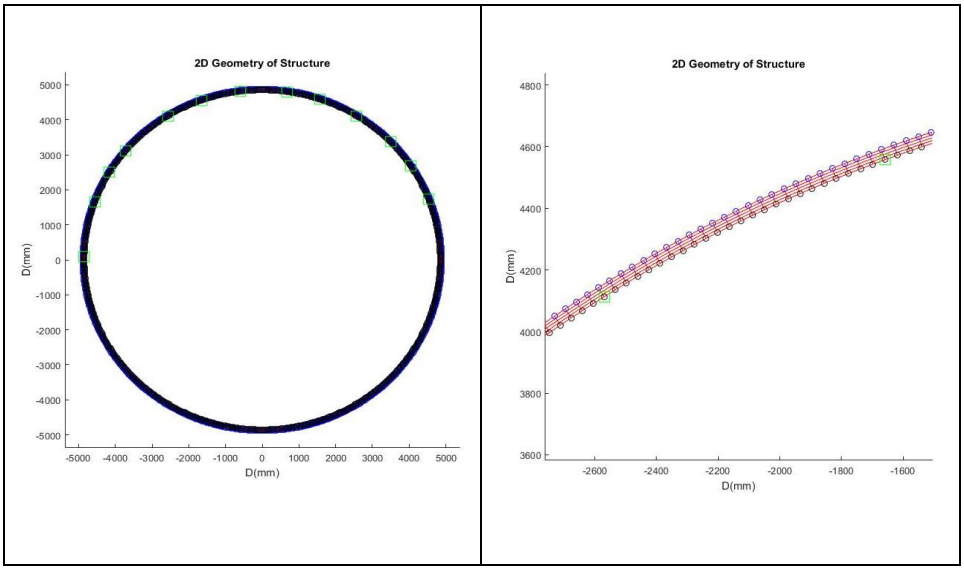

Figure 4-7 Recreating 2D geometry of structure by MATLAB (left)

rectangular mesh (right)

4.3.1 **Computation of load by Invers approach**

Considering the technical constraint of installing sensors in the interieur periphery of the tail skin, thirteen sensors are installed for measurement of inclination variation in upper parts of the tail skin. Structure inclination is captured for each sensor position. For the calculation of load, the inverse approach is developed, using deformation to calculate the load.

For implication of this approach, an optimization strategy is applied. The linear combination of the deformation is searched which sticks to the experimental deformation coming from sensors. The calculated coefficient based on deformation are used to calculate the load on the structure. As we do not apply a mathematical basis for the pressure, an approach based on the angular zone are developed for pressure calculation.

$$Deformation = a1 * D1 + a2 * D2 + a3 * D3 + \cdots$$

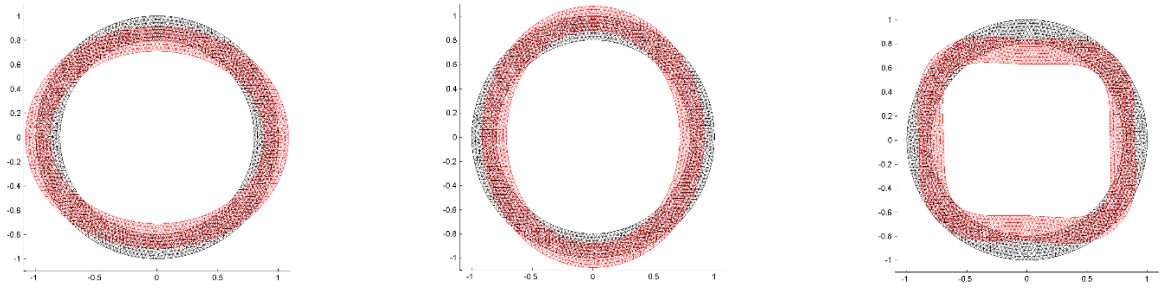

$$Pressure = a1 * P1 + a2 * P2 + a3 * P3 + \cdots$$

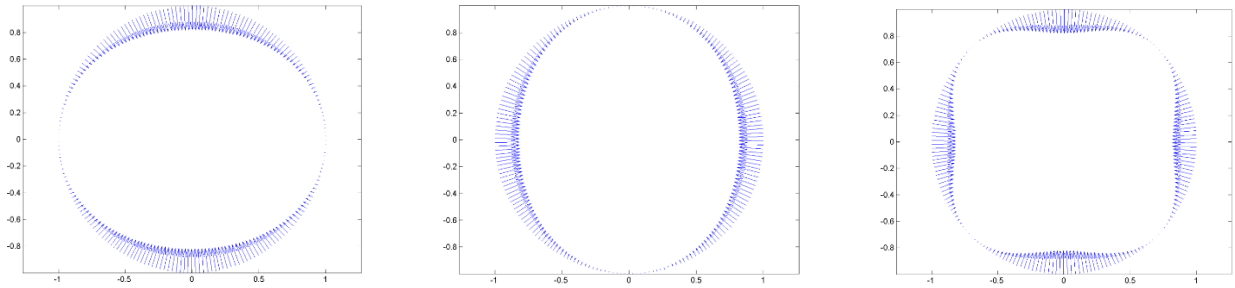

Angular zone approch

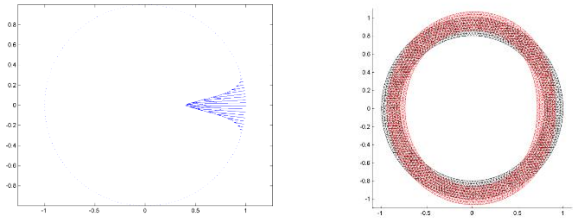

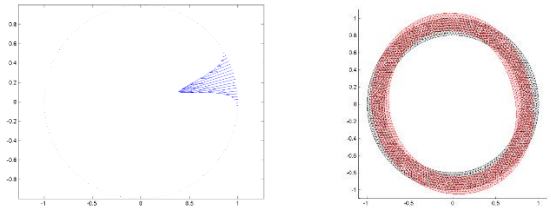

Figure 4-8 Hypothesis for calculation of load by invers approach

Figure 4-8 represents the hypotheses of computation of load by the inverse approach. For the computation of load the following hypotheses is considered:

- each pressure base distribution produces the solution of a system:

$$F_i = K * U_i \quad for \quad i = 1 \; to \; N \;\; (different \; angular \; distribution \; functions)$$

- then the displacement solution is written as follow:

$$U = \alpha_i * U_i$$

By using an optimization procedure, the α_i is calculated. The optimal value of α_i is chosen to calculate relative load on 2D transversal section on the tail skin. Based on the operational data of machine the earth pressure applied on excavation chambre of machine is around 1.75 to 2.25 bar during the first interval of investigations in September 2019. The calculated loads are between 10 to 60 kN/m2. After calculation of the load, the evaluation is made to find an association between calculated value and operational parameters of the TBM. The excavation of a TBM encountered different challenges because of technical issues and planning limits. For that reason, studies and evaluations were carried out for captured data in the periods when access was possible to both the operational data, the captured structure deformation data, and the computed loads. Figure 4-9 shows the distribution of calculated load for each sensor in a box plot during 12 days of investigation.

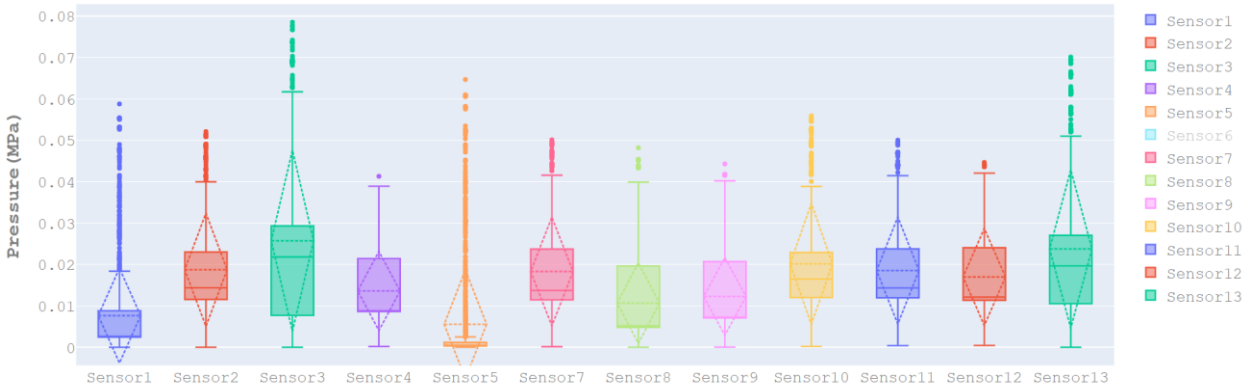

Figure 4-9 Box plot to evaluate the distribution of calculated relative load for each sensor over a period of 12 days

Figure 4-10 represents the evolution of load vs time. This observation was made for around twelve days of excavation of the TBM, as it is observable, the TBM excavated between 0 to 460 then it was stop until time 780. The variation of relative load is observable during excavation.

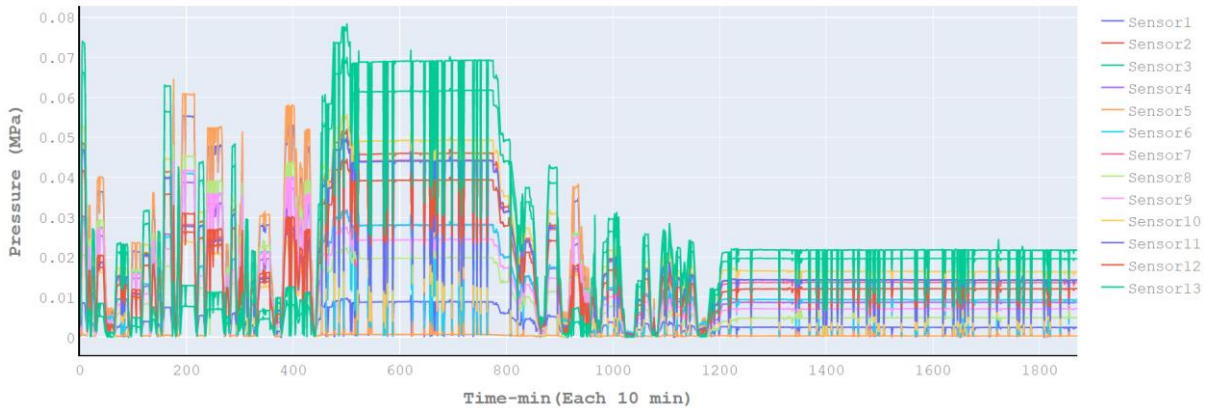

Figure 4-10 Visualization of variation of calculated relative load for each sensor during 12 days

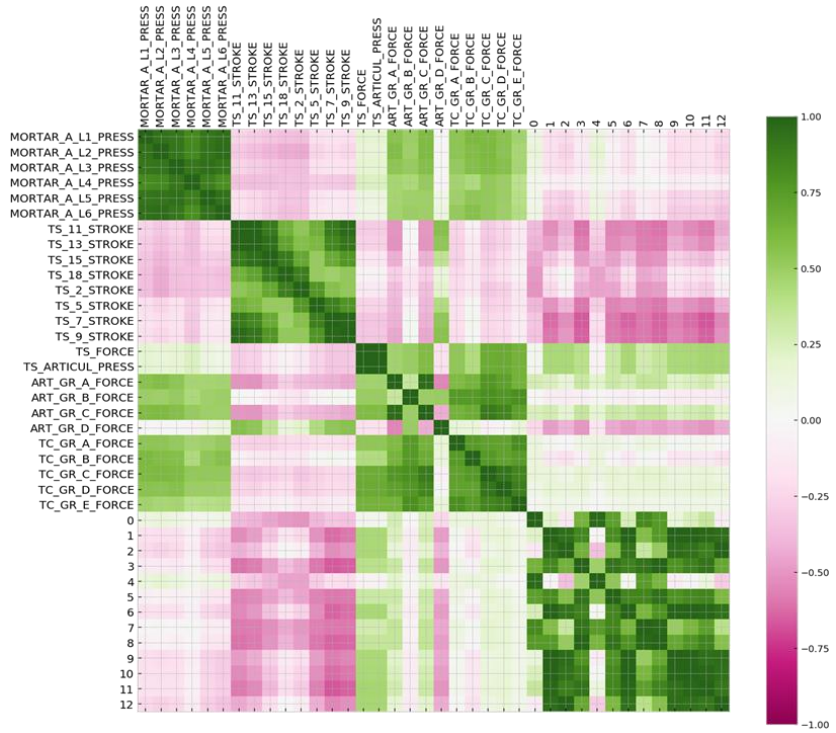

Figure 4-11 Correlation matrix of operational data and calculated relative load for 12 days of data

Figure 4-11 demonstrates the correlation matrix for operational excavation data (mortar injection pressure, elongation of tail skin cylinders, tail skin force, tail skin articulation pressure,

group of articulation cylinders force, and groups of thrust cylinders force) and calculated relative load for thirteen point. The operational excavation data are chosen based on previous parameter evaluations which have an influence on the variation of a load around a TBM body. The negative correlation is observable between calculated load and elongation of tail skin cylinders. Also, there is positive correlation between the tail skin force and pressure and calculated relative load for sensors. The second observation was made for 8 days in November 2019. Figure 4-12 represents box plot of calculated load for location of each sensors during 7 days of investigation.

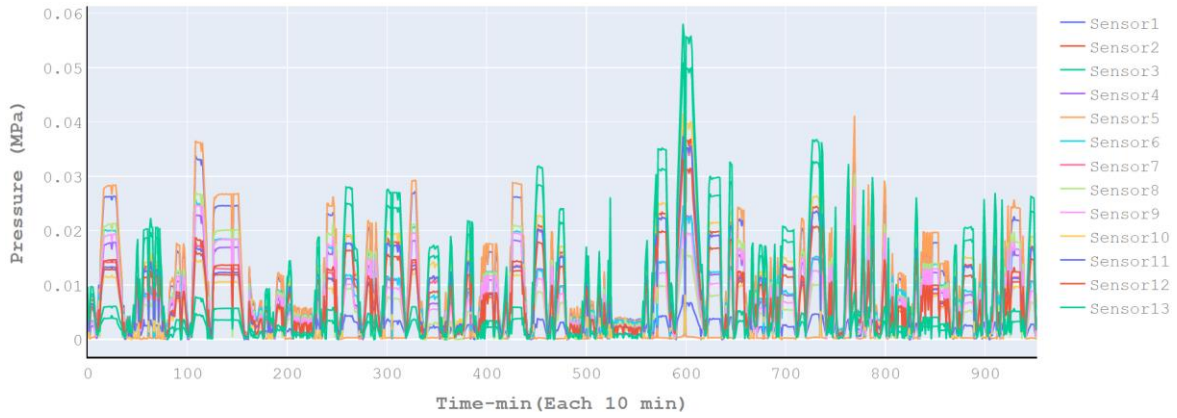

Figure 4-12 Box plot to observe distribution of calculated relative load over a period of 7 days

Figure 4-13 displays the evolution of load for second investigation. This observation was made for around 8 days of excavation of the a TBM. The variation of relative load is observable during excavation.

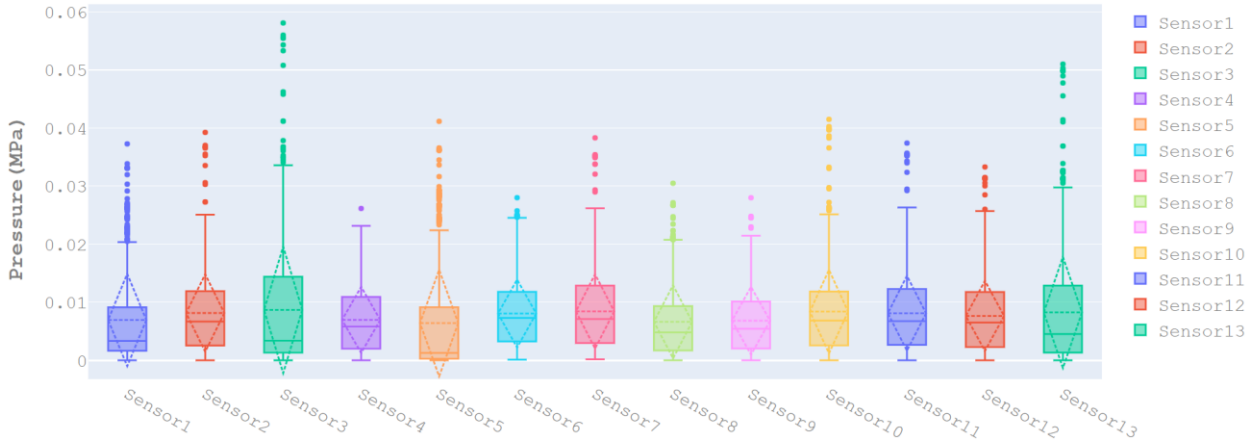

Figure 4-13 Visualization of variation of calculated relative load for each sensor over a period of 7 days

As observed in second investigation the calculated relative loads are between 10 to 50 kN/m2. Figure 4-14 demonstrates the correlation matrix for operational excavation data and calculated relative loads. Here there is not a similar correlation to a previous study between operational parameters and calculated load. There is a light correlation between mortar operational parameters (injection pressure, tail skin force and pressure and group of thrust cylinders force) and calculated loads.

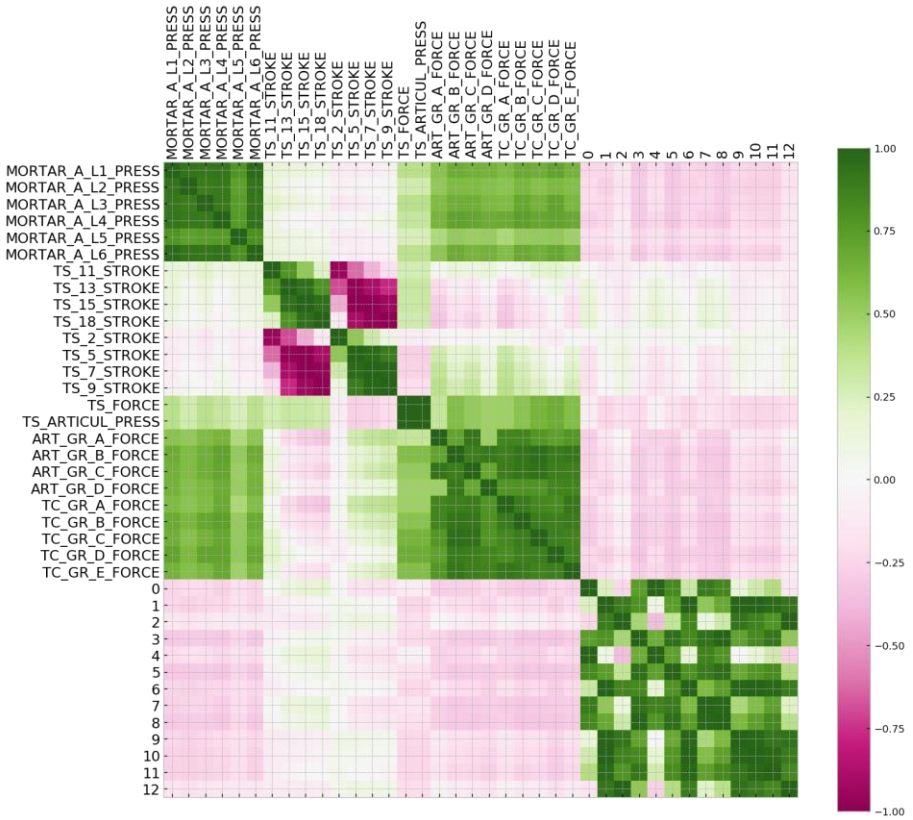

Figure 4-14 Correlation matrix of operational data and calculated relative load over a period of 7 days

In this case, correlation and anticorrelation between tail skin cylinders stroke is obvious as a result it may be more meaningful to investigate probable association of trajectory characteristics parameters, operational parameters and calculated loads.

4.4 Conclusion

As discussed, and reviewed in the second chapter, one of the challenges in TBM design and operational parameters assessment is the evaluation of load around TBM. This evaluation could be critical for improving the calculation of the required thrust force and required torque for the advancement of a TBM. Also, the calculation of load on the periphery of a TBM may improve our estimation of friction force due to interaction of a TBM and its environment.

The general idea was an inverse approach for the calculation of load based on structure deformation. As TBM operations and structural design is too complicated, there is not any available location to install sensors on the external section of TBM. Also, the internal part of a TBM has structural complexities; as a result, there are not many accessible positions for installation of sensors. One of the best locations for installation of sensors was the internal part of the tail skin. First, sensors are installed in a complete transversal section with one line in longitudinal section of the tail skin, however due to operational limits, thirteen sensors were installed on a transversal section of the tail skin (upper part) to calculate deformation based on inclination measured by sensors. The sensor data value (inclination of structure) is too small between 10^{-3} to 10^{-4} radian. For the first evaluation, data was captured during six months of excavation. There are some technical and planning issues during excavation of a TBM. As a result, the calculation and evaluations were developed for part of the accessible data.

The inclination calculated by sensors was in radian and the load was calculated on MPa. The Finite Element computation is applied to calculate the load on the tail skin. Our problem was observed in two-dimension structure (X-Y, transversal section) of a TBM. An optimization approach was applied to calculate the relative load on the structure, based on the comparison of the result between deformation calculated from FEM computation and experimental inclination that came from sensor data. By using the optimization approach, relative value of load applied on TBM are estimated. Finally, the potential association between calculated load and operational parameters of a TBM was observed. As observed, there are correlations between some of the operational parameters and calculated loads although these correlations could change according to different excavation intervals based on geological characteristics and trajectory characteristics.

5. Data-driven methods for TBM steering optimization

Chapter summary:

This chapter looks at a data-driven approach (finding a statistical learning model) between TBM data (operational parameters, geological parameters and trajectory characteristics) as inputs and steering parameters (Pitch and Yaw) of TBM as the output of the model (Pitch and Yaw considered as horizontal and vertical tendencies of TBM during advancement). As a first step, typical regression algorithms are observed. A spot-check of regression algorithms for this purpose is presented in this chapter. Then Multilayer Perceptron (MLP neural networks model) architecture on our data structure is implemented to find the optimal model for TBM operational data. A hyperparameter evaluation of algorithm is implemented to find the optimal configuration for the proposed model. Finally, the accuracy of the model is investigated by testing the model for different segmentations of the TBM trajectory characteristic.

5.1 Introduction

Following the rapid progress in hardware and software technologies (fast evolution of computational capabilities) and data acquisition system developments (accessibility to larger data) data-driven approaches has been used as efficient approach to solve many complex problems. During last year's data-driven approaches has been used to propose models for improvement of TBM performance and solving some of technical challenges during mechanized tunnelling.

In 2004, Benardos et al developed an Artificial Neural Network (ANN) approach to model the advance rate of tunnelling with respect to the geological and geotechnical site conditions [36]. In 2010, Javad et al developed the studies on the application of ANN techniques for modelling of the penetration rate of TBM. They used a database consist of TBM penetration rates, uniaxial compressive strengths of the rock, the distance between planes of weakness in the rock mass and rock quality designation (RQD) parameters [37]. In 2014, Mahdevari et al developed a regression model to predict penetration rate of TBM in hard rock conditions based on a Support Vector Regression (SVR) algorithm[38]. In 2016, Salimi et la developed an artificial intelligence models for TBM performance prediction. They performed different machine learning algorithms for this study such as Principle Component Analysis (PCA), Adaptive Neuro-Fuzzy Inference System (ANFIS) and Support Vector Regression (SVR). Based on their results they concluded that AI based methods can effectively be implemented for prediction of TBM performance[39]. In 2017, Namli et al created a model to predict daily advance rates of EPB-TBMs in a complex geology in Istanbul. The methodology was based on predicting field specific energies and comparing cutting power of EPB-TBMs[40]. In 2019, Xu et al developed the study and presented applications of supervised machine learning techniques in predicting the penetration rate of a TBM. They used an experimental data base based on field observations and laboratory tests for a tunnelling project in Malaysia. In the database, uniaxial compressive strength, Brazilian tensile strength, rock quality designation, weathering zone, thrust force, and revolution per minute of TBM were utilized as inputs to predict penetration rate of TBM[41].

In 2009, Yagiz et al proposed a study for the construction of non-linear multivariable prediction models to estimate TBM performance as a function of rock properties. They use Artificial Neural Networks(ANN) and the non-linear multiple regression methods [42].

In 2010, Boubou et al developed a research to find correlation between ground surface movements and TBM operation parameters. They used data from the excavation of the subway line B tunnel in Toulouse, France. They proposed two approaches (Least Square Approximation and ANN) [43]. In 2016, Lai et al published a review on application of ANNs on the tunnel performance prediction (tunnel deformation prediction). They determined that ANNs have some advantages, for prediction of rock mass deformation including self-learning ability, self-organized ability, high nonlinearity, good fault tolerance capability, and calculation inaccuracy[44].

In 2018, Wei et al proposed a dynamic load prediction approach based on using a data-driven technique. They used Random forest algorithm to construct the prediction model based on the integrated heterogeneous in-situ data[45]. In2019, Zhao et al proposed a data-driven framework to build a predictor for geological types of ground in front of TBM based on TBM operating data. The framework contains three stages: data acquisition, data pre-processing and learning models [46].

In 2020, Leng et al developed a hybrid data mining approach to process the real-time monitoring data from TBM automatically. Three different data mining techniques were combined to improve mining process and support safety management process[47]. In 2020, Shahrour et al published a review on soft computing technique to solve the complex problems related to TBM tunnelling. They proposed recommendations for the optimal use of these techniques. They concluded that engineering analysis is required to select the most significant input parameters for preparation of deployment of soft computing techniques [48].

5.2 What is Data-Driven model?

Data-Driven Modelling (DDM) is based on analysing and evaluation of the data about a system, specially finding connections between the system state variables (input, internal and output variables) without explicit knowledge of the physical behaviour of the system. These approaches consist of large, efficient fields and methods such as[49]:

- Artificial Intelligence (AI): developing of the computer systems to be able to perform normal human tasks (which require intelligence)

- Computational Intelligence (CI): include Machine Learning and Deep Learning (Artificial Neural networks)
- Soft Computing (SC): SC is close to CI; this term is presented by L.A. ZADEH in 1992. SC is defined as a group of computational techniques based on artificial intelligence (human like decision) and natural selection that provides quick and cost-effective solution to very complex problems for which analytical (hard computing) formulations do not exist [50]. SC focus more on fuzzy-ruled based systems induced from data.
- Data Mining and Knowledge Discovery in Databases are concentrated more on big data and its application on different sector such as finance, industry, customer services etc.

The benchmarking of typical statistical learning methods is observed (machine learning and deep learning algorithms) for our problems (optimization of TBM operation).

Artificial intelligence, statistical learning, machine learning and deep learning are terms that we hear too much these days. All of them can be considered as the Data-Driven approaches with a practical definition. As a simple definition Artificial intelligence can be considered as a program that can sense, reason, act, and adapt. Statistical learning includes Machine Learning and Deep Learning.

The term statistical learning is fairly new. The general definition of statistical learning is the combination of tools for understanding captured data. Those tools are divided into two categories, supervised learning and unsupervised learning. Supervised learning involves a statistical model for estimating or predicting an output based on one or multiple inputs. In unsupervised statistical learning there are inputs but there is no supervising output. In statistical learning we observe a quantitative response and different predictors (input variables). There is assumption that between output and input variables, a sort of relation exists as follow:

$$Y = f(X) + \epsilon \qquad \text{Equation 5.1}$$

Here f (target function) is some fixed but unknown function of X_1, $X_{2, \ldots.}$ $X_{p,}$ and ϵ is a random error term, which is independent of X and means zero. In this formulation f represents the systematic information that X provides about Y. There are two main reasons for the estimation of

f, estimation and inference[51]. There are also many linear and nonlinear approaches for estimation of f. This is general learning task; we aim to make a prediction for the future Y given a new example of input X. This approach is called predictive modelling or predictive analytics and the goal is to make the most accurate possible predictions.

Machine learning is the term born from the identification of pattern and the idea that computers learn for specific tasks. Artificial intelligence is interesting for researchers and scientists because they think these methods would help us to solve complex problems in different sectors. Machine Learning can be considered as algorithms whose performance improve as they are exposed to more data (data chosen based on the best understanding and characteristics of the problem) over time. A machine-learning system is trained rather than explicitly programmed. It is presented with many examples relevant to a task, and it finds statistical structure in these examples that eventually allows the system to come up with rules for automating the task[52].

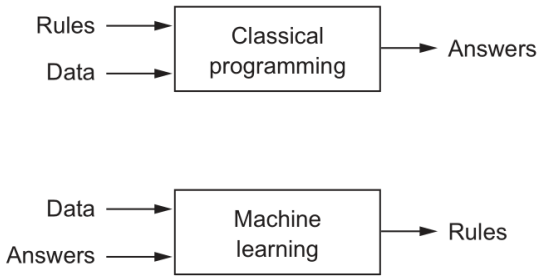

Figure 5-1 Programming a new paradigm: Machine learning (F. Chollet.2018)[52]

One of the most important challenges in machine learning and deep learning is to meaningfully transform data or to learn useful representation (different ways to look at, represent or encode) of input data which brings us closer to a desirable output. All Machine learning algorithms consist of transformations such as coordinate change, linear projection, translation, non-linear operations and so on to turn data into more effective and useful representations for a given task.

Deep learning is a subset of machine learning with networks capable of learning supervised and unsupervised to unstructured or unlabelled data. Deep Learning is considered a subset of machine learning in which Multi-layered Neural Networks learn from vast amounts of data. Deep learning puts an emphasis on learning successive layers of increasingly meaningful representations. Deep

learning dose not lead to a deeper understanding. In effect, the number of layers contributed to a model of the data is called the depth of the model.

5.2.1 Parametric and non-parametric machine learning approach

Parametric machine learning algorithms help us to simplify the mapping to a known functional form. Non parametric algorithms can learn any mapping from inputs to outputs[53]. A learning model that summarizes data with a set of parameters of fixed size (independent of the number of training examples) is called a parametric model. No matter how much data you throw at a parametric model, it won't change its mind about how many parameters it needs[54]. Some examples of parametric machine learning algorithms are logistic regression, linear discriminant analysis, and perceptron.

Algorithms that do not make strong assumptions about the form of the mapping function are called nonparametric machine learning algorithms. By not making assumptions, they are free to learn any functional form from training data. Nonparametric methods are good when you have a lot of data and no prior knowledge, and when you do not wish to worry too much about choosing just the right features[54]. As example of non-parametric machine learning algorithms, the K-Nearest Neighbours (KNN), Decision Trees, Naïve Bayes, Support Vector Machines (SVM), and Neural Networks could be mentioned.

5.2.2 Bias and variance

Generally bias refers to the simplifying assumption made in the algorithms structure to accomplish easier problem solving. The variance can represent either the sensitivity of a model or the changes to the training data. In supervised machine learning (supervised statistical learning) prediction error can be divided into three main group: Bias error, Variance error and irreducible error.

Th irreducible error cannot improve regardless which algorithm is used. The bias error is the assumption chosen by a model to make target function easier to learn. Generally parametric algorithms have a high bias, making them fast to learn and easier to understand although less flexible. Examples of low-bias machine learning algorithms include: Decision Trees, K-Nearest

Neighbours and SVM. Examples of high-bias machine learning algorithms include: Linear Regression, Linear Discriminant Analysis (LDA) and Logistic Regression.

Variance is the value of the change of estimation of the target function based on the change of training data. Low variance represents small changes to the estimation of the target function with changes to the training dataset. Hight variance represents large changes to the estimation of the target function with changes to the training dataset. Generally nonparametric machine learning algorithms that have a lot of flexibility have a high variance. For example, decision trees have a high variance, that is even higher if the trees are not pruned before use. Examples of low-variance machine learning algorithms include: Linear Regression, LDA and Logistic Regression. Examples of high-variance machine learning algorithms include: Decision Trees, KNN and SVM[53].

5.2.3 **Overfitting and underfitting in Machine Learning**

Overfitting means learning training data very well but the model is not really generalized. On the other hand, overfitting means there is a significant discrepancy between errors on the training data and errors on the test data. The Performance of machine learning algorithms is evaluated by overfitting or underfitting data. Overfitting is generally described when a model learns the detail and noise in the training data that negatively impacts the performance on the new data.

Underfitting refers to failing to learn the problem from the training data. An underfit machine learning model is not a suitable model and becomes obvious as it has poor performance on training data. A good fit model is the spot between underfitting and overfitting. Occurrence of overfitting and underfitting leads to poor model performance. Most of the time in applied machine learning overfitting is the main problem. There are two techniques that can be used for the evaluation of machine learning algorithms to limit overfitting, using resampling techniques to estimate model accuracy and creating a validation dataset. Validation data set is a subset of training data that are hold back from learning until the end of training. The learned models can be evaluated on the validation dataset to get a final objective idea of how the models might perform on unseen data. Cross-Validation (CV) is a technique in applied machine learning for evaluation of models by training several ML models on the subset of data.

5.3 TBM steering optimization using ML algorithms

TBM steering is an operation which depends on different parameters from operational parameters to guiding parameters and geological characteristics of the ground. Also, as mentioned in chapter two TBM interactions depends on the configuration of machine. In the first study the data driven approach for predictive modelling was observed. The goal is finding a statistical learning model (machine learning, deep learning model) for optimization of TBM operation. In the first study operational parameters for the learning procedure were chosen. Figure 5-2 shows the general diagram of applying statistical learning for optimization of TBM steering.

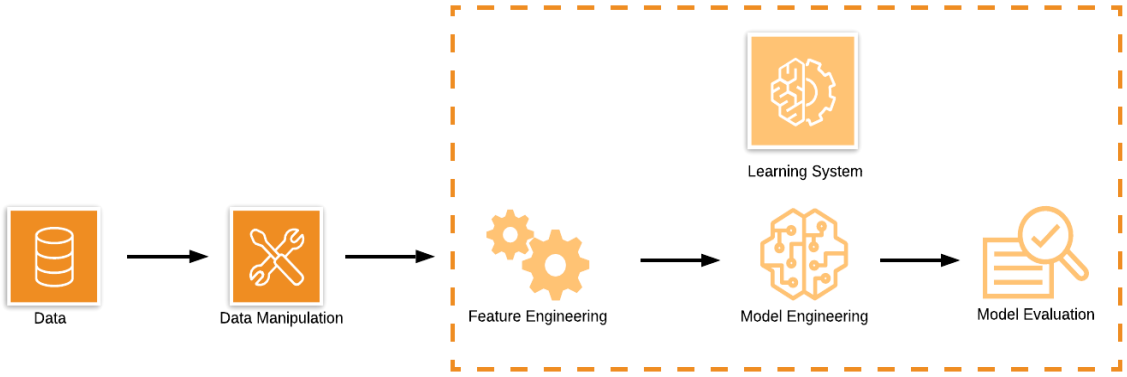

Figure 5-2 General diagram for statistical learning system

Table 5_1 shows the first group of operational parameters chosen as input and output parameters. There are different machine learning algorithms which are used for predictive analysis (regression problems). In Regression task, the computer program is asked to predict a numerical value given some input. To solve this task, the learning algorithm is asked to output a function.

There is a same principle and logic that lie beneath all supervised machine learning algorithms for predictive modelling. The most common type of machine learning is to learn the mapping Y = f(X) to make predictions of Y for new X. This is called predictive modelling or predictive analytics and the main goal is to make the most accurate predictions possible. By learning the mapping more was learnt about the relationship in the data (statistical inference). By learning a function, the form of function are estimated from the available data. Our estimation is not the perfect one. This estimation has errors and in applied machine learning many efforts is made to improve the

estimation. Machine Learning algorithms are tools for target function estimation. Different Machine Learning algorithms have different assumptions with regards to the function structure. Also, there are different methods for optimization and approximation of function representation.

For the benchmarking of machine learning algorithms for regression problems, 10 common regression algorithms run were chosen as an initial study. All the algorithms were carried out by using Scikit-learn library[55]. Without wishing to explain the details of each regression algorithms, main goal is to find the algorithms that could learn better generalized learning for data structure and creating a model with fewer errors. In this part all data are numeric.

Table 5-1 Input & output parameters for first study

Input	Output
Centre of thrust force	Pitch and Yaw (mm/m)
Thrust cylinders pressure	
Articulation cylinders pressure	Machine local position Y and Z (m)
Displacement cylinders pressure	
Mortar injection and grease injection pressure	
Backup force	Delta Y and Z Machine deviation (mm)
Contact force	
Confining pressure	

During the study, there were three important steps, choosing features, preparing data and the interpretation of the results. In the Spot-check of different algorithms same dataset (Nice-Tramway data) was used. In this study k-fold cross validation were employed to check each Machine Learning algorithms. Cross-validation is a statistical method applied to estimate the skill of machine learning models. By using the cross validation generally, lower bias is acquired. By using k-fold cross validation actually k different model is built. Prediction were made and as a result, the prediction is more accurate by using cross validation. More accurate metrics can be obtained and better decisions and conclusions regarding algorithm results and data. Another important role of cross validation method is the ability and usefulness in parameter fine tuning. Normally all learning

algorithms need a sort of parameter tuning. For example, the number of trees in a random forest, a hidden layer size or activation function in neural network etc. Cross validation is a powerful means to better use data and give further information about the performance of algorithms.

For the evaluation of algorithms performance based on the type of algorithms there are different metrics. In regression problems there are various metrics to evaluate the result of prediction, such as:

- Mean Squared Error (MSE),
- Root Mean squared Error (RMSE),
- Mean Absolute Error (MAE),
- R^2 (Coefficient of Determination).

Mean squared error is used as one of the preferred metrics for regression problems. MSE is the average of the squared difference between the target value and the value predicted by the model. One of the advantages of the MSE is that it is differentiable and is better optimized.

$$\text{MSE}\ (y, \hat{y}) = \frac{1}{n_{\text{samples}}} \sum_{i=0}^{n_{\text{samples}}-1} (y_i - \hat{y}_i)^2 \qquad \text{Equation 5.2}$$

True value: y_i,

The predicted value of ith sample: $\hat{y}_i$.

Root Mean Squared Error (RMSE) is the squared root of the MSE. In some cases, RMSE is preferred because the errors are first squared before averaging which poses a high penalty on large errors.

Mean Absolute Error (MAE) is the absolute difference between the target value and the predicted value. MAE is a linear score which means all the individual differences are weighted equally. It is not suitable for applications where you want to pay more attention to the outliers.

$$\text{MAE}\,(y,\hat{y}) = \frac{1}{n_{\text{samples}}} \sum_{i=0}^{n_{\text{samples}}-1} \left|y_i - \hat{y}_i\right| \qquad \text{Equation 5.3}$$

R2 or Coefficient of Determination is used to evaluate a model with a constant baseline. It represents the proportion of variance (of y) that has been explained by the independent variables in the model. It provides an indication of size accuracy of fit and therefore a measure of how well unseen samples are likely to be predicted by the model, through the proportion of explained variance.

$$R^2(y,\hat{y}) = 1 - \frac{\sum_{i=1}^{n}(y_i - \hat{y}_i)^2}{\sum_{i=1}^{n}(y_i - \overline{y})^2} \qquad \text{Equation 5.4}$$

The average of y_i: $\overline{y}$,

The benchmarking of regression algorithms is done for 4 linear algorithms and 6 non-linear algorithms. Table 5-2 shows the result of applying algorithms for two scenario using articulation parameters in input variable and without articulation parameters. The data used for this study is for the Nice Tramway project. Each time an algorithm for one output variable (single output) is run the accuracy of the result as a single variable prediction is evaluated.

As observed in the results the best algorithms for this project data (Nice Tramway) was non-linear algorithms giving results in comparison with a linear one. The main issue here is that the prediction is not generalized for other projects (TMCLK-880 &882). It means that the algorithm run for one project could not give accurate prediction for other projects. The first possible reason is the configuration difference between TBMs. Another issue of this study is that geological parameters are not considered in the input parameters which can have inevitable influence on the interaction of a machine with its environments.

Table 5-2 Algorithms results: benchmarking of regression algorithms

Algorithms	Different Output Scenarios							
	Machine No Articulation (1812(Ring)-62(Var)) (MachineParameters)		Machine with Articulation (1812(Ring)-84(Var)) (MachineParameters)		Ring No Articulation (1812(Ring)-62(Var)) (RingParameters)		Ring With Articulation (1812(Ring)-84(Var)) (Ring-Parameters)	
	Y	Z	Y	Z	Y	Z	Y	Z
	R2	R2	R2	R2	R2	R2	R2	R2
Linear Regression	0.836	0.717	0.872	0.756	0.836	0.845	0.872	0.884
Ridge	0.834	0.716	0.865	0.754	0.834	0.845	0.865	0.884
Lasso	0.814	0.582	0.849	0.621	0.814	0.677	0.849	0.721
ElasticNet	0.834	0.609	0.877	0.644	0.834	0.715	0.877	0.753
KNN	0.657	0.378	0.868	0.655	0.657	0.436	0.868	0.774
DecisionTreeRegressor	0.896	0.735	0.919	0.746	0.901	0.845	0.933	0.852
Random Forest Regressor	0.890	0.727	0.894	0.725	0.889	0.853	0.894	0.850
Extra Trees	0.967	0.835	0.980	0.834	0.966	0.955	0.982	0.964
MultiO/P GBR Regressor	0.861	0.699	0.878	0.827	0.878	0.833	0.906	0.875
MultiO/P AdaB	0.557	0.438	0.546	0.436	0.557	0.509	0.547	0.508

Figure 5-3 represents the comparison of root mean squared error calculated by different regression algorithms. This plot is used to find the response with minimum error.

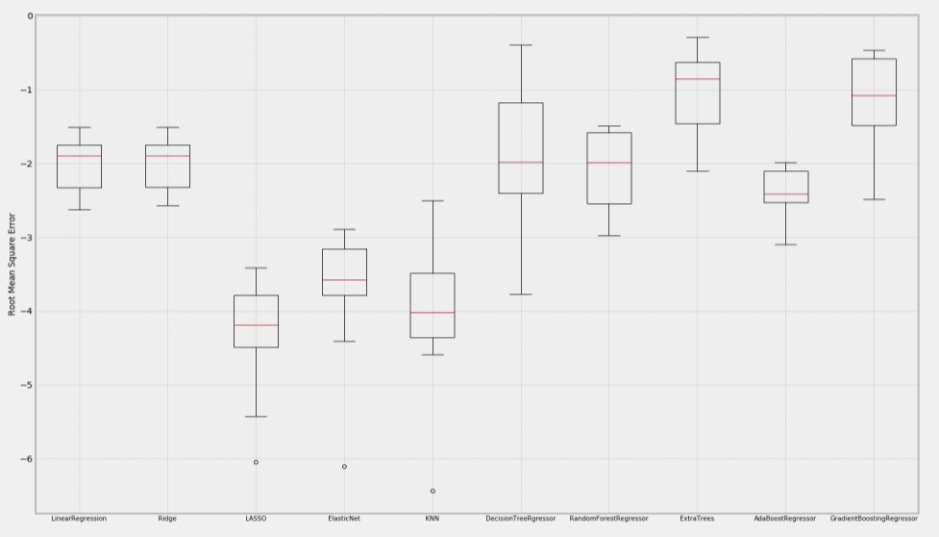

Figure 5-3 RMSE comparison for regression algorithms results (box plot)

Second study carried out on the portion of the project data such as the first 200 meters of tunnel advancement (between 50 to 250 meters) is then a verified learned model on the other portions. In this study the same input parameters and output parameters were used. The algorithms used for this purpose are linear regression, decision tree, random forest and extra tree regression.

Table 5-3 Algorithms results: benchmarking of regression algorithms (second study)

	Linear Regression		**Decision Regression**		**Random Forest**		**Extra Trees**	
	Yaw	**Pitch**	**Yaw**	**Pitch**	**Yaw**	**Pitch**	**Yaw**	**Pitch**
PM	**R2%**	**R2%**	**R2%**	**R2%**	**R2%**	**R2%**	**R2%**	**R2%**
50-250	67	30	82	29	86	65	90	72
50_275	66	36	71	1	94	78	92	80
50_300	-21	-527	51	-1	90	60	90	68
50_350	-136	-315	14	-80	77	47	74	51
50_500	-201	-356	-17	-15	66	20	63	4
50_700	-183	-15	-18	15	57	26	54	22
50_900	-159	-630	-19	16	45	19	51	11
50_1100	-151	-559	-21	16	41	21	43	13
50_1300	-140	-511	-19	12	32	18	37	11
50_1500	-128	-472	74	37	29	17	-6	11

As presented in Table 5-3 the results of the algorithms for different portion is not generalized. Here the input feature should be reviewed. Also, another issue here is that the configuration of a machine and the ground geomechanical characteristics are different for each project.

5.3.1 Feature engineering and data dimensionality reduction procedures, to simplify understanding and improve learning performance

As observed in previous section different Machine Learning algorithms cannot give us an appropriate answer. As a result, it was decided to reselect our input features and apply feature engineering techniques to improve feature selection.

Feature selection techniques consist of different methods which are used to improve learning procedures, such as:

- Imputation
- Handling outlier
- Binning

- Log transform
- One-Hot encoding
- Feature split
- Scaling

Imputation is applied for “Nan” values. There are different methods for handling “Nan” values in a data frame. Imputation is more preferable because it preserves the data size. Handling outlier by visualization is another step to take for high decision precision. Outlier detection can also be performed by statistical methodologies (using standard deviation or percentile), the advantage of using a statistical method is that they are fast.

Feature binning is another feature engineering technique of turning continuous variables into categorical values. It is used to make a model more robust and prevent overfitting, however, it has a cost to the performance. However, this has a performance cost. Each time binning is used, part of the information is forgone, making data more regularized.

Log transform (log transformation) is a mathematical transformation in feature engineering. It is used to handle skewed data; the distribution of data becomes more approximate to normal after transformation. Log transform could decrease the effect of the outliers (due to normalization of magnitude differences). Log transform applies only to positive values.

One-hot is mostly used for encoding data in machine learning. One-hot encoding spreads the column values to multiple columns and assigns 0 or 1 to them. Binary values show relationship between grouped and encoded columns. This method helps us to change categorical data which is challenging to understand for algorithms, to numerical value and enable us to use categorical data without losing any information.

Normally, in complex problems numerical features do not have the same unit and range. By using scaling, the continuous features could be comparable in terms of range. Some algorithms used only scaling features such as KNN or K-Mean (the algorithms based on distance calculation) but this process is not obligatory for many algorithms. There are two main types of scaling:

- Standardization
- Normalization

The standardization (Z-score normalization) would rescale features with the average (mean-μ) equal to zero and standard deviation (σ) of 1.

$$z = \frac{x - \mu}{\sigma} \qquad \text{Equation 5.5}$$

Standardizing the features so that they are centred around 0 with a standard deviation of 1 is not only important if we are comparing measurements that have different units, but it is also a general requirement for many machine learning algorithms.

Normalization (min-max normalization) rescaled all the feature values in a fixed range of 0 and 1. In this rescaling method, feature value distribution does not change due to the decrease of the standard deviation although the effect of outliers increases.

$$X_{\text{norm}} = \frac{X - X_{min}}{X_{\text{max}} - X_{\text{min}}} \qquad \text{Equation 5.6}$$

Which one should be used standardization or normalization? The answer depends on the application.

Dimensionality Reduction of Data

There are three fundamental techniques that will help us to summarize data information content of data set by transforming it onto a new feature subspace with lower dimensionality.

- Principle Component Analysis (PCA)
- Linear Discriminant Analysis (LDA)
- Non-linear dimensionality reduction via kernel principle component analysis.

Using dimension reduction techniques, such as PCA helps better understanding and extract features which help solve problems (find pattern between features and reduce dimension of datasets) with minimum loss of information. Feature extraction can be applied to minimize the number of features in our dataset (whenever there are many input features). Feature extraction can

be used to transform and project data onto new feature space. Dimension reduction is typically used to improve computational efficiency.

PCA is an unsupervised linear transformation technique that is widely used across different fields, most prominently for dimensionality reduction. It helps identify patterns in data based on the correlation between features. Desired result of the PCA is to project a feature space onto smaller subspace that represent the data. The orthogonal axes (principal components) of the new subspace can be interpreted as the directions of maximum variance given the constraint that the new feature axes are orthogonal to each other as illustrated in the following Figure 5-4 [56].

Applying PCA consists of following the main steps:

- Initial extraction of the components
- Determine the number of components
- Rotation of axes
- Interpretation of the rotated solution
- Created component

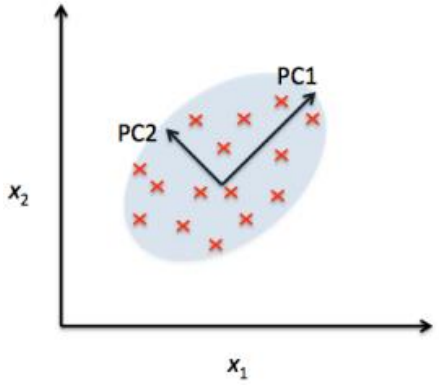

Figure 5-4 PCA orthogonal axes of the new space[56]

Data set preparation for PCA

After feature observation in chapter two another data set was selected to do dimension reduction (principle component analysis) then, to apply this data on another learning algorithm (multi-layered neural network). Figure 5-5 shows the correlation matrix of the new dataset. As can be seen there are more meaningful correlations between parameters (positive or negative correlation).

Correlation between altitude, total trust force and anti-thrust force is significant. A lower degree of correlation between Z projection of the thrust force centre (ThrustCenter_Z), thrust force and anti-thrust force are observed. Curvature projection on horizontal plane (Curvature_HP) shows modest negative correlation with thrust force and anti-thrust force.

Project geological information was also added in this data set including geological data from segmentation of geological plans. Based on geological plans 6 major type of geology were determined. Table 5-4 shows the geological segmentation for Nice Tramway project. This segmentation was considered as resume of the information existed in the geological plan. It can be interpreted as continuous characteristics of ground that will be apply for future evaluation of statistical learning algorithms. This data has categorical nature. It should be encoded so as to be used with continuous numerical data.

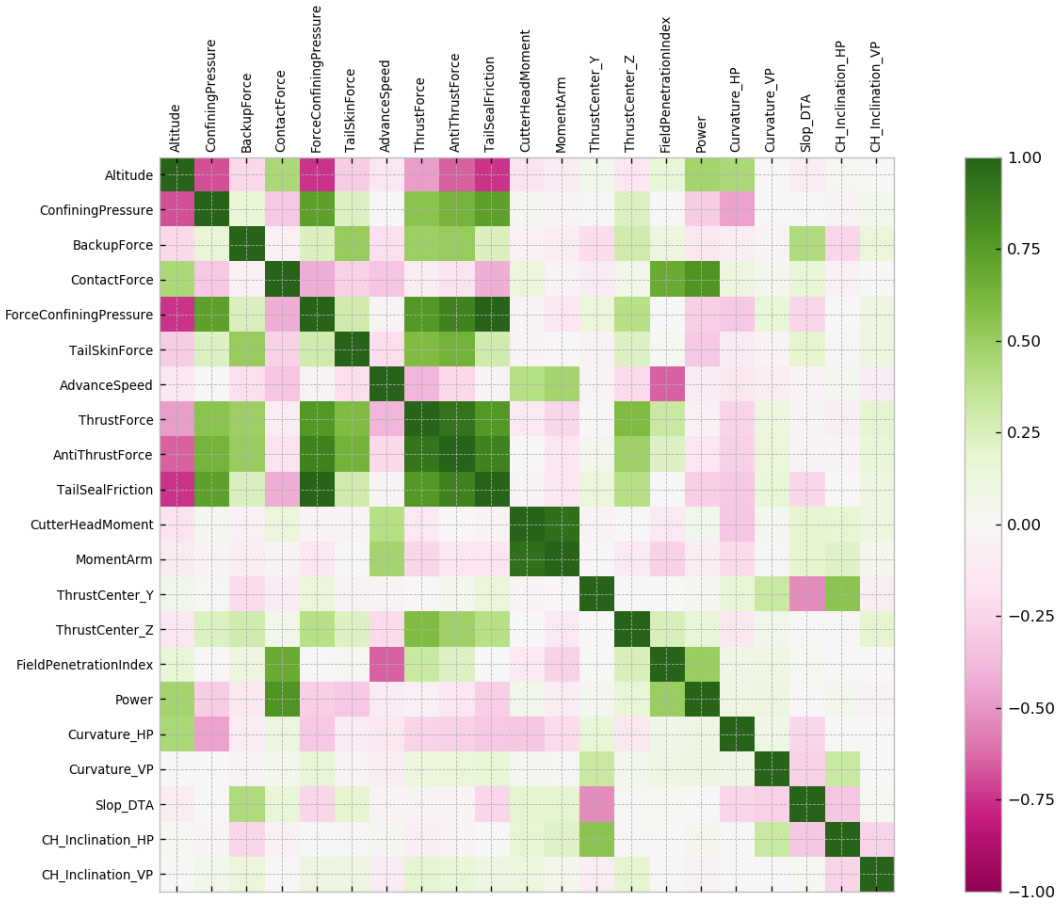

Figure 5-5 Correlation matrix of second data frame

Table 5-4 Geology segmentation (Nice Tramway project)

Geology Type	Length in project profile(m)
Sandy-Silt (SL)	956
SandyGravel-Silt (SGL)	933
SandyGravel-Silt-Clay (SGLA)	480
Soft Silty-Clay (LA)	266
Silt	153
Limestone	113

The final data frame for further studies consists of 21 parameters (operational data and guiding data) and geological characteristics of ground (6 types of geological formation after segmentation of the geological profile).

Explained variance in PCA

The total variance definition in PCA is the summery of all individual principle components. Figure 5-6 shows the explained variance by each principle component (in percentage).

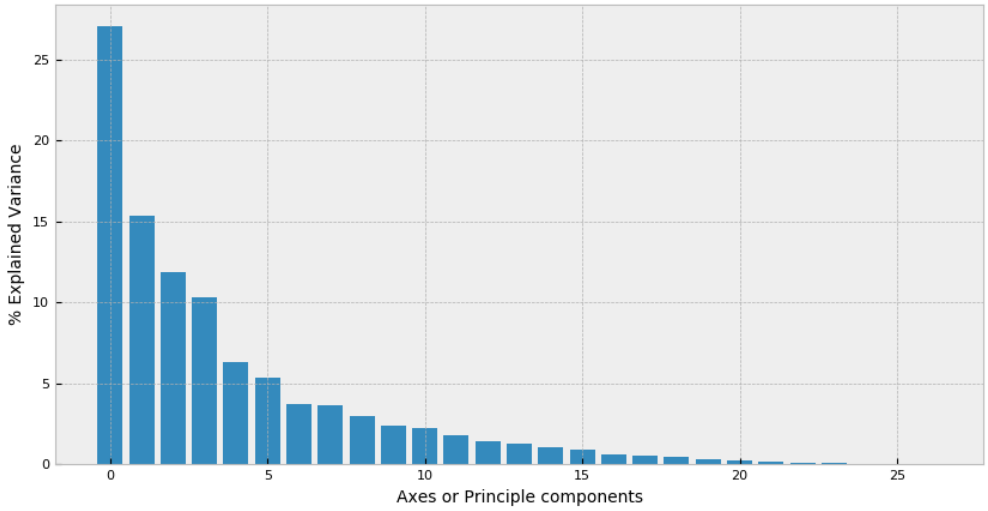

Figure 5-6 Explained variance by principle component in %

The highest fraction of explained variance among these variables is around 27%, and the lowest one is around 1%. We can also compute these fractions for subsets of variables. Figure 5-7 displays the cumulative explained variance by principle components.

PCA computes a new set of components and represents the data in terms of new components These new components represent the same amount of information and the total variance remains the same. Generally, the first n principle components (n could be 1,2,3 etc.) explain the most variance any n variables can explain. We could choose the first n components, and not just some k components, because they have the highest variance out of all principal components. We also choose the first n components big enough to reduce the information loss.

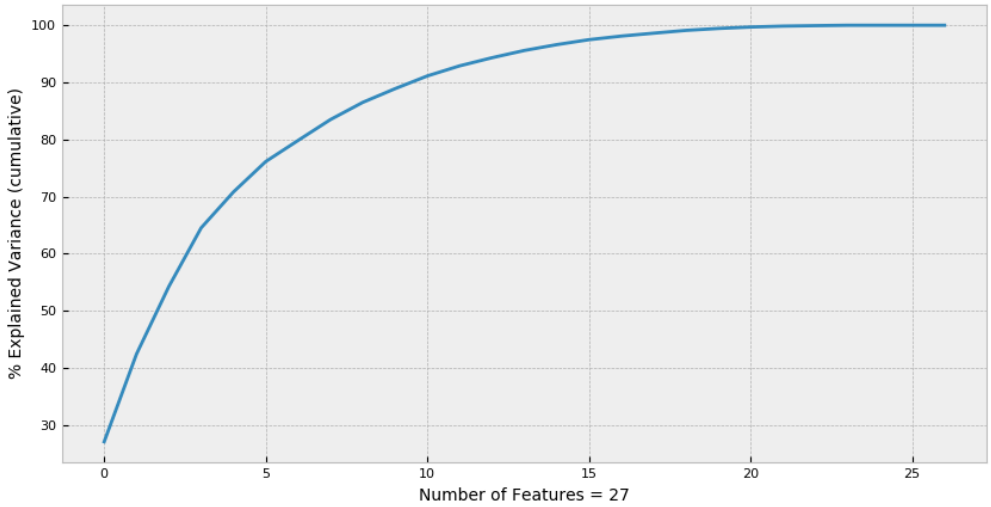

Figure 5-7 Cumulative explained variance in %

There are different methods to select the number of components to retain:

- Kaiser criterion: Eigenvalue >1
- Percent variance accounted for
- The Scree Test: Keep components before the break
- Parallel analysis
- MAP test
- The interpretability criteria

Figure 5-8 represents the scree plot for our components.

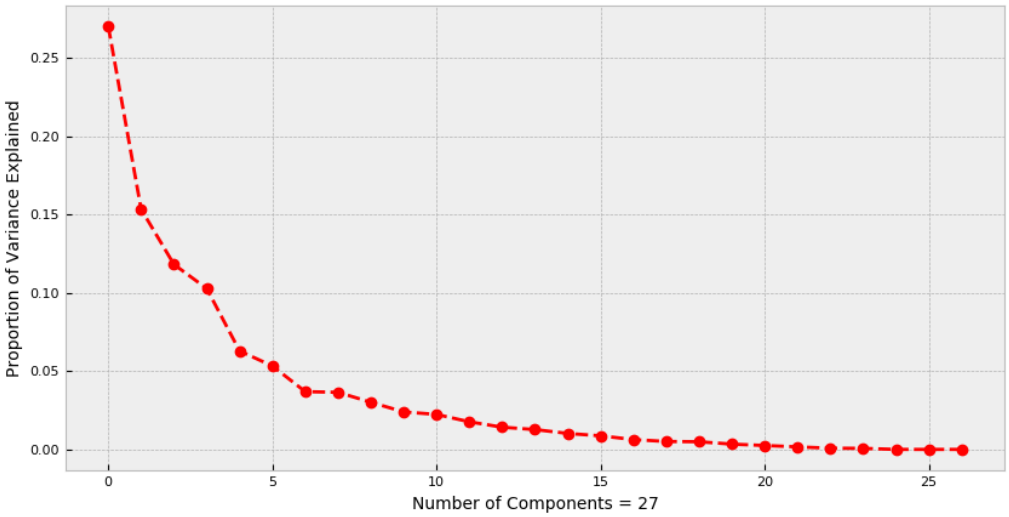

Figure 5-8 PCA Scree plot

Figure 5-9 represents the feature importance for the 6 first components (axis) of PCA.

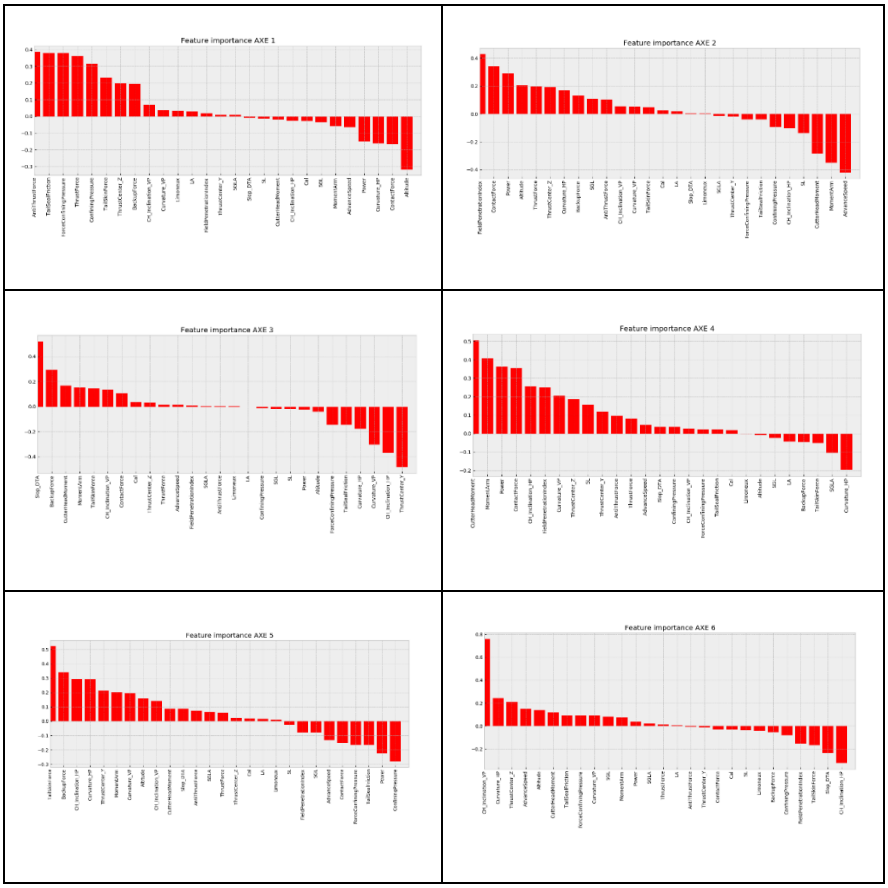

Figure 5-9 Feature importance evaluation for first six components

5.4 TBM steering optimization using Neural Networks

Finally, regression algorithms were observed to solve our problem. The task (steering of TBM) to be optimize by statistical learning is very complex. Also, due to uncertainty, (soil and rock geomechanicial characteristics) and the number of features involved during TBM operations, the model created by machine learning algorithms are not generalized for our problem.

During the last few years and decades different neural networks developed such as Multilayer feedforward networks, recurrent neural networks and statistical networks. They can be very efficient for complex and difficult problems such as[57]:

- Lack of physical/statistical understanding of problem
- Statistical variation in the observed data
- Non-linear mechanisms responsible for generation of data

Artificial Neural Networks (Deep learning neural networks) are generally developed to solve generalization problem for high-dimensional data. In the AI development the expression of (Curse of Dimensionality) was encountered, this means that many machine learning problems become exceedingly difficult when the number of dimensions in the data is high [58]. The challenge created by the curse of dimensionality is a statistical challenge.

5.4.1 Summary of Neural Networks Anatomy

In the literature introduced three basic mapping neural networks[59]:

- Recurrent networks: They are nonlinear, fully interconnected systems and form an auto associative memory.
- Universal feedforward neural networks: They produce a nonlinear mapping between input and output and are nonlinear function approximators. Multilayer Perceptron (MLP), the backpropagation-type neural network, the radial basis neural networks and the Support Vector Machine (SVM) which are the most well-known universal feed forward neural networks.

- Local Interaction-based neural networks: These networks are based on competitive learning; the output neurons of the network compete among themselves to be activated. The output that wins the competition is called a winning neuron.

One of the basic models of deep learning neural networks is called Multilayer Perceptron (MLP). MLPs are one of the most important types of neural nets because many applications are successful implementations of MLPs. The architecture of the MLP is completely defined by an input layer, one or more hidden layers, and an output layer[59]. Perceptron is a single neuron of a larger neural network. Perceptron could be considered as the simplest part of a model of biological brain that is used to solve complex computational tasks such as predictive modelling tasks. The main advantage of neural networks is their capabilities to learn representation in the training data. Neural Networks (MLPs) are also considered as providing a nonlinear mapping between an input vector and a output vector [57]. The predictive capability of neural networks comes from the hierarchical or multi-layered network structure. The data structure can pick out (learn to represent) features at different scales or resolutions and combine them into higher-order features[60].

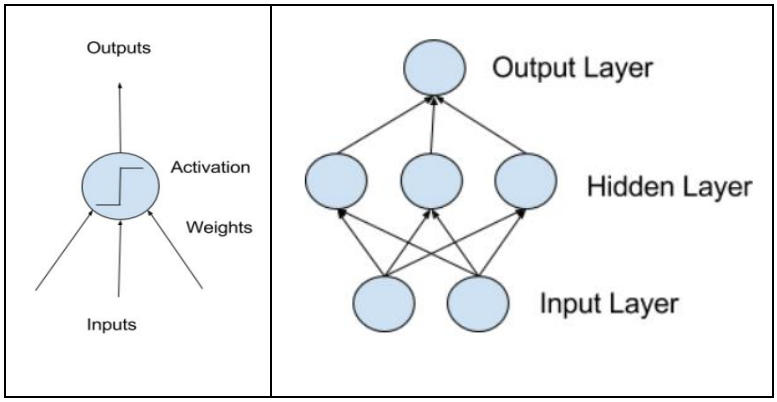

Figure 5-10 Schematic of single neuron (left) and simple network(right)[60]

Neurons are the smallest part of neural networks. They are units that contain weighted inputs and produce an output by using an activation function (the weighted input is added then passed through an activation function). Activation functions are mathematical equations that determine the output of a neural network. Activation functions should be computationally efficient. Activation functions can be linear or non-linear. Neurons are arranged into networks of neurons. A row of neurons is called a layer and one network can have multiple layers. The architecture of the neurons in the network is often called the network topology. The basic data structure in neural networks is the layer.

A typical anatomy of neural networks are presented by F.Cholet as follow[52]:

- Layers, which are combined into a network,
- The input data and corresponding targets
- The loss function which defines the feedback signal used for learning
- The optimizer, which determines how learning proceeds

For the configuration of the learning process the proper loss function and optimizer should be chosen. The loss function (objective function) represents a measure of success for the task that we want to model (predict). The function we want to minimize or maximize is called the objective function or criterion. When we are minimizing it, we may also call it the cost function, loss function, or error function[58].

Optimizers are used to update weights and bias and to determined how the network will be updated based on the loss function. It implements a specific variant of Gradient Descent (GD) or Stochastic Gradient Descent (SGD). Gradient Descent is an iterative machine learning optimization algorithm to decrease the lost function error and help to make accurate predictions. Also, other global designed optimization algorithms can be used for non-convex optimization problems.

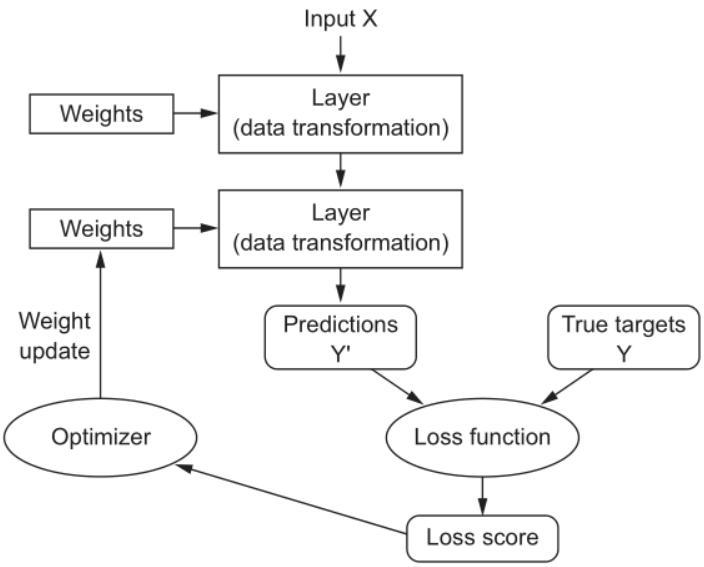

Figure 5-11 Illustration of relation between neural networks objects[52]

5.4.2 **Implementing Multi-layered Neural Network on TBM data**

In this section the implementation of the MLP on our data input is presented to find learning functions between our inputs and outputs. The input parameters consist of operational parameters of a TBM. Guiding parameters (trajectory characteristics), geological characteristics such as thrust force, anti-thrust force, centre of thrust force, slope and curvature of trajectory and geological segmentation (used as parameters) represent geological characteristics of excavated ground). There are 22 inputs features and 2 output features (Pitch and Yaw of TBM). Like previous studies, the data came from Tramway Nice project. For the development of a model, TensorFlow and Keras libraries were used. TensorFlow is an interface for expressing machine learning algorithms and an implementation for executing such algorithms[61]. Keras is a deep learning API written in Python, running on top of the machine learning platform TensorFlow.

To choose the best Neural network model there is not any analytical calculation to find optimal configuration. However, some techniques can be used to better train our model and find the best configuration. There are three types of problems with regards to performance evaluation of a deep learning neural network model:

- Problem with learning,
- Problem with generalization
- Problem with predictions

Problem with learning means that a model cannot effectively learn a training dataset and show bad performance. Problems of generalization means that a model overfits the training dataset. Problems of predictions reveal in the stochastic training algorithm having a great impact on the final model, causing high variance in behaviour and performance of model. To improve these problems, some techniques can be used. These techniques are used to make better configuration for neural network model and to choose better hyperparameters for the neural network model optimization[62].

Here the procedure is observed to control the capacity of a neural network model and how capacity impacts what a model is capable of learning. The capacity of a neural network model is controlled by two aspect of the model, the number of nodes and the number of layers in the model. The number of nodes in a layer considered as width of networks. The number of layers is

considered as depth of the networks. the depth generally increases the capacity of the model. In practice there are not any recommendations to find sufficient width (number of nodes in a layer) and depth (number of layers) of networks. An iterative search was applied to find model with the best width and depth for the problem. Training the depth of a model increases the capacity of the model although more time is added for computation and it may add the problem of vanishing gradient.

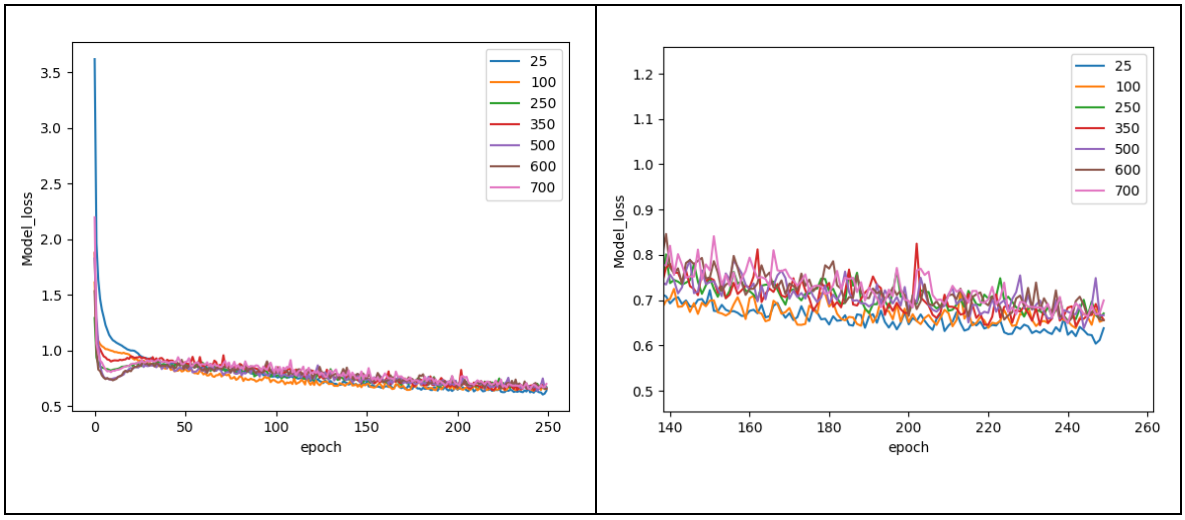

Figure 5-12 Model width (number of nodes) evaluation

Figure 5-12 represents the evaluation of different nodes number. Base on this iterative study it is observed that model with 25 and 100 nodes have the lowest model loss values. Figure 5-13 shows the evaluation of best layer number. Here the best layer numbers would be 6 and 8.

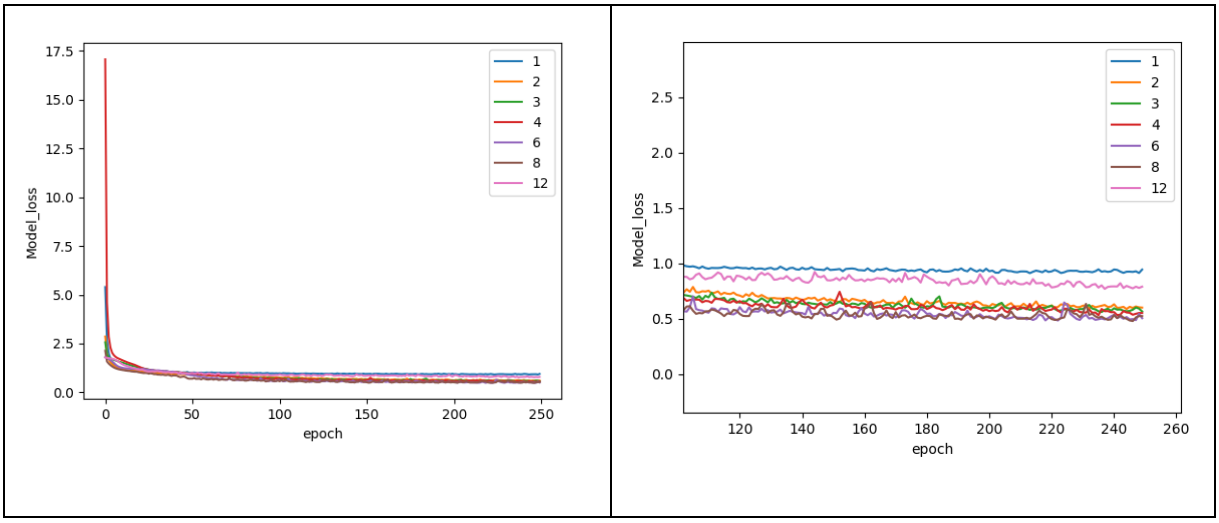

Figure 5-13 Model depth (number of layer) evaluation

As explained previously, neural networks are trained using the SGD optimization algorithm. Optimization algorithms that use the entire training set are called batch or deterministic gradient methods, because they process all of the training examples simultaneously in a large batch [58]. The number of training examples used in the estimate of the error gradient is a hyperparameter for the learning algorithm called the batch size, or simply the batch. A batch size of 32 means that 32 samples from the training dataset will be used to estimate the error gradient before the model weights are updated [62].

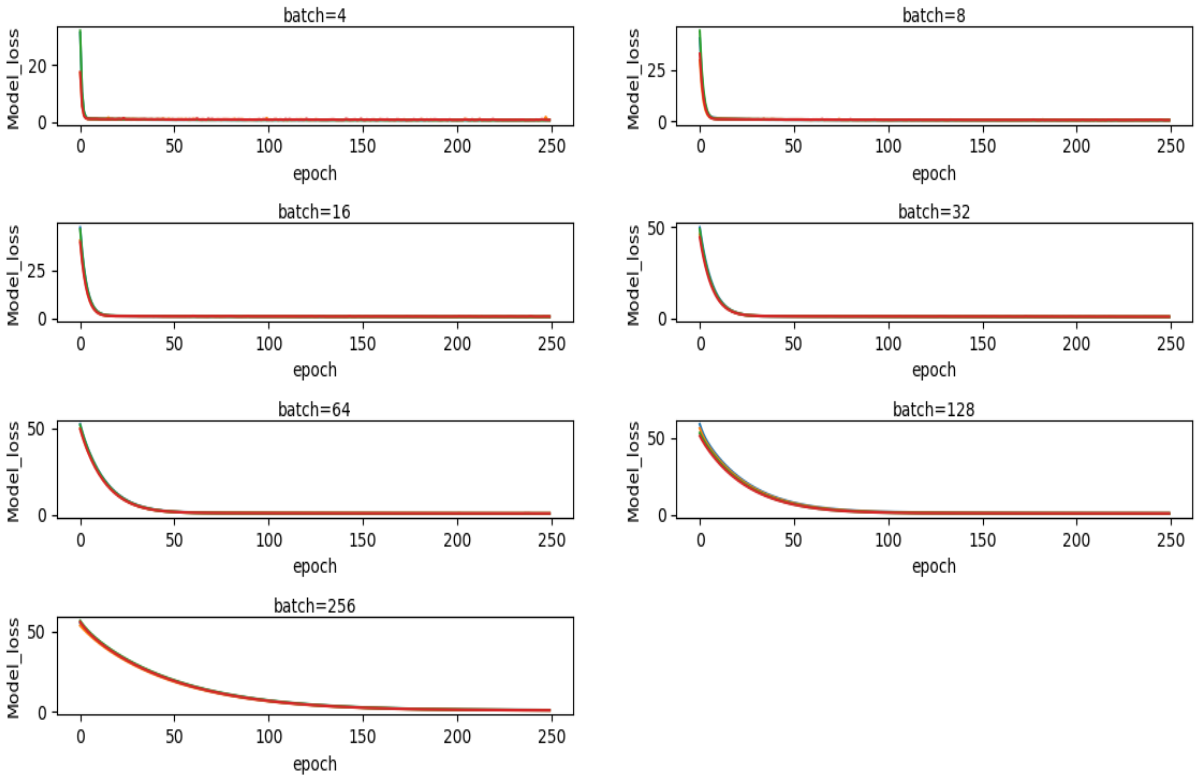

Figure 5-14 Batch size evaluation to find a model optimal batch size

The next step is to set up a neural network model configuration of the learning rate on the training dataset. The learning rate is perhaps the most important hyperparameter that controls how much we are adjusting the weights of our network respecting the loss gradient[58]. Generally, a large learning rate allows the model to learn faster, at the cost of arriving on a sub-optimal final set of weights. A smaller learning rate allows the model to learn a more optimal or even globally optimal set of weights however this may take significantly longer to train[62]. There are not any

analytical calculations for finding the optimal learning rate. The general method to find optimal learning rate is via trial and error.

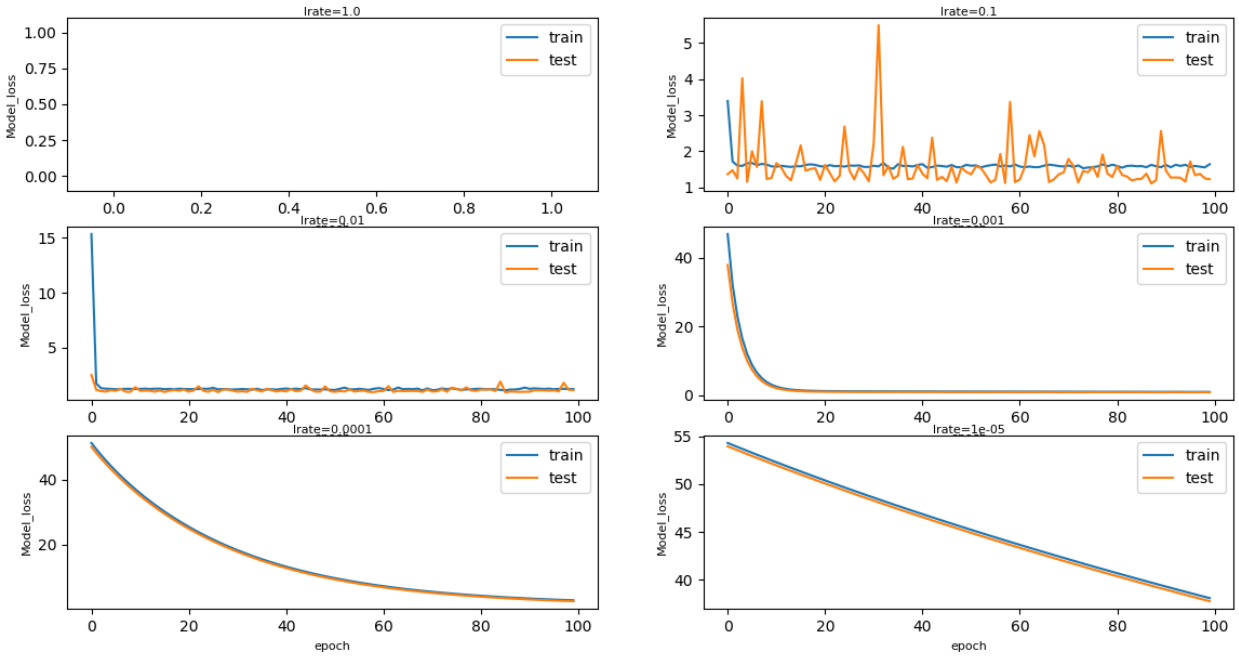

Figure 5-15 Learning rate evaluation

The Figure 5-15 displays the variation in behaviour for the too-large learning rate of 1.0 and the inability of the model to learn anything with the too-small learning rates of 1E-4 and 1E-5. Here it is observed that the model was able to learn the problem well with the learning rates of 1E-2 and 1E-3, although successively slower as the learning rate decreased. With the chosen model configuration, the results suggest a moderate learning rate of 0.001 resulting in a successful good model performance on the train and test sets.

TensorFlow provides a suite of extensions of a simple stochastic gradient descent that support adaptive learning rates. As each method adapts to the learning rate, little configuration is often required for one learning rate per model weight. Commonly used adaptive learning rate optimizers are: RMSProp, Adagrad, Adam, Nadam, Adamax.

Figure 5-16 represents the evaluation of different optimizers to find optimal learning for our model. As observed, oscillation of response for different optimizers, Adam, Adamax and Nadam give the best learning rate for this model.

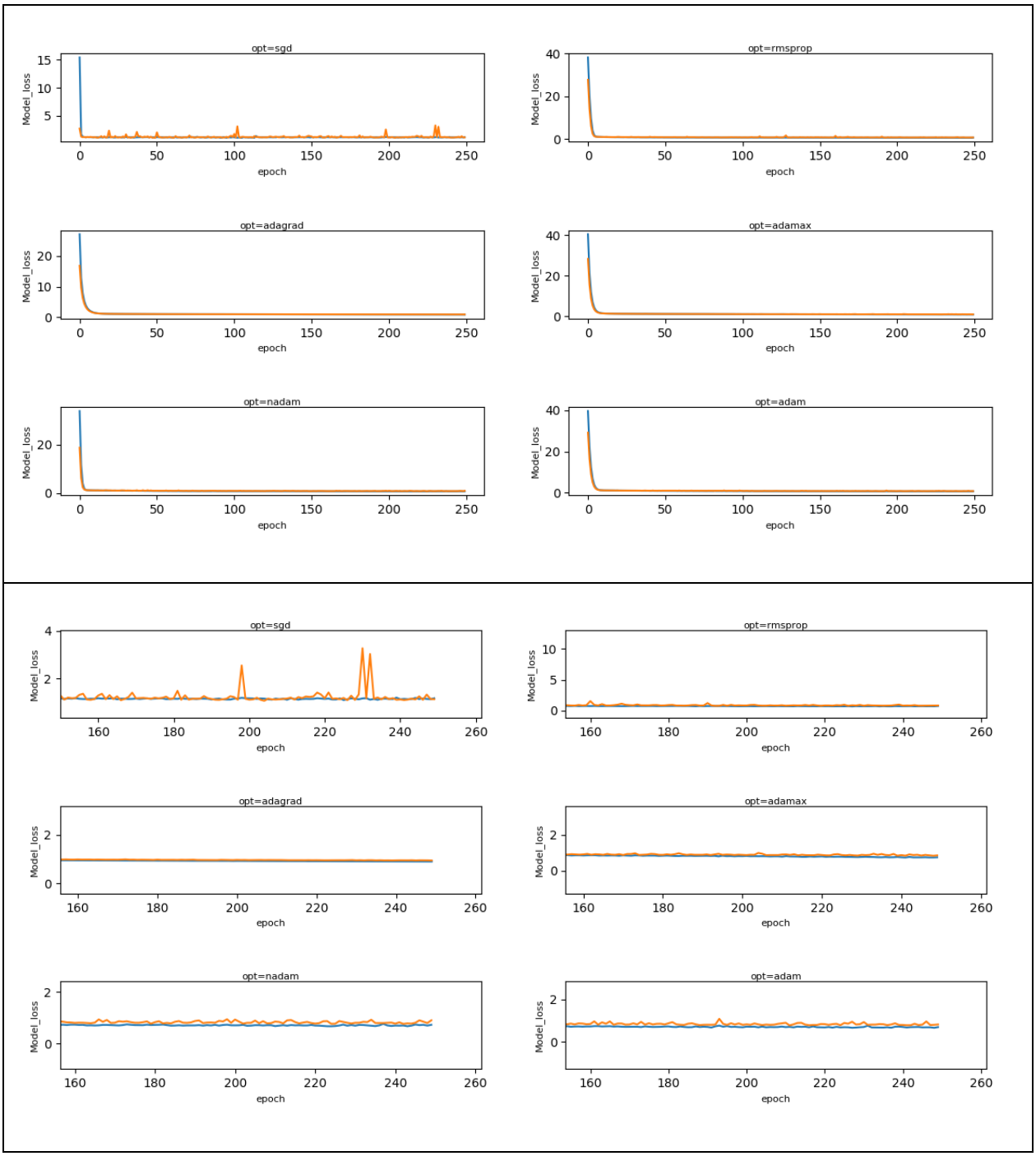

Figure 5-16 Finding the best optimizer to find optimal learning rate

After configuration evaluation to find the optimal architecture of neural network models (the best learning model), the model is trained on the first 1000 meters of the Nice Tramway project data project.

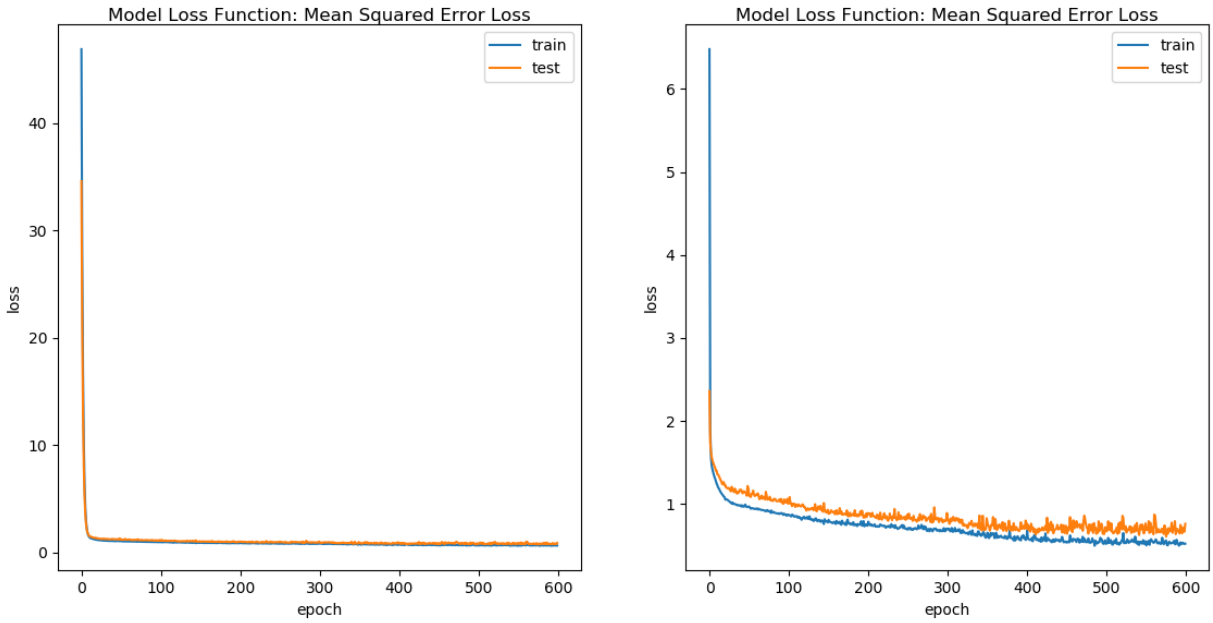

Figure 5-17 Model Loss evaluation (MSE Loss Function)

Figure 5-17 represents the model loss on a training set and tests set of our data frame for validation of the model then the model is implemented on the second 1000 meters (between PM (1000 and 2000)) of our data and the MSE and RMSE for our output parameters (Pitch and Yaw) are verified. Other portions of trajectory are also observed to evaluate the prediction along different trajectory properties such as 2200 to 2600 meter, 2600 to 3100 meter and 2000 to 3100 meters.

Table 5-5 Model performance on the test data (data comes from different parts of tunnel trajectory)

Test Model on different parts of Trajectory															
PM (1000-2000)				**PM (2200-2600)**				**PM (2600-3100)**				**PM (2000-3100)**			
Pitch		Yaw		Pitch		Yaw		Pitch		Yaw		Pitch		Yaw	
MSE	RMSE	MSE	RMSE	MSE	RMSE	MSE	RMSE	MSE	RMSE	MSE	RMSE	MSE	RMSE	MSE	RMSE
0.709	0.842	0.966	0.983	0.841	0.917	1.447	1.203	3.001	1.732	5.328	2.308	1.200	1.599	2.559	1.442

5.5 Conclusion

In this chapter, a summary of previous researches on using data-driven methods is presented to evaluate a TBM performance and the modelling of TBM parameters. Then, a brief introduction is presented with regards to statistical learning, machine learning and deep learning.

The evaluation of machine learning regression algorithms is presented for the optimization of TBM performance. In this study, the operational parameters of a TBM were used as the input features and the guiding parameters (deviation of machine and relative tendency of the TBM) were investigated as the output parameters. The algorithm results were not generalized for different projects (3 projects evaluated). There were two main reasons: first, the configuration of the TBM was different for each project (which leads to a different number of input features). Second, different geological characteristics (it was essential to add parameters which can represent geomechanical characteristics of the ground) influenced the model to be generalized or not. As observed in this chapter, two strategies were examined to find regression (linear or non-linear) algorithm which is capable of generalizing the results for the learning procedure, but they were not appropriate to find the best learning algorithms for our problem.

As a next step, a dimensionality reduction algorithm (PCA) was implemented on the selected parameters (operational parameters, guiding parameters and geological feature as a representative of ground characteristics) to find the essential features as a new component which can represent the most significant variance of all features by a smaller number of features (components).

Then the MLP algorithm was implemented to model steering parameters of TBM (pitch and yaw) based on operational parameters as inputs being used. After trial and error application, the architecture of neural nets defined in the chapter, were capable to converge the learning model which used operational parameters, guiding parameters and geological characteristics as input. The pitch and yaw (considered as relative tendency of TBM during each excavation step) of TBM as output. The different configuration optimization processes were carried out to improve and optimize hyperparameters of our algorithms (number of layers, type of activation function, evaluation of the batch size, finding the optimized batch size, optimization of learning rate and finding efficient optimizer function). The importance of the geological characteristics was

observed (using geological characteristics was crucial, if the geological parameters were eliminated then the algorithms were not capable to converge with a good precision for train and test set of learning). These primary results showed that more refining for input and output parameters lead to better learning algorithm for our problem.

6. Conclusion and recommendation

Regarding technical advances during the few last decades, TBM tunnelling is one of the most popular and reliable excavation methods in different types of geological conditions from soft ground to hard rock. This study mainly focused on using data driven approaches to evaluate and model behaviour of a TBM. To better understand the behaviour of TBMs, a summary of the analytical (mathematical) model is investigated. In parallel, the study is conducted to evaluate the forces exerted on a TBM to understand its behaviour and evaluate the parameters which have important influence in TBM steering. The parameters were chosen based on the state of the art of previous studies and the discussion with engineers and field experts. Next, an EDA was carried out to discover the statistical distribution of the parameters based on the most the accurate and accessible resolution (each meter of the TBM advancement-project chainage).

This study focused on an evolution of the operational data and steering parameters (trajectory characteristics). The antithrust force was proposed as a combination of forces against advancement of a TBM. The antitrust force consisted of different components such as, the force exerted on a bulkhead due to confining pressure, the corrected contact force, the articulation cylinders force, the back-up force, and the tail seal friction resistance. The box plots were presented to assess the distribution of forces exerted on different parts of a TBM based on data captured during TBM excavation. Some variables such as the centre of thrust force, the inclination of the cutter head and the cutter head moment arm were calculated by using the TBM data. These variables give more comprehensible and understanding of the TBM behaviour. The centre of thrust force was calculated using cylinders geometry and thrust cylinders force. Cutter head inclination is calculated by using displacement cylinders data. The slope of the trajectory and curvature in the horizontal and vertical plane is calculated using DTA data. Then, the EDA was carried out to find the association and potential correlation between operational data of a TBM, the trajectory characteristics and the steering parameters. For further study in this part the evaluation of operational data, in smaller resolution, is proposed to assess and compare the result for the most significant behaviour. Implementation of the EDA was one of the most essential and time-consuming steps during this study. Evaluation of different operational parameters, trajectory

characteristics and finding a potential association between these parameters was an inevitable step to better choose significant parameters for solving problem and implementing data-driven modelling.

In parallel, an instrumentation strategy was proposed to capture angular deformation of the tail skin structure. Then the finite element strategy with an optimization procedure was used for the calculation of load exerted on the periphery of the TBM. The inclination calculated by sensors was in radian and the load was calculated on MPa. Our problem was observed in a two-dimension structure (X-Y, transversal section) of a TBM. An optimization approach was applied to calculate the relative load on the structure, based on the comparison of the result between deformation calculated from FEM computation and experimental inclination that came from sensor data. By using the optimization approach, the relative value of load applied on a TBM are estimated. The study was conducted over two periods of time (these two periods was chosen based on the accessibility of data). Finally, the potential association between calculated load and operational parameters of a TBM were observed. As observed, there are correlations between some of the operational parameters and calculated loads although these correlations could change according to different excavation intervals based on geological and trajectory characteristics. For future studies the correlation between calculated load, trajectory characteristics and operational parameters for more cases can be observed and compared with in this study in order to gain more accurate evaluation. Also due to technical limits the number of installed sensors were limited in this study. As a result, the calculation conducted in two dimensions, by installation of more sensors in the longitudinal and transversal section of the structure, further studies can be implemented. Another evaluation can be carried out by evaluation of different intervals of the time based on the accessibility of the operational data and the calculated load with different resolution of time and investigation of the results.

Next, the previous evaluations and investigations were used to apply a data-driven approach (statistical learning, machine learning and deep learning algorithms) and model the tendency of machines by using the operational parameters, geological characteristics and trajectory characteristics. The benchmarking of the regression algorithms was evaluated, but they did not generalize the learning process for different case studies. Then a dimensionality reduction algorithm (PCA) was implemented on the selected parameters (operational parameters, guiding

parameters and geological features as a representative of ground characteristics) to find the essential features as a new component which can represent the most significant variance of all features by a smaller number of features (components). The MLP algorithm was implemented to model steering parameters of TBMs (pitch and yaw) based on using operational parameters as inputs. As a first result the model was convenient. Different configuration optimization processes were carried out to improve and optimize hyperparameters of the algorithm (number of layers, type of activation function, evaluation of the batch size, finding the optimized batch size, optimization of learning). As a perspective more refinement can be implemented on the input and output parameters mainly using the local position of TBMs as a parameter which can represent tendency of machine. Also, further investigation and assessment can be done to find a more accurate neural network architecture (the other algorithms such as Recurrent Neural Networks can be studied to observe the capacity of the algorithm to make a more appropriate model for our problem).

A- Appendices

A1. Exploratory Data Analysis of TBM data (TMCLK-S882 project)

The EDA is demonstrated for the summery of the important operational data of TMCLK-S882 project.

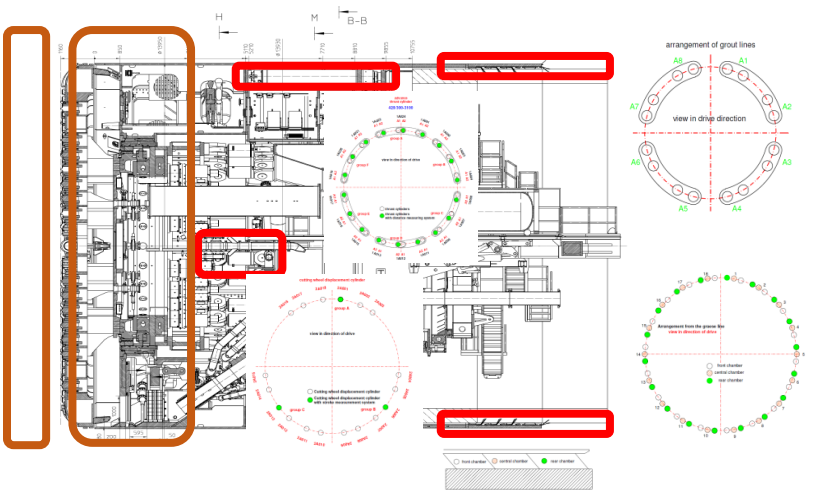

A.1. 1 The configuration of TMCLK-S882 TBM, mortar injection lines, grease injection configurations, thrust cylinders and displacement cylinders configuration.

A.1. 2 The configuration of TMCLK-S882 TBM, mortar injection lines, grease injection configurations, thrust cylinders and displacement cylinders configuration.

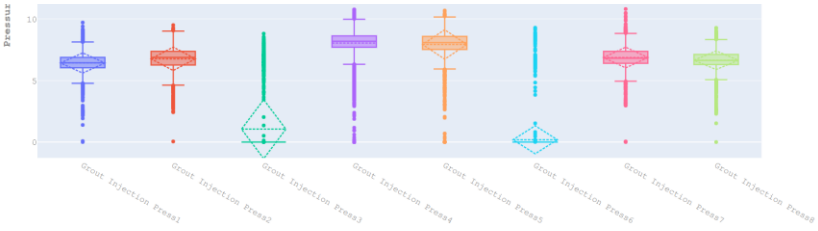

A.1. 3 Distribution of mortar injection pressure, box plot illustrated eight injection lines of mortars. As observed in the figure the distribution of pressure in line 3 and 5 was not normal. The data came from these two lines was not used in the future study due to the defects existed in the grout line data.

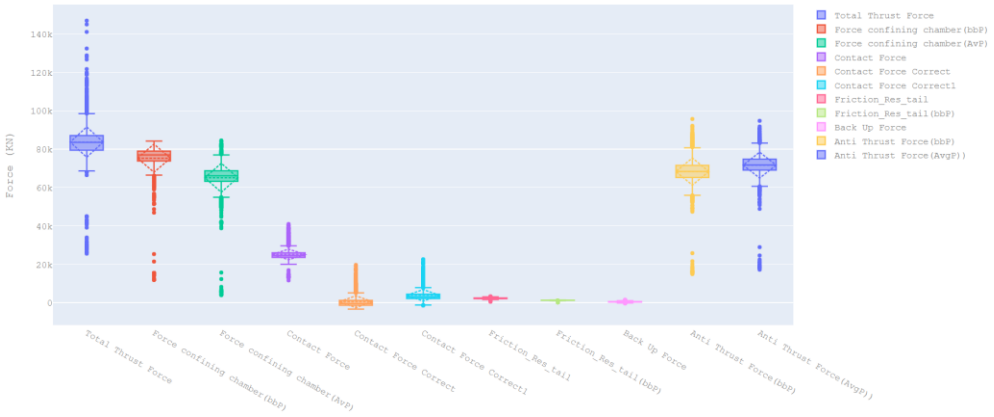

A.1. 4 Evaluation of forces exerted on TBM S882 (internal and external interactions) based on data captured during excavation. Figure presented distribution of , total thrust force, force exerted on the confining chamber calculated based on bubble pressure(bbP) and average pressure(AvgP) in working chamber, contact force, corrected contact force calculated based on bbp and AvgP, Tail skin resistance force due to injection of grease between tail skin and segments, back up train traction force and anti-thrust force calculated based on bbP and AvgP.

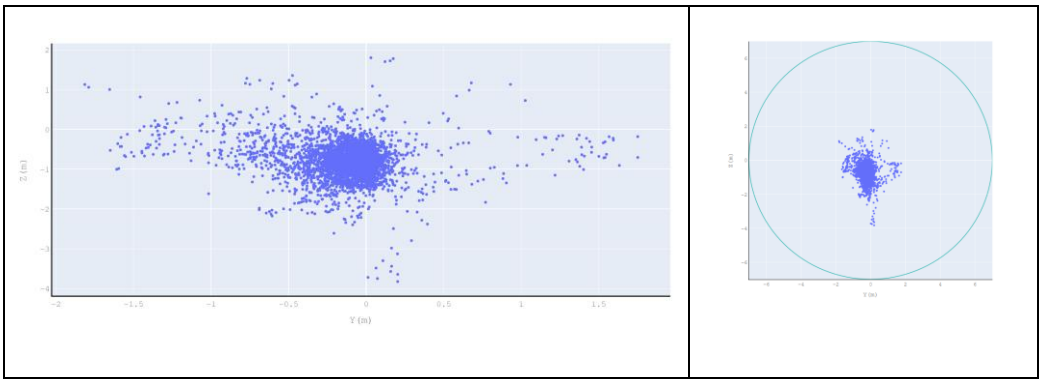

A.1. 5 Centre of thrust force calculated and visualized for each meter of excavation by S882 TBM. Right plot showed scatter plot of the center of thrust force in the transversal section of the TBM S882 with 14 m diameters.

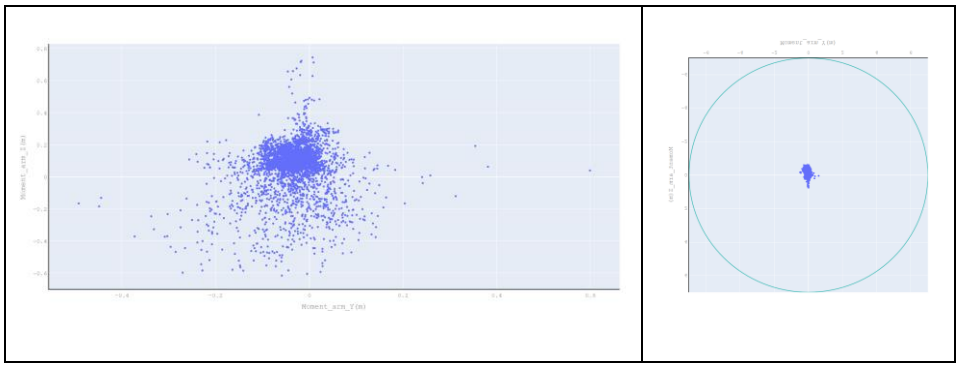

A.1. 6 Evaluation of the distribution of the cutter head moment arm for TBM S882. Right plot showed scatter plot of the cutter head moment arm in the transversal section of the TBM S882 with 14 m diameters.

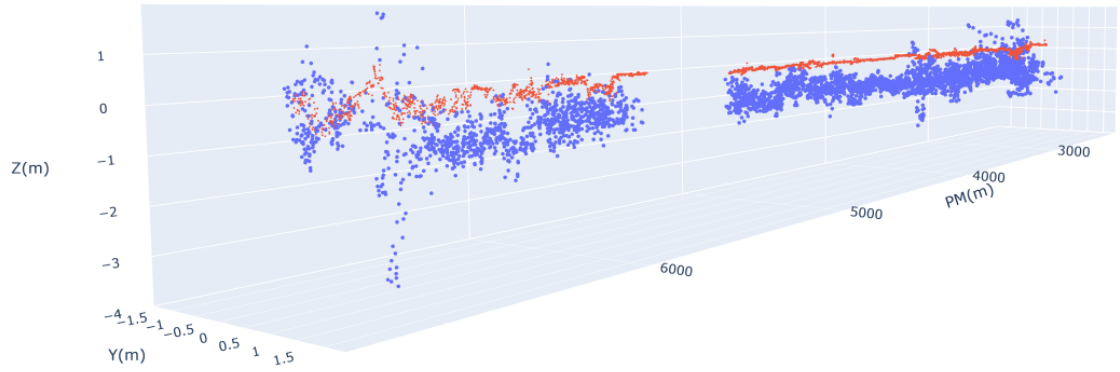

A.1. 7 3D visualization of the centre of the thrust force (blue point) and the moment arm (red point)

A.1. 8 Main drive displacement cylinders evolution vs chainage, the cylinders configuration established in three position 12h, 4h and 8h.

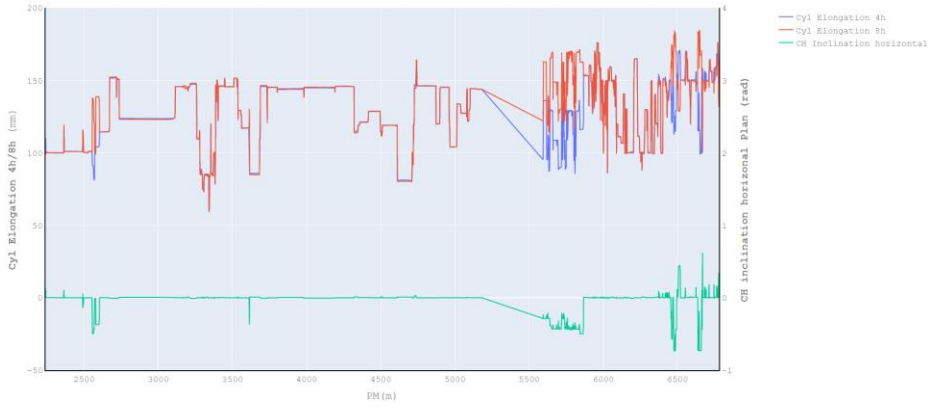

A.1. 9 Evaluation of the cutter head inclination (horizontal plane) vs TBM chainage. The inclination is calculated by using elongation of cylinders located at 4h and 8h. Right axis shows cylinder's elongation in mm. Left axis demonstrates inclination fluctuation of cutter head during each meter of advancement.

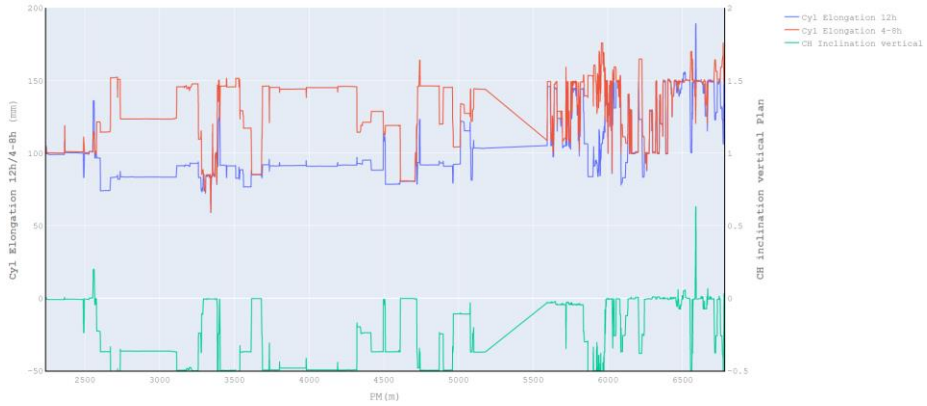

A.1. 10 Evaluation of the cutter head inclination (vertical plane) vs TBM chainage. The inclination is calculated by using elongation of cylinders located at 12h and 4h/8h. Right axis shows cylinder's elongation in mm. Left axis demonstrates inclination fluctuation of cutter head during each meter of advancement.

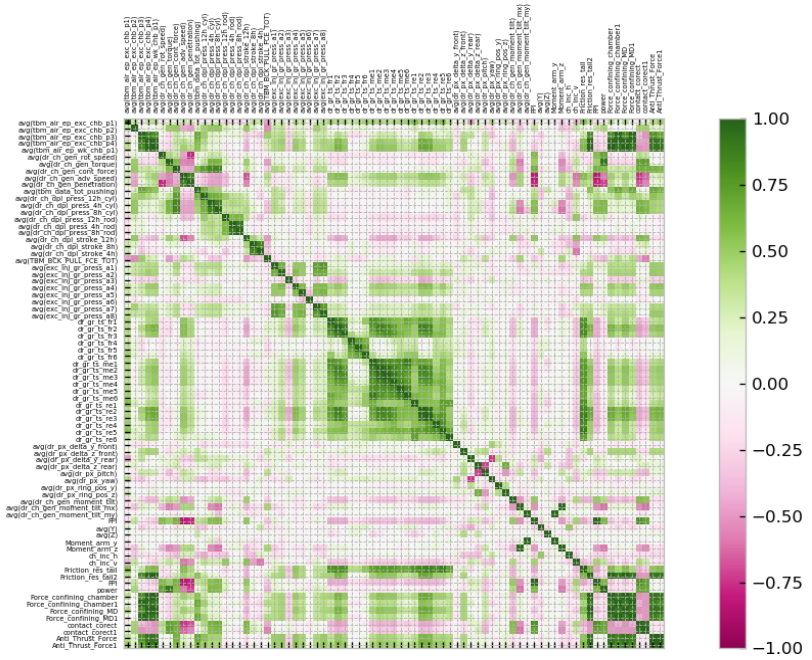

A.1. 11 Correlation matrix for operational parameters of TBM (S882) is investigated. Correlation matrix shows the correlation coefficients between each two variables. Correlation matrix help us to summarize relation between data into more advance analysis. It gives information about relation of each two parameters and the direction of that relation. Two properties are important for interpretation of correlation matrix, magnitude and direction of relation. The magnitude range in magnitude from 1 to -1, the larger the absolute value of the coefficient the greater the magnitude of the relationship. The direction of the relationship between each two values is indicated by the sign of the coefficient.

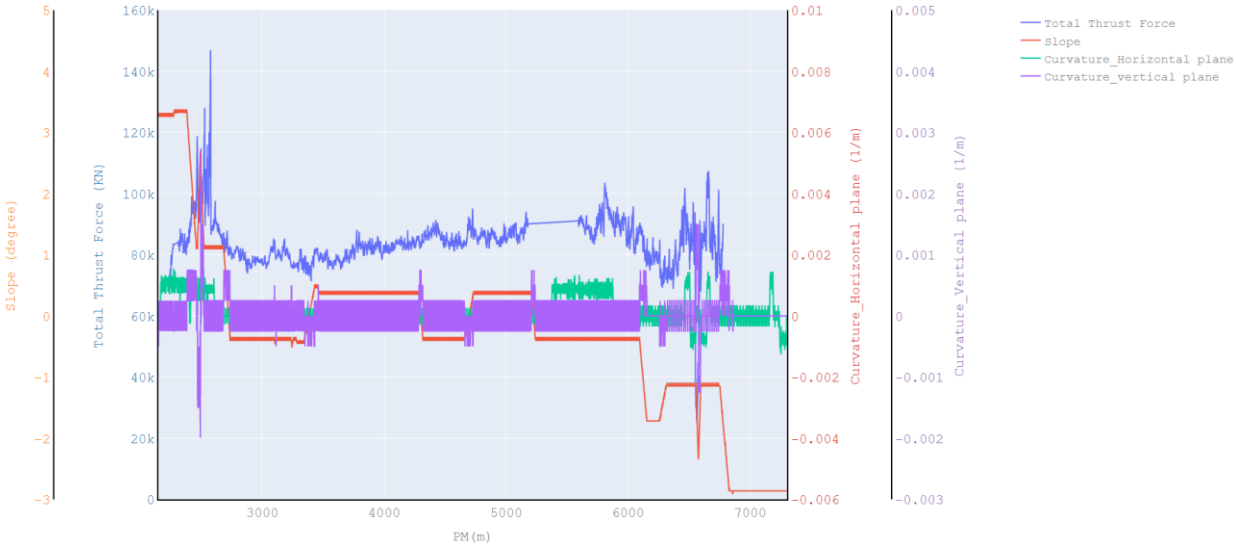

A.1. 12 line plot investigates fluctuation of total thrust force vs chainage and compare with guiding (trajectory) properties(characteristics) for TBM(S882). The potential relation between total thrust force evolution with trajectory properties can be evaluated.

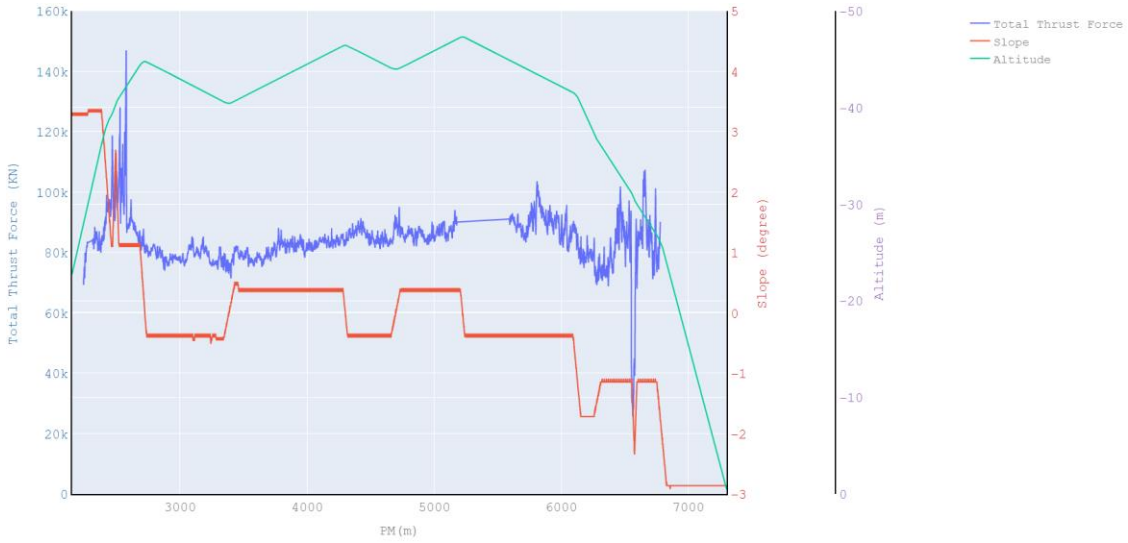

A.1. 13 line plot investigates fluctuation of total thrust force vs chainage and compare with guiding (trajectory) properties(characteristics) for TBM(S882). The potential relation between total thrust force evolution with altitude and slope is investigated.

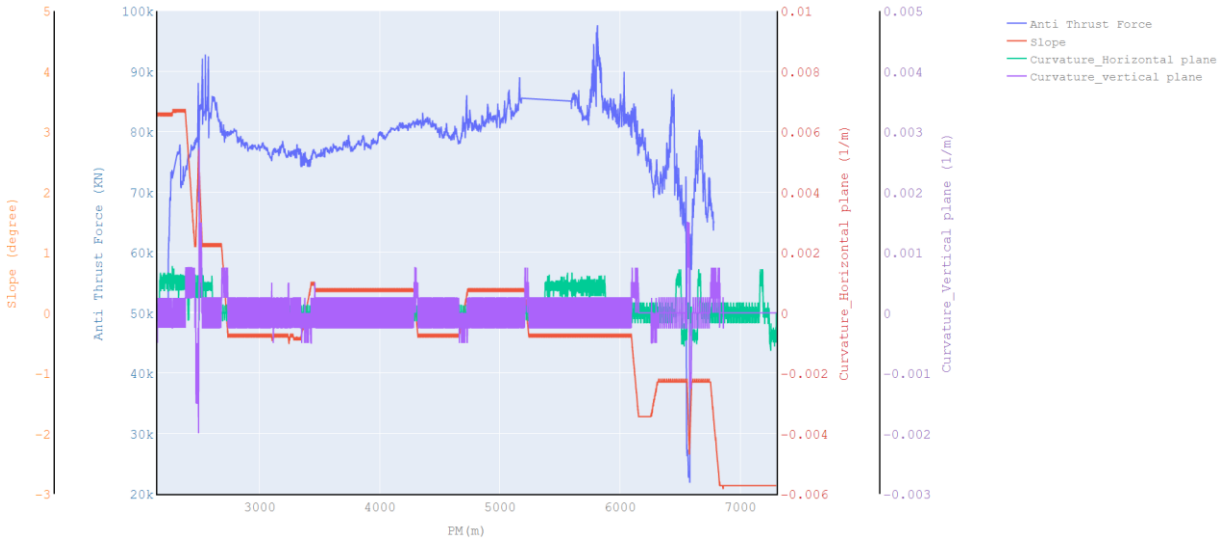

A.1. 14 line plot investigates fluctuation of anti-thrust force vs chainage and compare with guiding (trajectory) properties(characteristics) for TBM(S882). The potential relation between anti-thrust force evolution with trajectory properties can be evaluated.

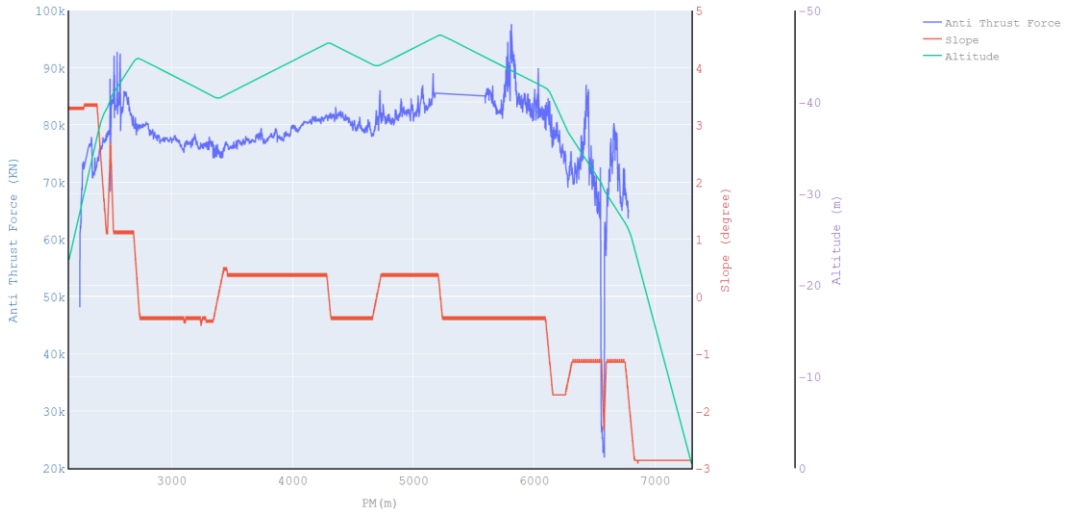

A.1. 15 line plot investigates fluctuation of anti-thrust force vs chainage and compare with guiding (trajectory) properties(characteristics) for TBM(S882). The potential relation between anti-thrust force evolution with altitude and slope is investigated.

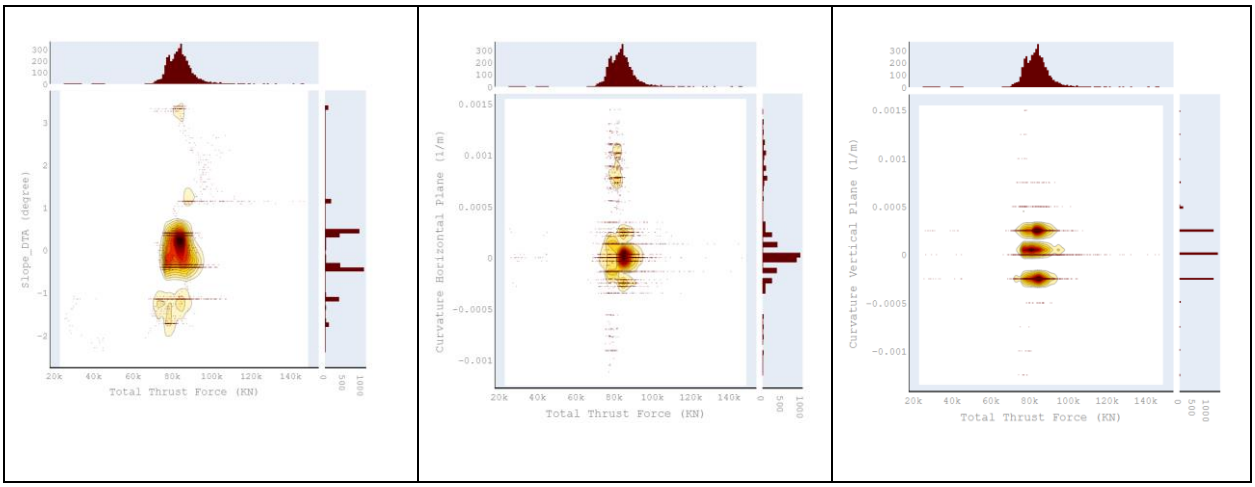

A.1. 16 Histograme2DConture plot: total thrust force vs trajectory characteristics

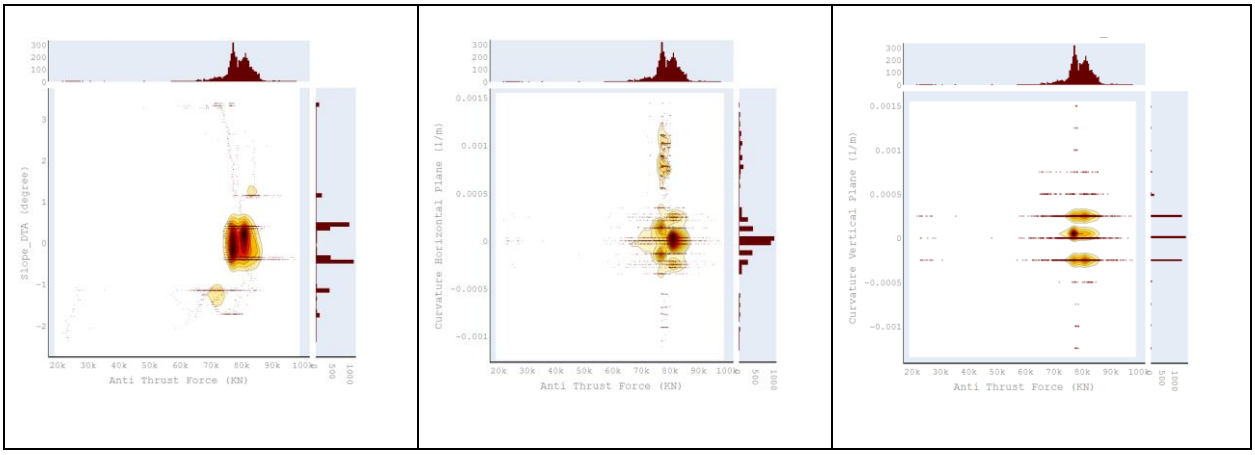

A.1. 17 Histograme2DConture plot: anti-thrust force vs trajectory characteristics

A2. Exploratory Data Analysis of TBM data (TMCLK-S881 project)

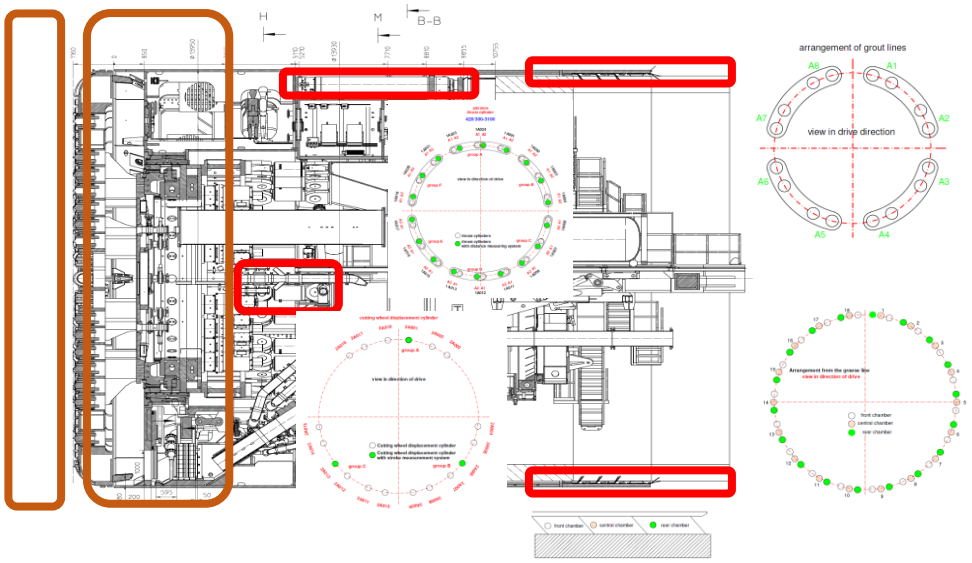

A.2. 1 The configuration of TMCLK-S881 TBM, mortar injection lines, grease injection configurations, thrust cylinders and displacement cylinders configuration.

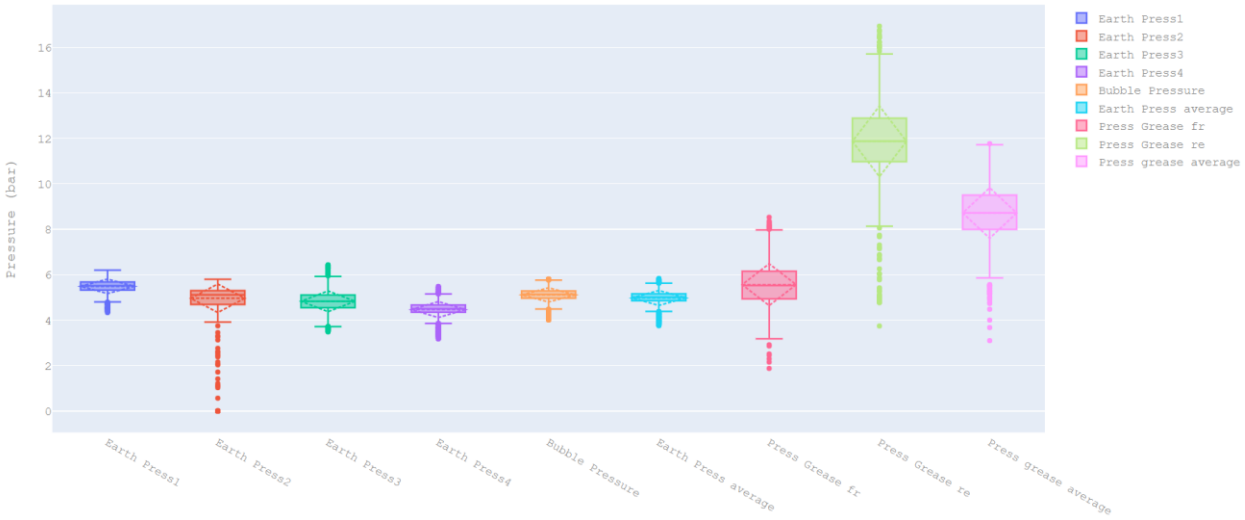

A.2. 2 Evaluation of earth pressure in excavation chamber and grease injection pressure. Pressure in excavation chamber is measured in four position and bubble pressure is measured in working chamber.

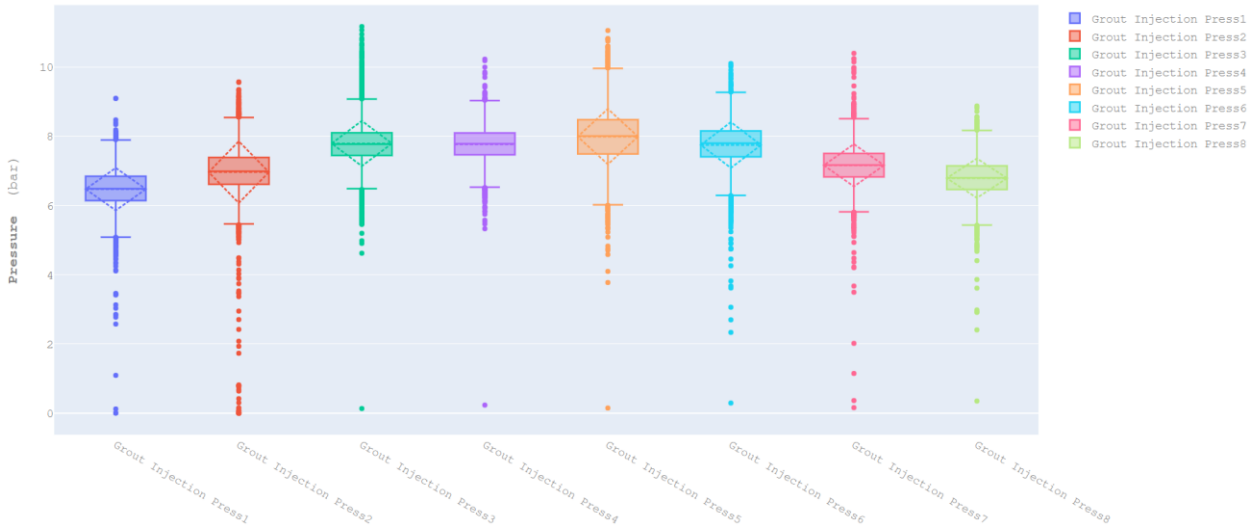

A.2. 3 Distribution of mortar injection pressure, box plot illustrated eight injection lines of mortars. As observed in the figure the distribution of pressure in line 3 and 5 was not normal. The data came from these two lines was not used in the future study

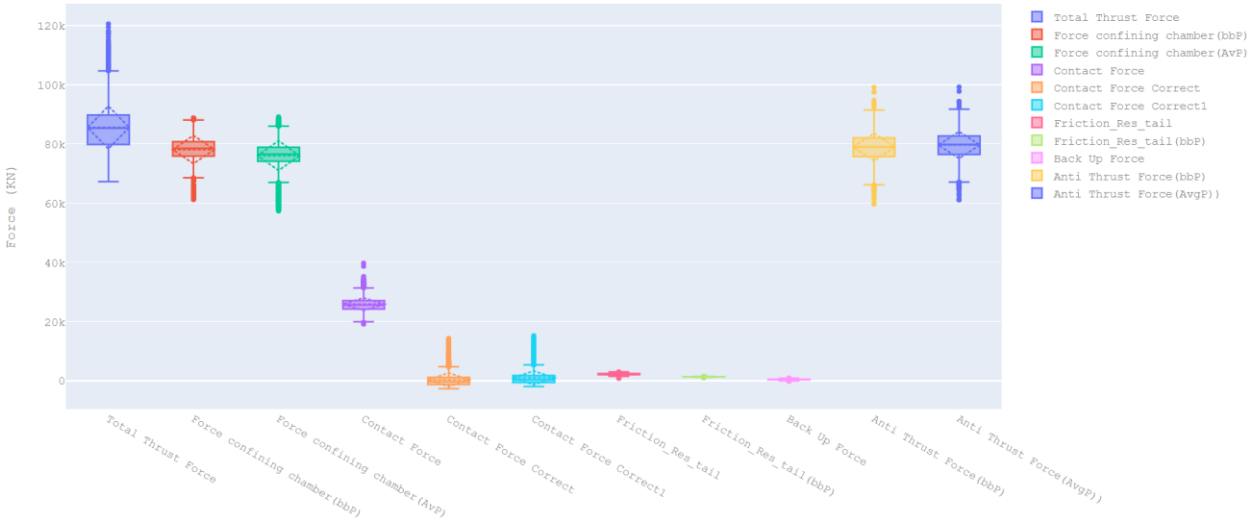

A.2. 4 Evaluation of forces exerted on TBM S881 (internal and external interactions) based on data captured during excavation. Figure presented distribution of total thrust force; force exerted on the confining chamber calculated based on bubble pressure

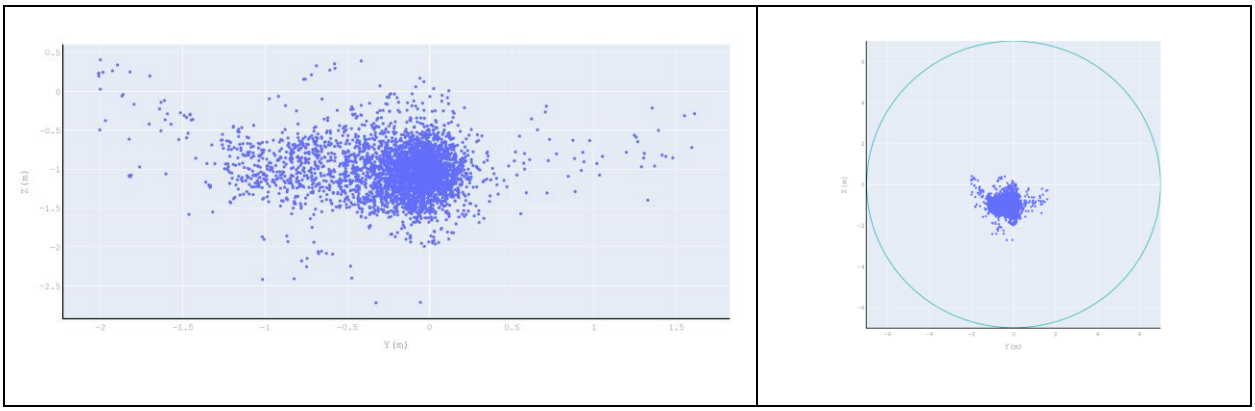

A.2. 5 Centre of thrust force calculated and visualized for each meter of excavation by S881 TBM. Right plot showed scatter plot of the center of thrust force in the transversal section of the TBM S882 with 14 m diameters.

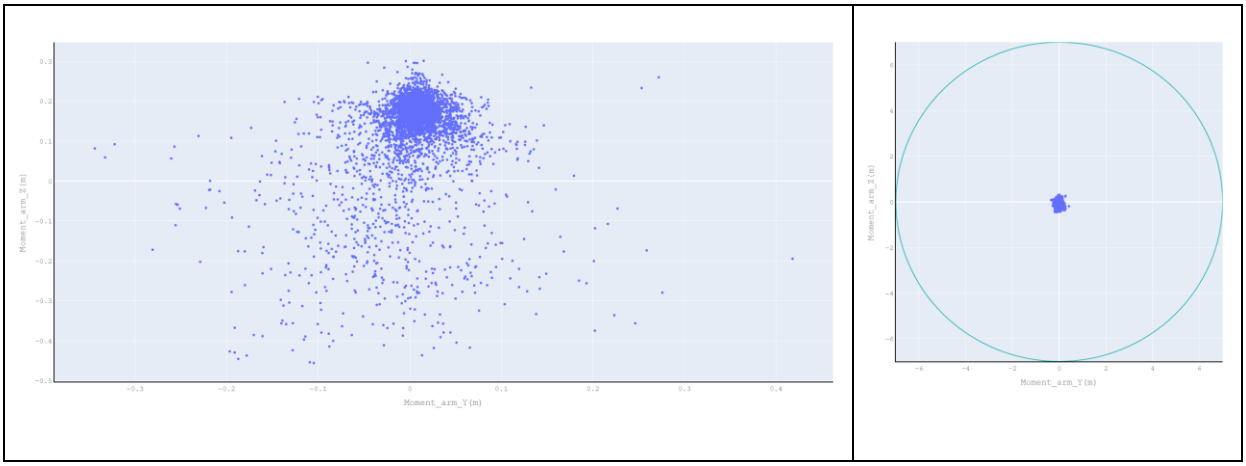

A.2. 6 Evaluation of the distribution of the cutter head moment arm for TBM S881. Right plot showed scatter plot of the cutter head moment arm in the transversal section of the TBM S882 with 14 m diameters.

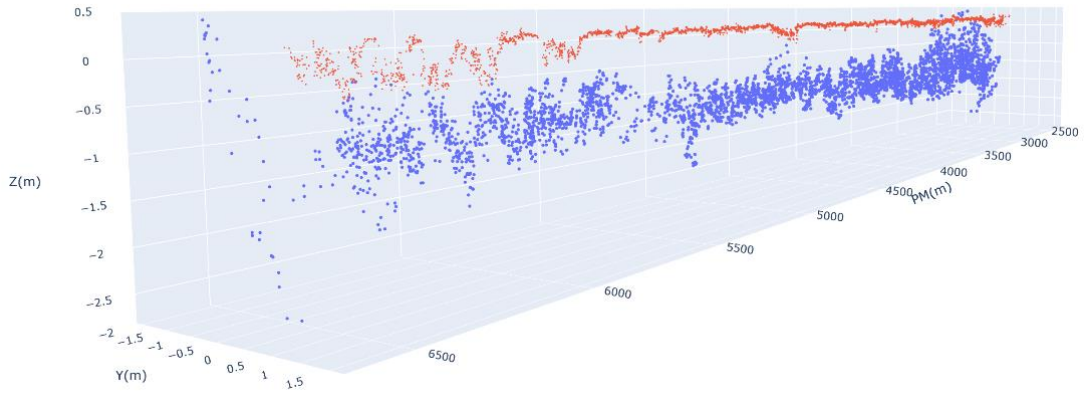

A.2. 7 3D visualization of the centre of the thrust force (blue point) and the moment arm (red point)

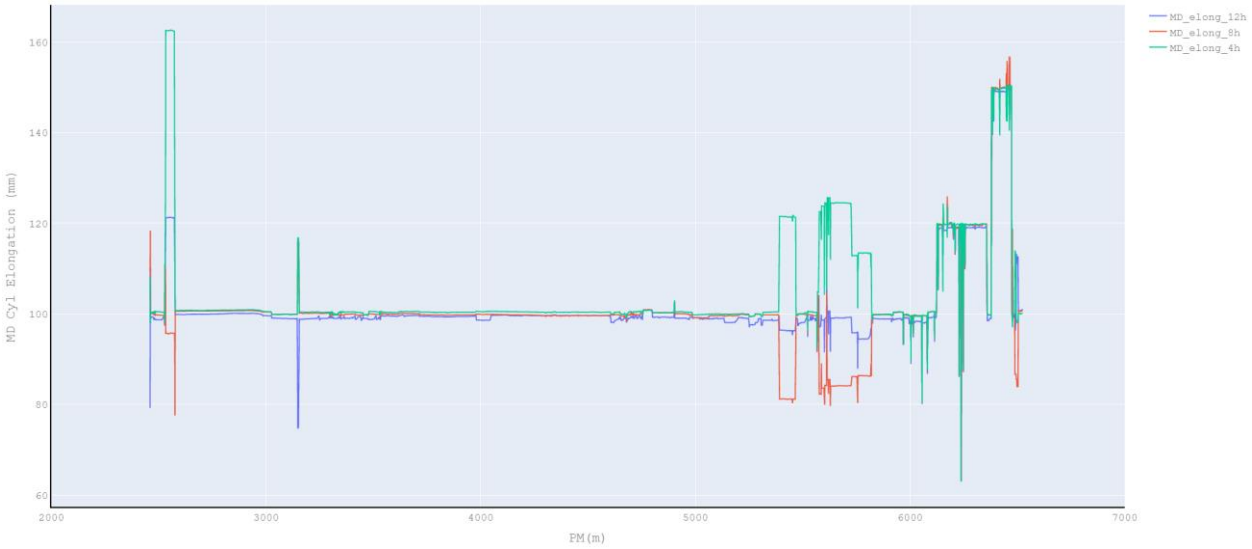

A.2. 8 Main drive displacement cylinders evolution vs chainage, the cylinders configuration established in three position 12h, 4h and 8h.

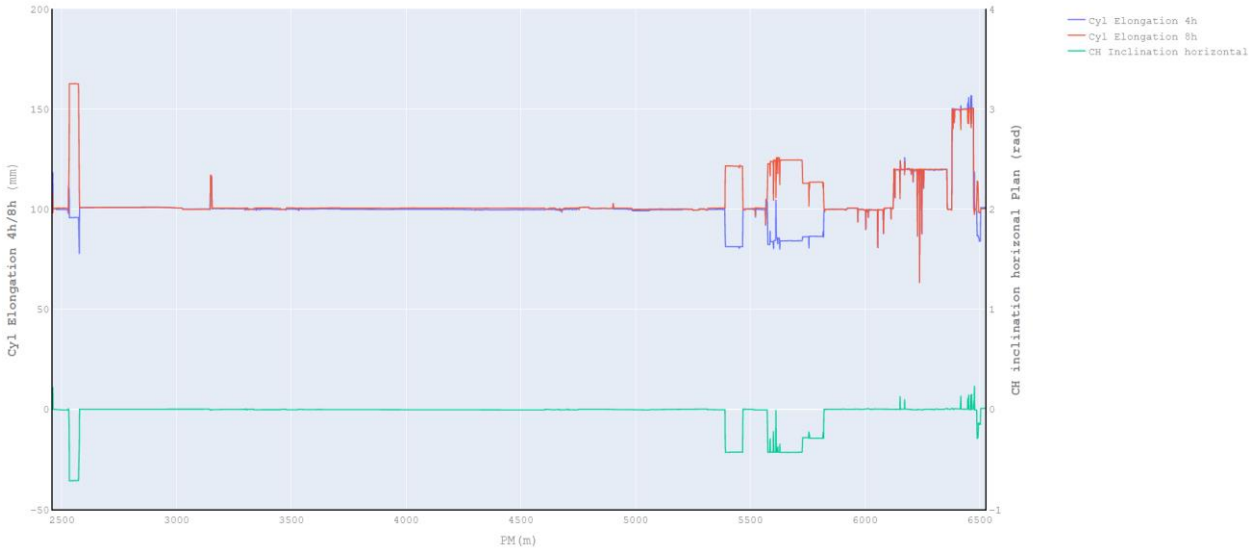

A.2. 9 Evaluation of the cutter head inclination (horizontal plane) vs TBM chainage. The inclination is calculated by using elongation of cylinders located at 4h and 8h. Right axis shows cylinder's elongation in mm. Left axis demonstrates inclination fluctuation of cutter head during each meter of advancement.

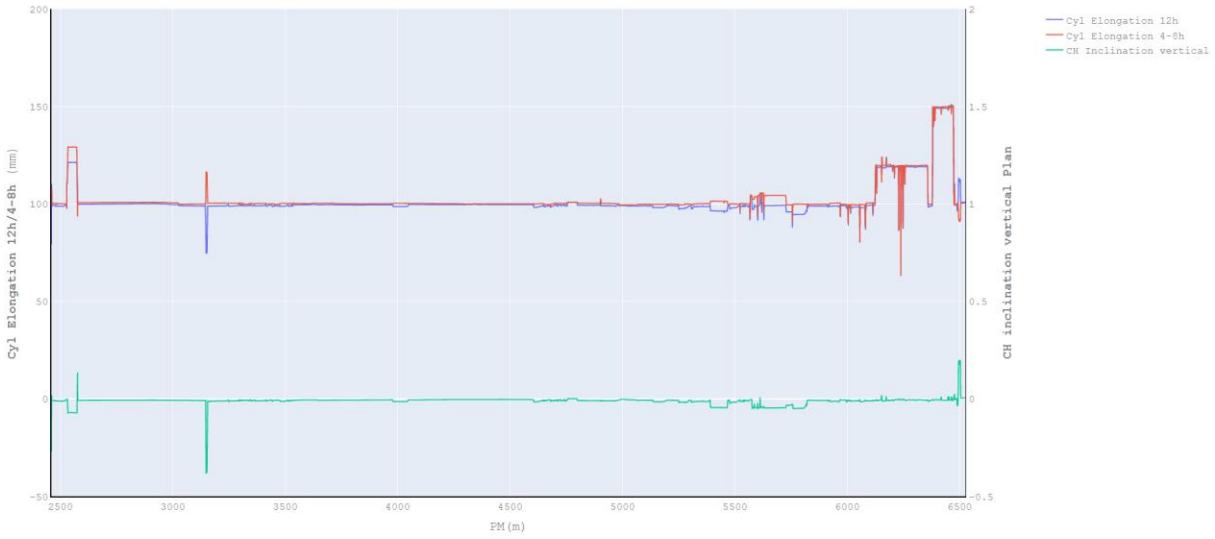

A.2. 10 Evaluation of the cutter head inclination (vertical plane) vs TBM chainage. The inclination is calculated by using elongation of cylinders located at 12h and 4h/8h. Right axis shows cylinder's elongation in mm. Left axis demonstrates inclination fluctuation of cutter head during each meter of advancement.

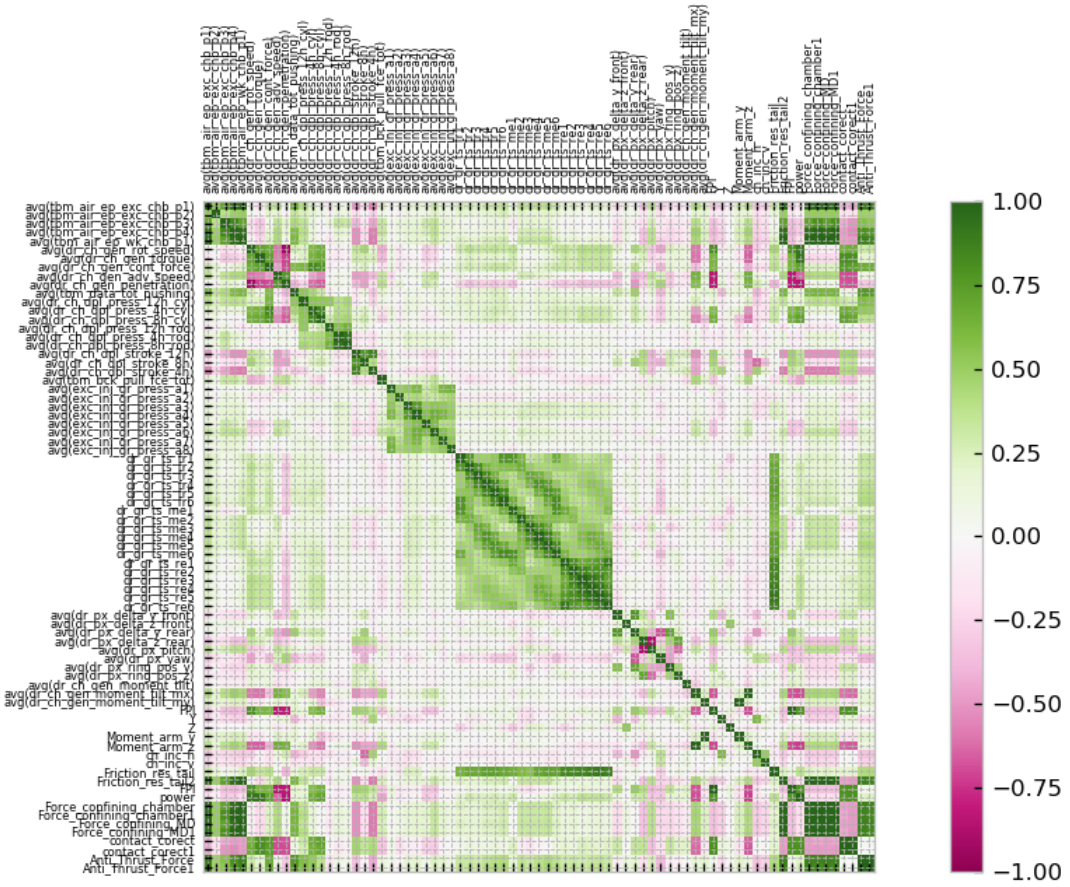

A.2. 11 Correlation matrix for operational parameters of TBM (S881) is investigated.

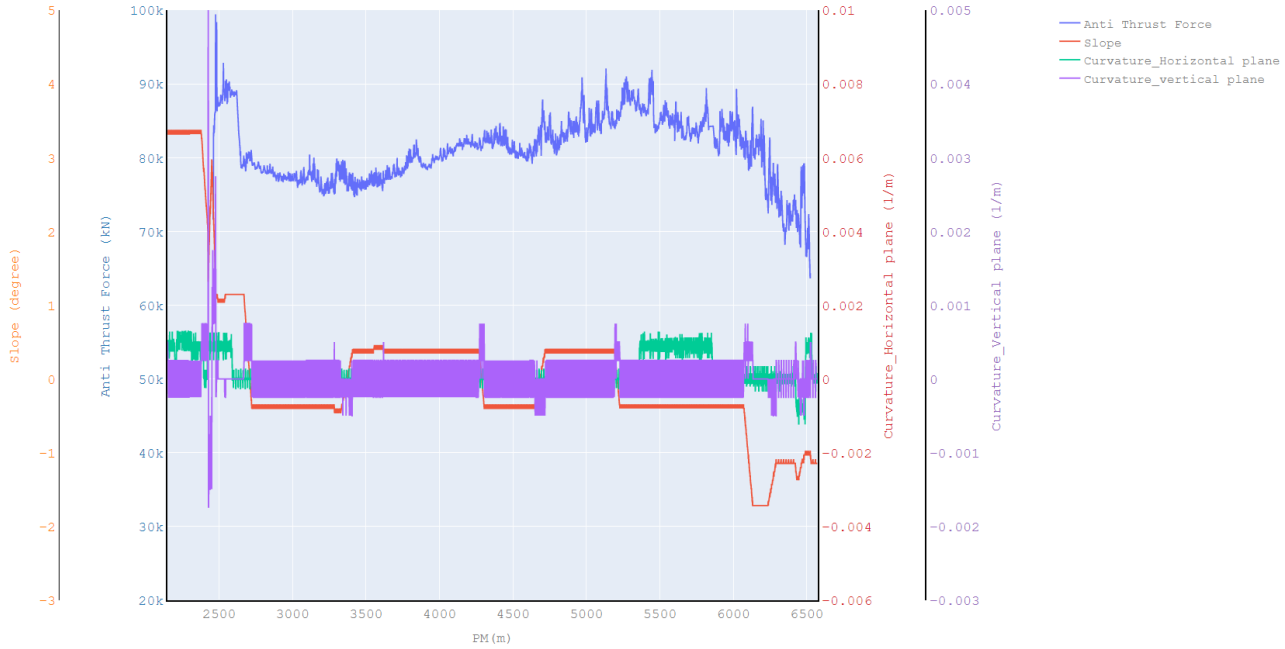

A.2. 12 line plot investigates fluctuation of anti-thrust force vs chainage and compare with guiding (trajectory) properties(characteristics) for TBM(S881). The potential relation between anti-thrust force evolution with trajectory properties can be evaluated.

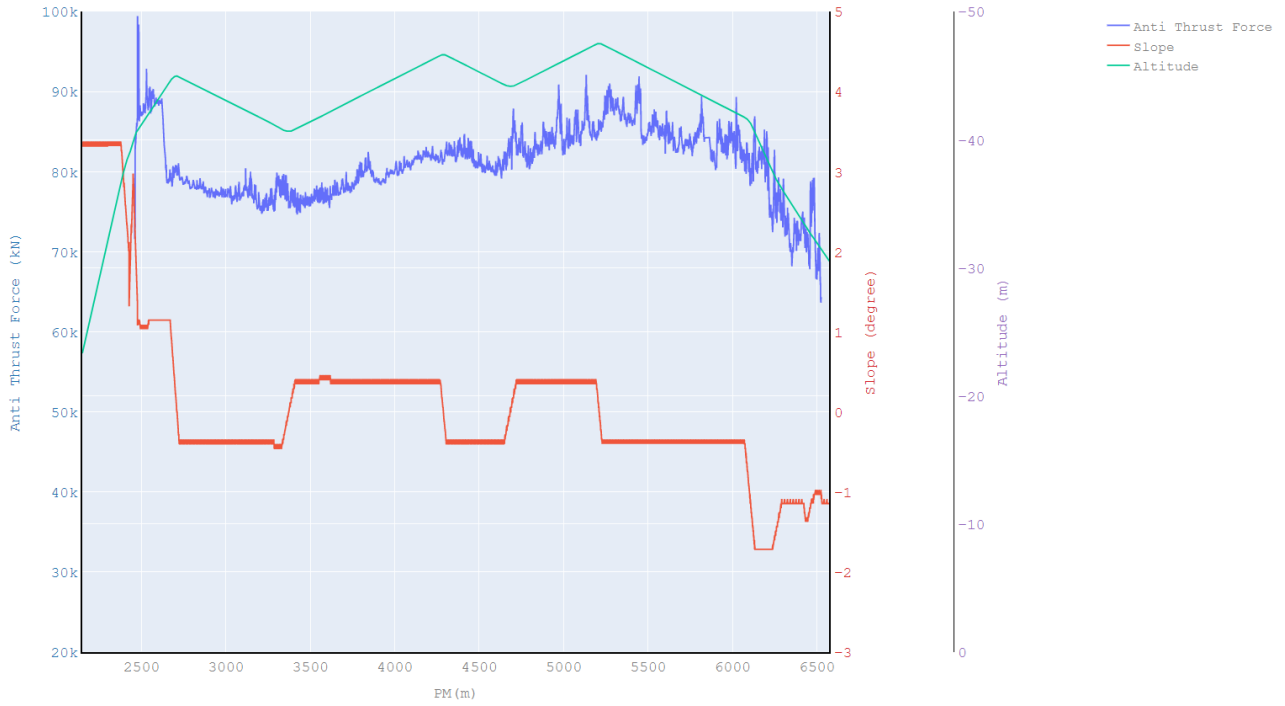

A.2. 13 line plot investigates fluctuation of anti-thrust force vs chainage and compare with guiding (trajectory) properties(characteristics) for TBM(S881). The potential relation between ant-thrust force evolution with altitude and slope is investigated.

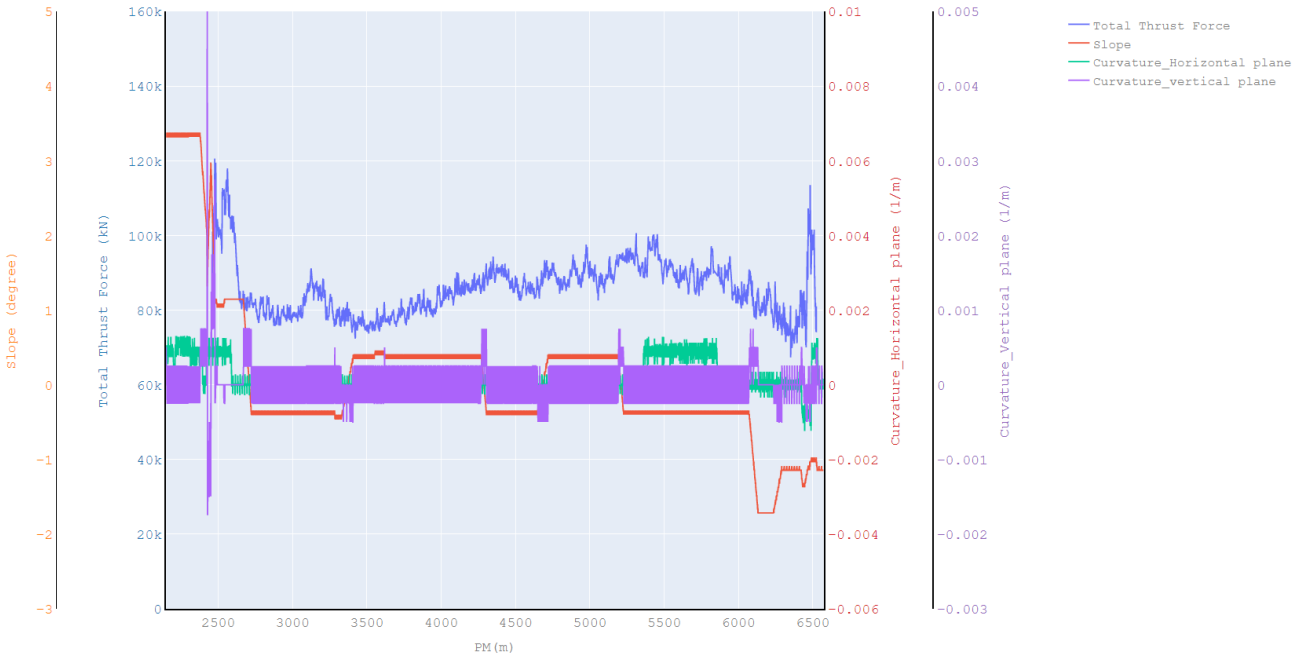

A.2. 14 line plot investigates fluctuation of total thrust force vs chainage and compare with guiding (trajectory) properties(characteristics) for TBM(S881). The potential relation between total thrust force evolution with trajectory properties can be evaluated

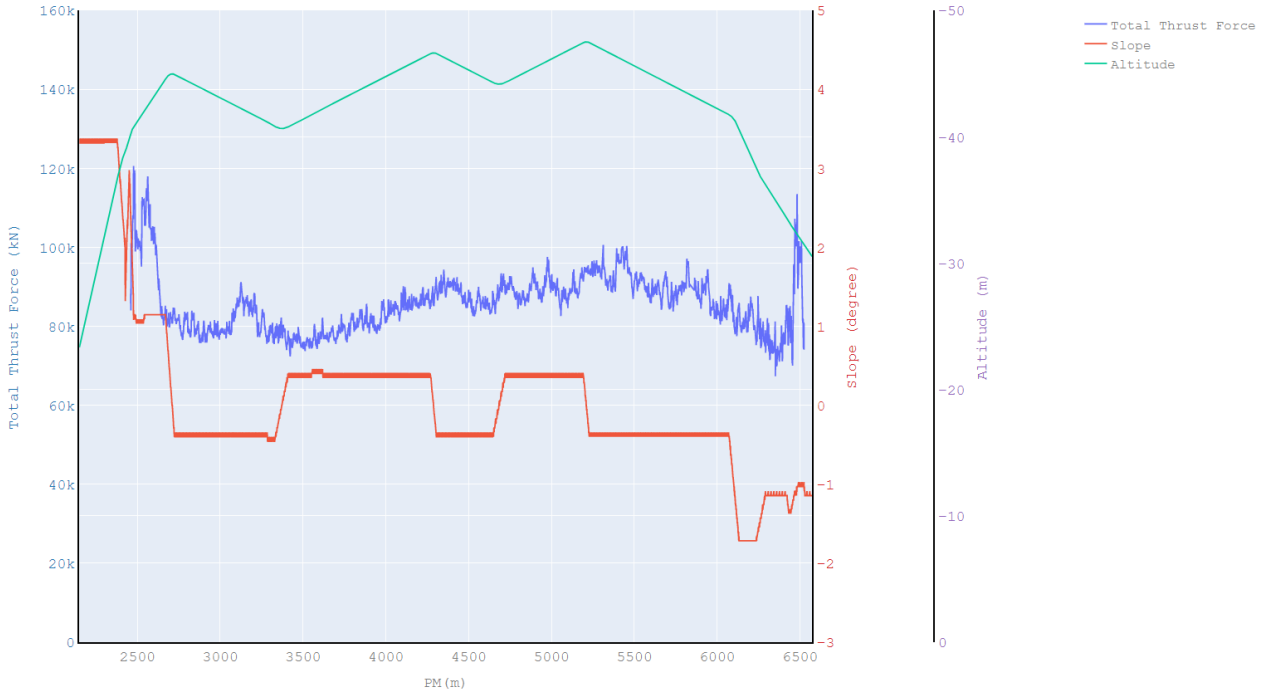

A.2. 15 line plot investigates fluctuation of total thrust force vs chainage and compare with guiding (trajectory) properties(characteristics) for TBM(S882). The potential relation between total thrust force evolution with altitude and slope is investigated.

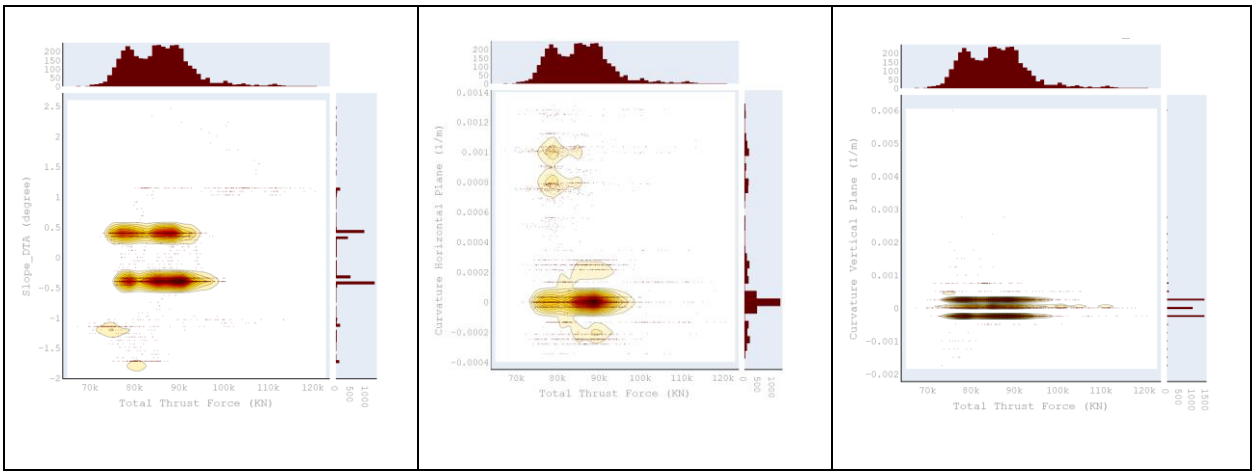

A.2. 16 Histograme2DConture plot: total thrust force vs trajectory characteristics

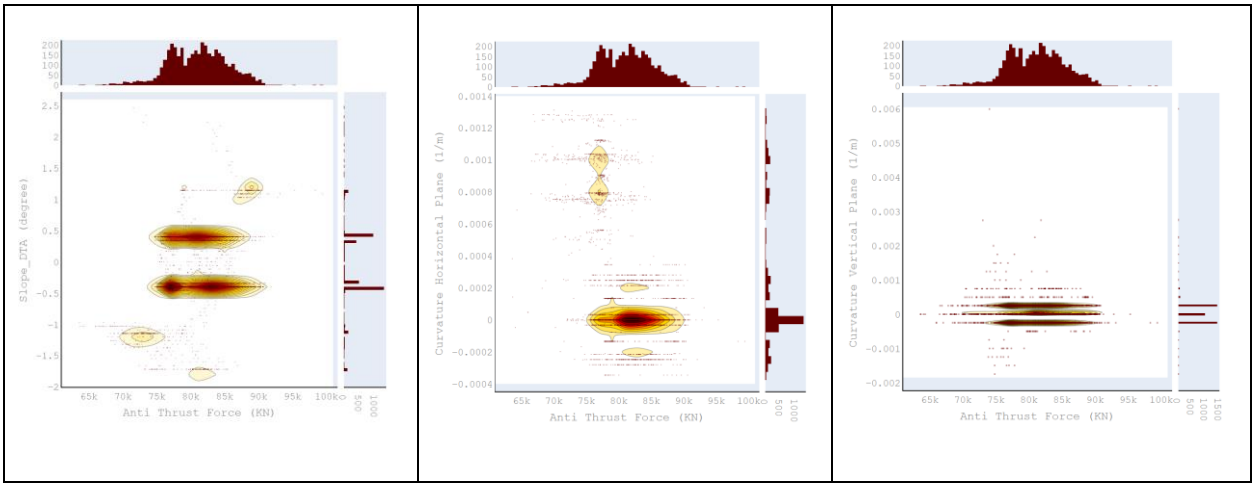

A.2. 17 Histograme2DConture plot: anti-thrust force vs trajectory characteristics

A3. Dimension reduction (PCA) result and evaluation on TMCLK-S882 project

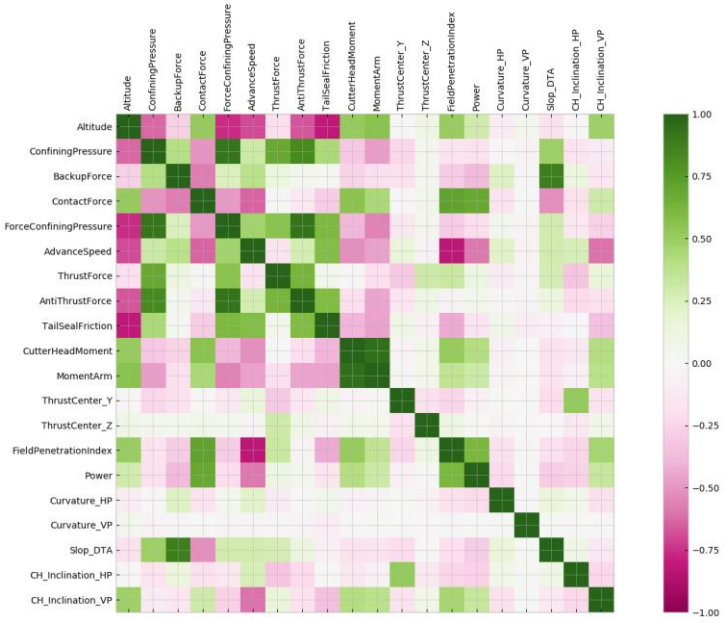

A3. 1 Correlation matrix for TMCLK S882 parameters

A3. 2 Geology segmentation (TMCLK Project, TBM S882)

Geology Type	Length in project profile(m)
ALLUVIONS	1740
G45	1140
ALLUVIONS_G45	820
G345	387

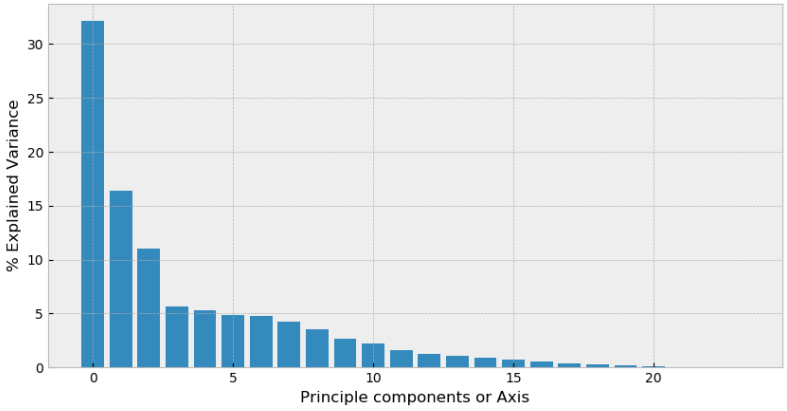

A3. 3 Explained variance by principle component in %

A3. 4 Left: Cumulative explained variance in %, Right: PCA Scree plot

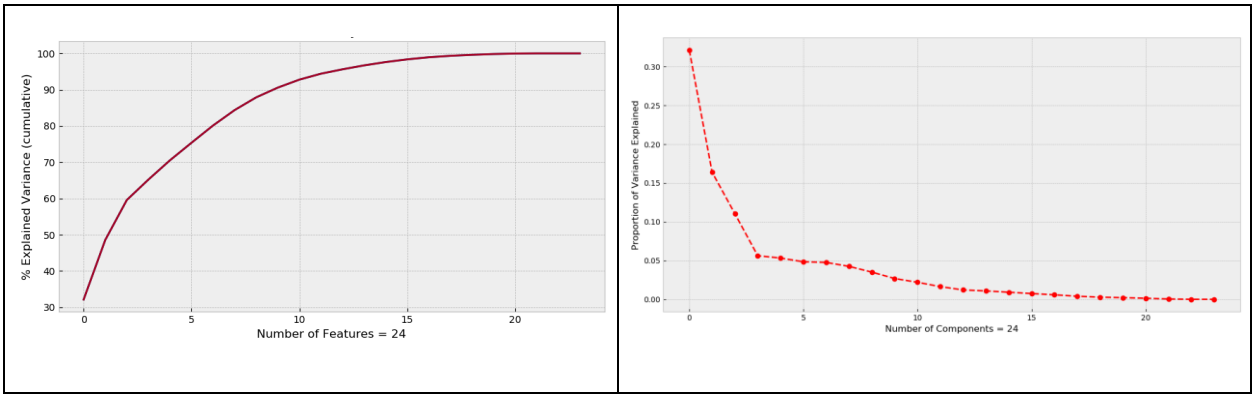

A3. 5 Feature importance evaluation for first six components (TMCLK S882)

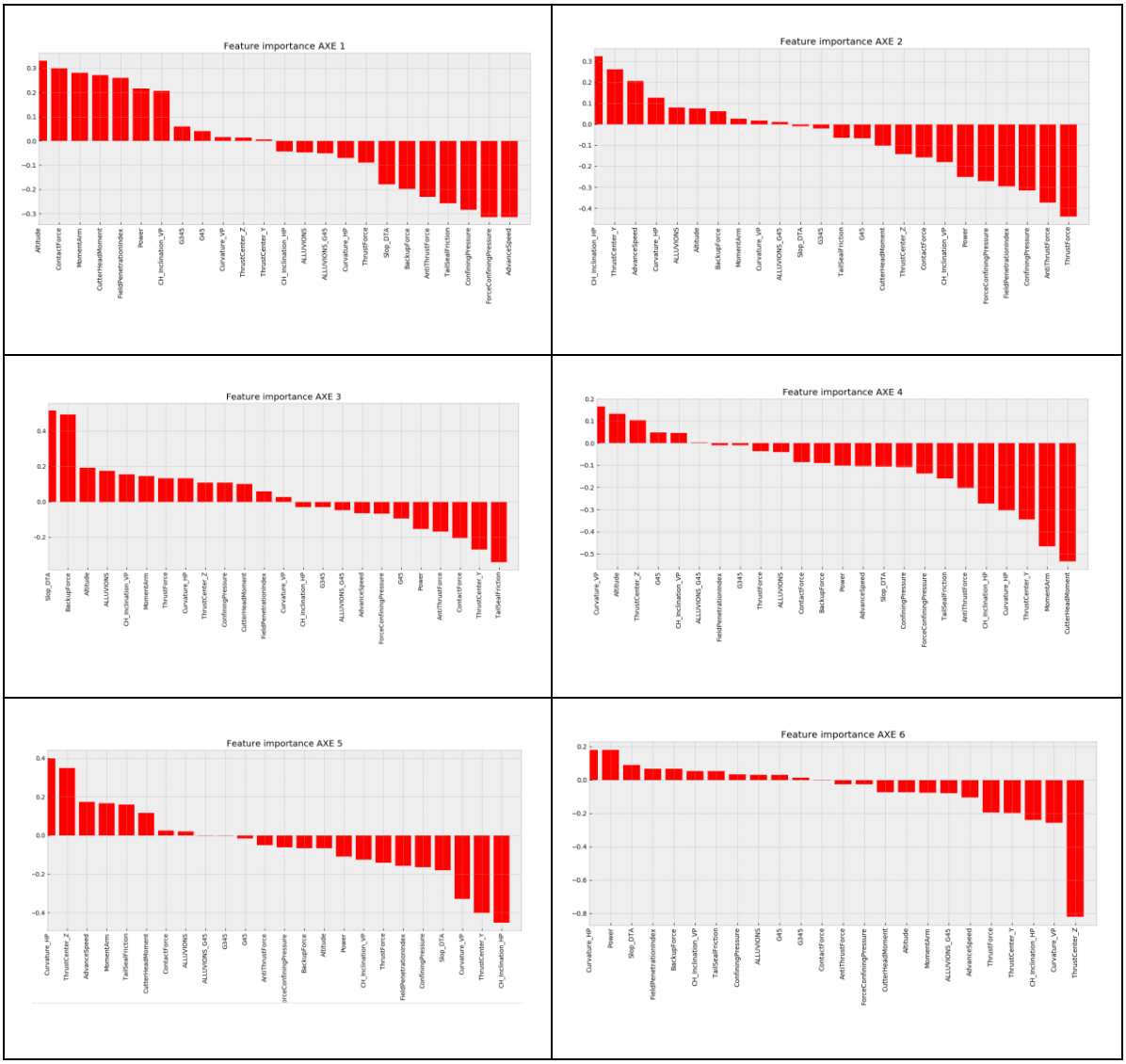

A4. Dimension reduction (PCA) result and evaluation on TMCLK-S881 project

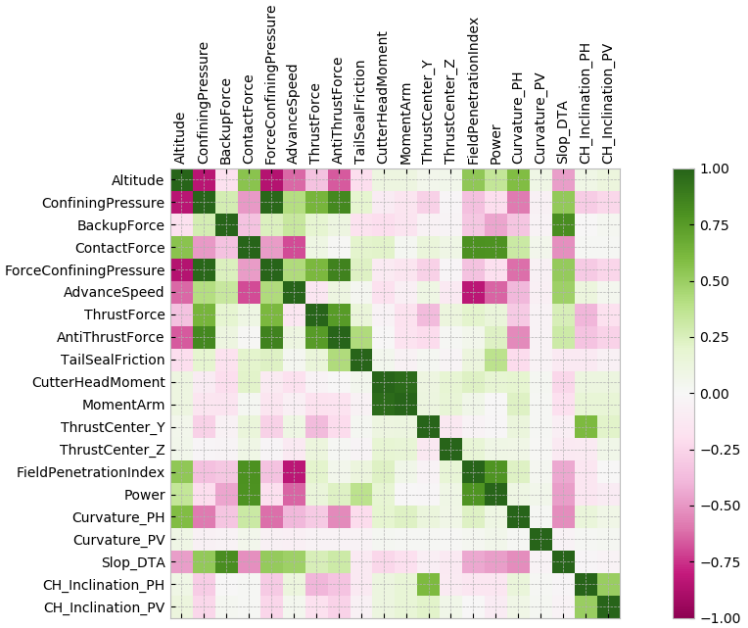

A4. 1 Correlation matrix for TMCLK S881 parameters

A4. 2 Geology segmentation (TMCLK Project, TBM S881)

Geology Type	Length in project profile(m)
ALLUVIONS	1740
G45	1140
ALLUVIONS_G45	820
G345	387

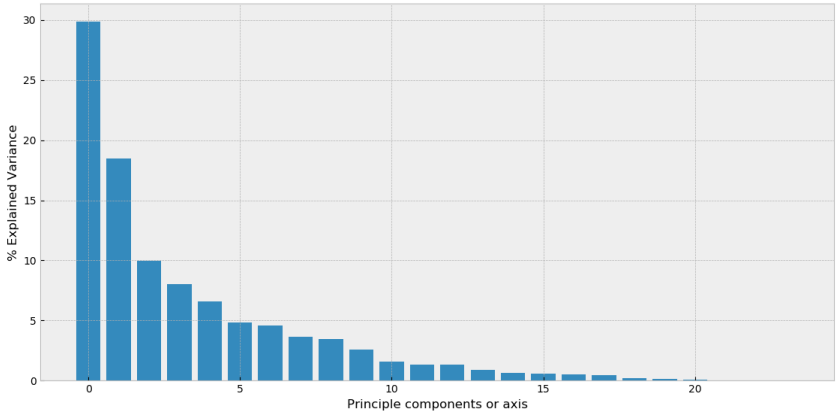

A4. 3 Explained variance by principle component in %

A4. 4 Left: Cumulative explained variance in %, Right: PCA Scree plot

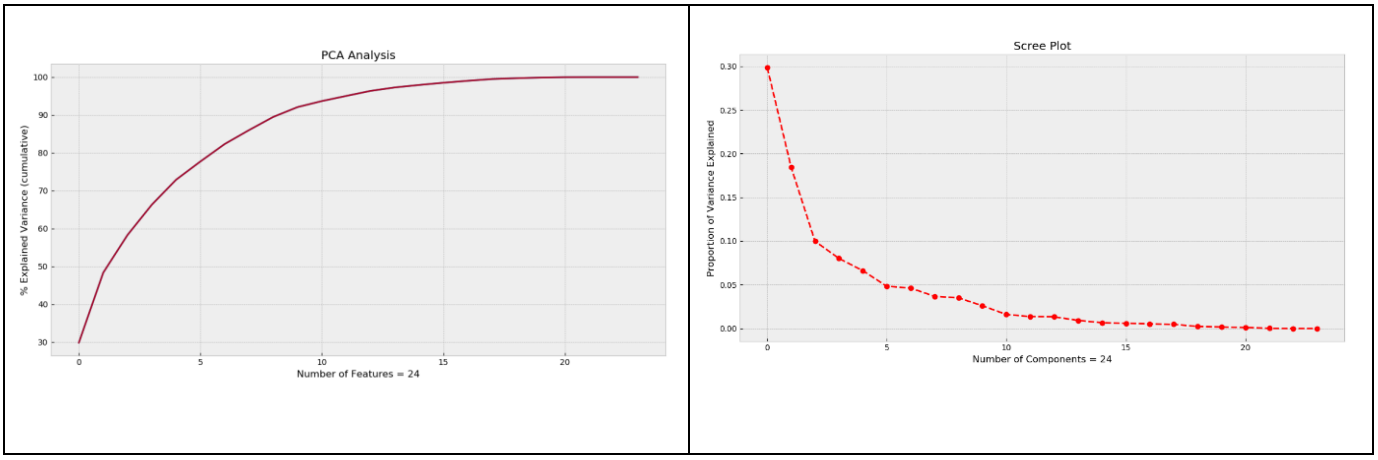

A4. 5 Feature importance evaluation for first six components (TMCLK S881)

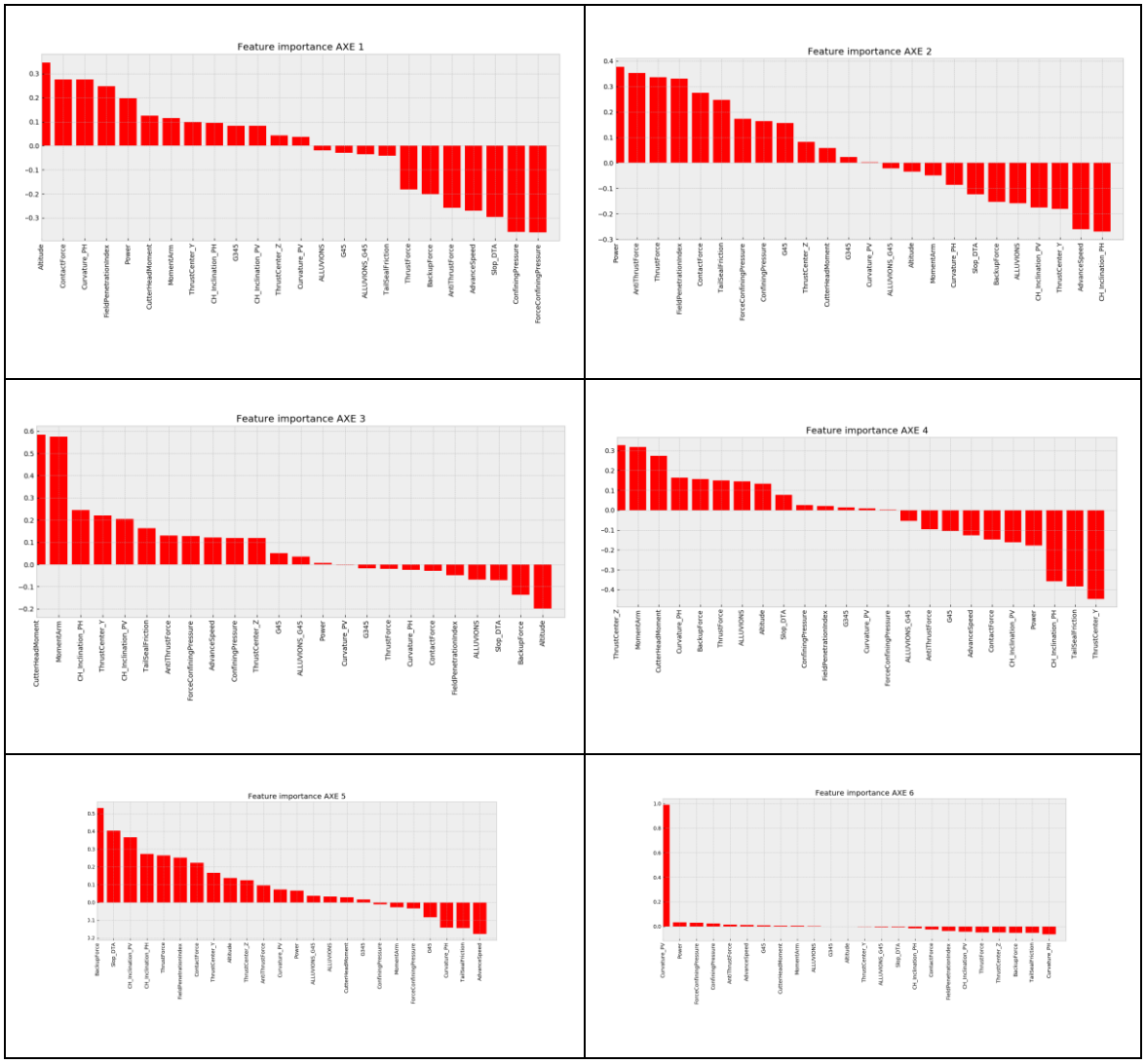

References

[1] Peck R.B, “Deep excavations and Tunnelling in soft Ground,” 1969.

[2] H. Ma, L. Yin, Q. Gong, and J. Wang, “TBM tunneling in mixed-face ground: Problems and solutions,” *Int. J. Min. Sci. Technol.*, vol. 25, no. 4, pp. 641–647, 2015.

[3] K. J. Bakker, P. van den Berg, and Jan Rots, “Monitoring soft soil tunnelling in the Netherlands: an inventory of design aspects,” 1997.

[4] B. B. Broms and H. Bennermark, “Stability of Clay at Vertical Openings,” 1967.

[5] B. Maidl, M. Herrenknecht, U. Maidl, and G. Wehrmeyer, *Mechanised Shield Tunnelling, Second Edition*. 2012.

[6] N. Bilgin, H. Copur, and C. Balci, *Mechanical Excavation in Mining and Civil Industries*. 2014.

[7] Japan Society of Civil Engineers, *Standards Specifications for Tunneling 2016: Shield Tunnels*. 2016.

[8] I. T. A. ITA, “Guidelines for the Design of Shield Tunnel Lining,” 2000.

[9] M. Zizka, Z., & Thewes, “Recommendations for Face Support Pressure Calculations for Shield Tunnelling in Soft Ground,” 2016.

[10] K. H. Chen and F. Le Peng, “An improved method to calculate the vertical earth pressure for deep shield tunnel in Shanghai soil layers,” *Tunn. Undergr. Sp. Technol.*, vol. 75, no. January, pp. 43–66, 2018, doi: 10.1016/j.tust.2018.01.027.

[11] W. Wittke, C. Erichsen, and J. Gattermann, *Stability Analysis and Design for Mechanized Tunnelling*. 2006.

[12] A. Bezuijen and A. Talmon, “Processes around a TBM,” 2008.

[13] A. Bezuijen and K. J. Bakker, “The influence of flow around a TBM machine,” *Geotech.*

Asp. Undergr. Constr. Soft Gr. - Proc. 6th Int. Symp. IS-SHANGHAI 2008, 2009.

[14] A. Bezuijen, "Bentonite and grout flow around a TBM," *"Proceedings 33rd ITA-AITES World Tunn. Congr. - Undergr. Sp. - 4th Dimens. Metropolises,"* vol. 1, no. March, pp. 383–388, 2007, doi: 10.1201/noe0415408073.ch64.

[15] PJA and Pipe Jacking Association, "Guide to Best Practice for the Installation of Pipe Jacks and Microtunnels," 1995.

[16] N. Bilgin, H. Copur, C. Balci, D. Tumac, M. Akgul, and A. Yuksel, "The selection of a TBM using full scale laboratory tests and comparison of measured and predicted performance values in Istanbul Kozyatagi-Kadikoy metro tunnels," *Proc. World Tunn. Congr. Akra, India*, pp. 1509–1517, 2008.

[17] N. Bilgin *et al.*, "The performance prediction of a TBM in Tuzla-Dragos Sewerage Tunnel," *Challenges 21st Century. Proc. World Tunn. Congr. '99, Oslo, June 1999. (2 vols).*, pp. 817–822, 1999.

[18] M. Sugimoto, A. Sramoon, and M. Asce, "Theoretical Model of Shield Behavior During Excavation. I: Theory," doi: 10.1061/ASCE1090-0241200212812138.

[19] S. R. Sukumar, M. Olama, and J. J. Nutaro, "Concept of Operations for Knowledge Discovery from ' Big Data ' Across Enterprise Data Warehouses," no. May, 2013, doi: 10.1117/12.2016321.

[20] G. R. Schleder, A. C. M. Padilha, C. M. Acosta, M. Costa, and A. Fazzio, "From DFT to machine learning: recent approaches to materials science–a review," *J. Phys. Mater.*, vol. 2, no. 3, p. 032001, 2019, doi: 10.1088/2515-7639/ab084b.

[21] J. W. Tukey, *Exploratory Data Analysis*. 1977.

[22] P. Bruce, A. Bruce, and P. Gedeck, *Practical Statistics for Data Scientists*. 2017.

[23] J. D. Hunter, "Matplotlib: A 2D graphics environment," *Comput. Sci. Eng.*, vol. 9, no. 3, pp. 99–104, 2007, doi: 10.1109/MCSE.2007.55.

[24] Plotly Technologies Inc, “Collaborative data science.” 2015, [Online]. Available: https://plot.ly.

[25] P. Virtanen *et al.*, “SciPy 1.0: fundamental algorithms for scientific computing in Python,” *Nat. Methods*, vol. 17, no. 3, pp. 261–272, 2020, doi: 10.1038/s41592-019-0686-2.

[26] T. E. Oliphant, “Guide to NumPy,” *Methods*, vol. 1, p. 378, 2010, doi: 10.1016/j.jmoldx.2015.02.001.

[27] W. McKinney, “Data Structures for Statistical Computing in Python,” *Proc. 9th Python Sci. Conf.*, vol. 1697900, no. Scipy, pp. 51–56, 2010, [Online]. Available: http://conference.scipy.org/proceedings/scipy2010/mckinney.html.

[28] Bouygues TP, “SCL1128_PYXIS_Surveyor Manual_V1.0,” 2016.

[29] Bouygues TP, “SLC1128_ Pyxis_PilotManual_v3.0,” 2016.

[30] T. Kasper and G. Meschke, “On the influence of face pressure, grouting pressure and TBM design in soft ground tunnelling,” *Tunn. Undergr. Sp. Technol.*, vol. 21, no. 2, pp. 160–171, 2006, doi: 10.1016/j.tust.2005.06.006.

[31] J. F. Nagel, “Numerical modelling of partially saturated soil and simulation of shield supported tunnel advance,” 2009.

[32] D. Festa, W. Broere, and J. W. Bosch, “An investigation into the forces acting on a TBM during driving - Mining the TBM logged data,” *Tunn. Undergr. Sp. Technol.*, 2012, doi: 10.1016/j.tust.2012.06.006.

[33] D. Festa, W. Broere, and J. W. Bosch, “Tunnel-boring in soft soil: a study on the driving forces applied to a slurry-shield TBM.”

[34] D. Festa, W. Broere, and J. W. Bosch, “Tunnelling in Soft Soil: Tunnel Boring Machine Operation and Soil Response,” no. 95530, pp. 978–89, 2013.

[35] D. Festa, W. Broere, and J. W. Bosch, “Kinematic behaviour of a Tunnel Boring Machine in soft soil: Theory and observations,” *Tunn. Undergr. Sp. Technol.*, 2015, doi:

10.1016/j.tust.2015.03.007.

[36] A. G. Benardos and D. C. Kaliampakos, “Modelling TBM performance with artificial neural networks,” *Tunn. Undergr. Sp. Technol.*, vol. 19, no. 6, pp. 597–605, 2004, doi: 10.1016/j.tust.2004.02.128.

[37] J. Gholamnejad and N. Tayarani, “Application of artificial neural networks to the prediction of tunnel boring machine penetration rate,” *Min. Sci. Technol.*, vol. 20, no. 5, pp. 727–733, 2010, doi: 10.1016/S1674-5264(09)60271-4.

[38] S. Mahdevari, K. Shahriar, S. Yagiz, and M. Akbarpour Shirazi, “A support vector regression model for predicting tunnel boring machine penetration rates,” *Int. J. Rock Mech. Min. Sci.*, vol. 72, pp. 214–229, 2014, doi: 10.1016/j.ijrmms.2014.09.012.

[39] A. Salimi, J. Rostami, C. Moormann, and A. Delisio, “Application of non-linear regression analysis and artificial intelligence algorithms for performance prediction of hard rock TBMs,” *Tunn. Undergr. Sp. Technol.*, vol. 58, pp. 236–246, 2016, doi: 10.1016/j.tust.2016.05.009.

[40] M. Namli and N. Bilgin, “A model to predict daily advance rates of EPB-TBMs in a complex geology in Istanbul,” *Tunn. Undergr. Sp. Technol.*, vol. 62, pp. 43–52, 2017, doi: 10.1016/j.tust.2016.11.008.

[41] H. Xu, J. Zhou, P. G. Asteris, D. J. Armaghani, and M. M. Tahir, “Supervised machine learning techniques to the prediction of tunnel boring machine penetration rate,” *Appl. Sci.*, vol. 9, no. 18, pp. 1–19, 2019, doi: 10.3390/app9183715.

[42] S. Yagiz, C. Gokceoglu, E. Sezer, and S. Iplikci, “Application of two non-linear prediction tools to the estimation of tunnel boring machine performance,” *Eng. Appl. Artif. Intell.*, vol. 22, no. 4–5, pp. 808–814, 2009, doi: 10.1016/j.engappai.2009.03.007.

[43] R. Boubou, F. Emeriault, and R. Kastner, “Artificial neural network application for the prediction of ground surface movements induced by shield tunnelling,” *Can. Geotech. J.*, vol. 47, no. 11, pp. 1214–1233, 2010, doi: 10.1139/T10-023.

[44] J. Lai, J. Qiu, Z. Feng, J. Chen, and H. Fan, “Prediction of Soil Deformation in Tunnelling Using Artificial Neural Networks,” *Comput. Intell. Neurosci.*, vol. 2016, 2016, doi: 10.1155/2016/6708183.

[45] W. Sun, M. Shi, C. Zhang, J. Zhao, and X. Song, “Dynamic load prediction of tunnel boring machine (TBM) based on heterogeneous in-situ data,” *Autom. Constr.*, vol. 92, no. March, pp. 23–34, 2018, doi: 10.1016/j.autcon.2018.03.030.

[46] J. Zhao *et al.*, “A Data-Driven Framework for Tunnel Geological-Type Prediction Based on TBM Operating Data,” *IEEE Access*, vol. 7, pp. 66703–66713, 2019, doi: 10.1109/ACCESS.2019.2917756.

[47] S. Leng, J. R. Lin, Z. Z. Hu, and X. Shen, “A Hybrid Data Mining Method for Tunnel Engineering Based on Real-Time Monitoring Data from Tunnel Boring Machines,” *IEEE Access*, vol. 8, no. May, pp. 90430–90449, 2020, doi: 10.1109/ACCESS.2020.2994115.

[48] I. Shahrour and Z. Wengang, “Use of soft computing techniques for tunneling optimization of tunnel boring machines,” *Undergr. Sp.*, 2020, doi: 10.1016/j.undsp.2019.12.001.

[49] D. Solomatine, L. M. See, and R. J. Abrahart, “Data-Driven Modelling: Concepts, Approaches and Experiences,” *Pract. Hydroinformatics*, pp. 17–30, 2008, doi: 10.1007/978-3-540-79881-1_2.

[50] B. Choudhury and R. Mohan Jha, *Soft computing techniques*. 2016.

[51] T. Hastie, R. Tibshirani, J. Friedman, and G. James, *An Introduction to Statistical Learning*. 2013.

[52] F. Cholet, *Deep Learning with Python*. 2018.

[53] J. Brownlee, *Master Machine Learning Algorithms*. 2017.

[54] S. J. Russell and P. Norvig, *Artificial Intelligence: A Modern Approch*, Third Edit. 2010.

[55] G. Varoquaux, L. Buitinck, G. Louppe, O. Grisel, F. Pedregosa, and A. Mueller, “Scikit-learn,” *GetMobile Mob. Comput. Commun.*, vol. 19, no. 1, pp. 29–33, 2015, doi:

10.1145/2786984.2786995.

[56] S. Raschka, *Python Machine Learning*. 2015.

[57] P. GUPTA and N. K. SINHA, *Neural Networks for Identification of Nonlinear Systems: An Overview*. Academic Press, 2000.

[58] I. Goodfellow, Y. Bengio, and A. Courville, “Deep Learning,” 2016.

[59] A. Meyer-Baese and V. Schmid, *Foundations of Neural Networks*. 2014.

[60] J. Brownlee, *Deep Learning with Python, Develope Deep Learning models on TensorFlow using Keras*. 2020.

[61] J. Dean and M. Rajat, “TensorFlow: Large-Scale Machine Learning on Heterogeneous Distributed Systems,” 2015.

[62] J. Brownlee, *Better Deep Learning, Train faster, Reduce overfitting and make better prediction*. 2020.

Modélisation du comportement du tunnelier et impact sur son environnement

Résumé : Le tunnelier, l'une des méthodes les plus fiables de creusement de tunnels mécanisés, a des acteurs scientifiques et professionnels de premier plan dans le monde entier, du Japon à l'Europe et à l'Amérique du Nord. Le développement du tunnelier a bénéficié de différentes approches analytiques, numériques et expérimentales.

Au cours de ce projet de recherche, nous avons déterminé l'importance de l'exploration et de l'analyse des données opérationnelles des TBM. Les compétences en science des données, en particulier l'analyse exploratoire des données (EDA), nous permettent d'étudier les paramètres opérationnels de l'excavation, de découvrir des relations significatives entre les paramètres et de trouver des paramètres efficaces pour décrire plus précisément l'interaction du tunnelier avec son environnement. Ensuite, des algorithmes mathématiques et statistiques (algorithmes d'apprentissage automatique) seront utilisés pour étendre nos capacités de modélisation et d'optimisation du pilotage de la TMB en utilisant des paramètres sélectionnés de l'AED.

Cette étude de recherche nous a permis d'évaluer et d'identifier une méthode applicable pour trouver une corrélation significative entre les paramètres opérationnels du TBM et pour évaluer son comportement avec l'environnement. Cette évaluation basée sur les données nous donne des capacités d'interprétation améliorées pour trouver des paramètres efficaces afin de réduire l'incertitude dans nos opérations techniques. Nous avons également proposé une stratégie instrumentale pour mesurer la déformation du corps cylindrique de la structure (la jupe) et calculer la charge exercée sur la périphérie de la jupe. Les paramètres proposés sont utilisés dans des approches data-driven pour optimiser le pilotage des TBM. Les approches data-driven permettent également aux experts de terrain (ingénieurs de tunnel) d'observer les données opérationnelles mesurées afin d'améliorer la résolution des problèmes.

Mots clés : Tunnelier, Modélisation Analytique, Analyse Exploratoire des Données, Optimisation, Apprentissage Automatique.

Modelling the behaviour of the Tunnel Boring Machine and impact on its environment

Summary: Tunnel Boring Machine (TBM) tunnelling as one of the most reliable mechanized tunnel excavation methods has prominent worldwide scientific and professional actors from Japan to Europe and North America. The development of TBM tunnelling has benefited from different analytical, numerical, and experimental approaches. Given the progress of new technologies, data-driven methods can be used as practical tools to realize and solve optimization and operational problems. The data-driven approaches support us in optimized decision-making based on data analysis and interpretation.

For this study, TBM operational excavation data are used, the data came from roadway and transportation tunnel projects. During this research project, the importance of TBM operational data exploration and analysis is determined. Data science skills, especially Exploratory Data Analysis (EDA), give us further capacities to investigate the operational excavation parameters, discover meaningful relation between parameters, and find useful parameters to describe the TBM interaction with its surroundings accurately.

This research study allowed us to assess and identify an applicable method to find a meaningful association between operational parameters of TBM, trajectory characteristics, geological characteristics of ground and to assess TBM behaviour with the surrounding. The data-driven assessment gives us improved interpretational capabilities to find effective parameters to reduce uncertainty in our technical operations. In parallel, an instrumentational strategy is proposed and developed to measure the deformation of the cylindrical body of the tail skin structure and calculate the exerted load on the periphery of the tail skin. Proposed parameters are used in data-driven approaches to optimize the steering of TBM. data-driven approaches also enable field experts (tunnel engineers) to observe measured operational data to improve problem-solving capacities.

Keywords: TBM, Analytical Modelling, Data-Driven Methods, Exploratory Data Analysis, Optimization, Machine Learning, Deep Learning.